Performance Analysis of Train Communication Systems

Waled Ali Mohamed Gheth

PhD 2021

Performance Analysis of Train Communication Systems

Waled Ali Mohamed Gheth

A thesis submitted in partial fulfilment of the requirements of
Manchester Metropolitan University for the degree of
Doctor of Philosophy

Department of Engineering
Manchester Metropolitan University

2021

Table of contents

List of figures

List of tables

List of Symbols

A	Area
a	Acceleration
B	Bandwidth
C	Capacitance
C	Capacity
D	Destination
d	Distance
G	Conductance
G	Gain
$g(\Psi_K)$	Optical Concentration Gain
h	Channel Gain
f	Operating Frequency
I	Current
L	Inductance
L	Vertical Distance to the User Plane
l	Length
M	Number of Links
N	Number of Relays
n	Noise
O	Outage Probability
P	Transmit Power
R	Resistance
S	Source
t	Time
$U(\Psi_K)$	Optical Filter Gain
V	Voltage
v	Speed
X	Leakage Reactance
$y(t)$	Received Signal
Z	Impedance

List of Symbols

α	PLC Channel Attenuation Factor
δ	Conductivity
ε_0	Free Space Permittivity
ε_r	Permittivity of the Medium
γ	Propagation Factor
μ	Permittivity of Conductors
ρ	Resistivity
ϕ	Total Angle of the LED

Abstract

Trains are considered as a highly efficient transport mode which generate significant challenges in terms of their communication systems. For improved safety, to cope with the expected rapid increase in traffic, and to meet customer demands, an enhanced and reliable communication system is required for high-speed trains (HSRs). Mobile phone and laptop users would like to make use of the non-negligible time that they spend commuting but current HSR communication systems have a foreseeable end to their lifetime and a reliable, efficient, and fast communication replacement system has become essential. Encouraged by the use of existing power line networks for communication purposes, this research investigates the possibility of developing a train communication system based on the use of overhead line equipment (OLE). The ABCD transfer line model is developed to represent the transfer function of the OLE channel and is evaluated using computer simulations. The simulations of the OLE system used are based on orthogonal frequency division multiplexing as the chosen modulation scheme.

Within the train, for the provision of broadband services, developing a reliable communication system which is a combination of power line communication and optical wireless communication services using visible light communication (VLC) is considered. Mathematical methods were developed for these networks to assess the overall capacities and outage probabilities of the hybrid systems. Derivation of such analytical expressions offered opportunities to investigate the impact of several system parameters on the performance of the system. To assess the possibility of improving the performance of the proposed integrated systems, their performance in the presence of different relaying protocols has been comprehensively analyzed in terms of capacity and outage probability. This thesis studied the outage probability and energy per bit consumption performance of different relaying protocols over the VLC channel. Accurate analytical expressions for the overall outage probability and energy-per-bit consumption of the proposed system configurations, including the single-hop and multi-hop approaches were derived.

It was found that the transfer function of the OLE channel can be represented by the two-port network model. It was also revealed that transmission over OLE is negatively affected by the speed of the train, frequency, and length of the OLE link. In train,

relay-based communication systems can provide reliable connectivity to the end-user. However, choosing an optimal system configuration can enhance system performance. It was also shown that increasing relay numbers on the network contributes to the total power consumption of the system.

Declaration

I Waled Ali Mohamed Gheth hereby declare that the work referred to in this thesis submitted by me, under the guidance of Prof. Bamidele Adebisi is my original work and has not been submitted to any other University or Institute or published earlier.

Waled Ali Mohamed Gheth
2021

I would like to dedicate this thesis to my family.

Acknowledgements

First of all, I would like to extend my sincere thanks to my parents and my lovely brothers, sisters, nephews, and nieces for their love, encouragement and support. Special thanks to my wonderful wife and children for being patient and providing such an environment for my study particularly during the unprecedented times of the COVID-19 pandemic. Although, an effort have been taken by me in completing this project but this would not have been possible without the considered support of many individuals.

I would like to express my gratitude towards the project supervisor Prof. Bamidele Adebisi and supervisory team Dr. Khaled Rabie and Dr. Muhammad Ijaz for providing me with the possibilities to finish this thesis properly. My deepest appreciation and thanks to Dr. Georgina for giving me such attention and time. My thanks and appreciations also go to colleagues and friends in Manchester Metropolitan University for the encouragement which really helped me in completion of this thesis. I am really grateful to my office mates who shared with me the good and hard times. Finally, I would like to express my special thanks of gratitude to my government for giving me this golden opportunity to study in this university.

List of publications

Journal Papers

1. Waled Gheth, Khaled M. Rabie, Bamidele Adebisi, Muhammad Ijaz, Georgina Harris. COMMUNICATION SYSTEMS OF HIGH-SPEED RAILWAY: A Survey. *Transactions on Emerging Telecommunications Technologies*, 2020.

   https://doi.org/10.1002/ett.4189.

2. Waled Gheth, Khaled M. Rabie, Bamidele Adebisi, Muhammad Ijaz, Georgina Harris. Performance Analysis of Cooperative and Non-Cooperative Relaying over VLC Channel. *Sensors*, doi 10.3390/s20133660, Volume 20, 2020.

   https://doi.org/10.3390/s20133660.

3. Waled Gheth, Khaled M. Rabie, Bamidele Adebisi, Muhammad Ijaz, Georgina Harris. Energy-per-bit performance analysis of relay-based visible-light communication systems. *Physical Communication*, 1874-4907, Volume 35, 2019.

   https://doi.org/10.1016/j.phycom.2019.04.013.

Conference Papers

1. Waled Gheth, Khaled M. Rabie, Bamidele Adebisi, Muhammad Ijaz, Georgina Harris. Channel Modeling for Overhead Line Equipment for Train Communication. In *2020 IEEE International Symposium on Power Line Communications and its Applications (ISPLC)*, 2020.

   https://ieeexplore.ieee.org/document/9115413.

2. Waled Gheth, Bamidele Adebisi, Muhammad Ijaz, Georgina Harris. Hybrid Visible-Light/RF Communication System for Mission-Critical IoT Applications. In *2019 IEEE 2nd British and Irish Conference on Optics and Photonics (BICOP)*, pages 1–4, December 2019.

   https://ieeexplore.ieee.org/document/9059572.

3. Waled Gheth, A. Alfitouri, K. M. Rabie, B. Adebisi and K. A. Hamdi. Performance Analysis of Cooperative Diversity in Multi-user Environments. In *2019 8th International Conference on Modeling Simulation and Applied Optimization (ICMSAO)*, pages 1–4, 2019.

   https://ieeexplore.ieee.org/document/8880443.

4. Waled Gheth, Khaled M. Rabie, Bamidele Adebisi, Muhammad Ijaz, Georgina Harris. A Survey on Impulsive Noise Mitigation Strategies over Power Line Channels. In *Int. Telecommun. Conf., (Singapore)*, 2019.

   https://www.researchgate.net/publication/326233086.

5. Waled Gheth, Khaled M. Rabie, Bamidele Adebisi, Muhammad Ijaz, Georgina Harris. EMC Measurements in Indoor Power Line Communication Environments. In *Int. Telecommun. Conf., (Singapore)*, 2019.

   https://link.springer.com/chapter/ 10.1007/978-981-13-0408-8-16.

6. Waled Gheth, Khaled M. Rabie, Bamidele Adebisi, Muhammad Ijaz, Georgina Harris. On the Performance of DF-based Power-Line/Visible-Light Communication Systems. In *2018 International Conference on Signal Processing and Information Security (ICSPIS)*, pages 1–4, November 2018.

   https://ieeexplore.ieee.org/document/8642750.

7. Waled Gheth, Khaled M. Rabie, Bamidele Adebisi, Muhammad Ijaz, Georgina Harris. Performance Analysis of Integrated Power-Line/Visible-Light Communication Systems with AF Relaying. In *2018 IEEE Global Communications Conference (GLOBECOM)*, 2018.

   https://ieeexplore.ieee.org/document/8647270.

8. W. Gheth, K. M. Rabie, B. Adebisi, M. Ijaz, G. Harris and A. Alfitouri. Hybrid Power-Line/Wireless Communication Systems For Indoor Applications. In *2018 11th International Symposium on Communication Systems, Networks and Digital Signal Processing (CSNDSP)*, pages 1-6, July 2018.

   https://ieeexplore.ieee.org/document/8471777.

Abbreviations

Acronyms / Abbreviations

2G	Second-Generation
3G	Third-Generation
4G	Fourth-Generation
5G	Fifth-Generation
AC	Alternating Current
ADC	Analog-to-Digital Converter
AF	Amplify-and-Forward
AT	Auto-transformer
AWGN	Additive White Gaussian Noise
BER	Bit-Error-Rate
BPSK	Binary Phase Shift Keying
BT	Booster Transformer
CP	Cyclic Prefix
CTF	Channel Transfer Function
DAC	Digital-to-Analog Converter
DF	Decode-and-Forward
EMC	Electromagnetic Compatibility
FFT	Fast Fourier Transform
GMD	Geometric Mean Distance

GSM-R	Global System for Mobile Communications-railway
HD	Half-Duplex
HSR	High-Speed Trains
IDF	Incremental Decode-and-Forward
IDFT	Inverse Discrete Fourier Transform
IFFT	Inverse Fast Fourier Transform
LEDs	Light Emitting Diodes
LoS	Line-of-Sight
LTE-R	Long Term of Evaluation-railway
LTE	Long Term of Evaluation
MV-PLC	Medium-Voltage Power Line Communication
OFDM	Orthogonal Frequency Division Multiplexing
OLE	Overhead Line Equipment
OWC	Optical Wireless Communication
PER	Packet Error Rate
PLC	Power Line Communication
PSC	Parallel-to-Serial Converter
QoS	Quality of Service
SDF	Selective Decode-and-Forward
SNR	Signal-to-Noise Ratio
SPC	Serial-to-Parallel Converter
TLT	Transmission Lines Theory
VLC	Visible Light Communication

Chapter 1

Introduction

This chapter provides a brief description of railway communication systems and discusses communication systems within the train. The chapter also presents the major motivations and challenges of the thesis. The aim and objectives are also discussed and the novelty of the thesis is outlined.

1.1 Research Motivations and Challenges

Trains are considered the most efficient form of land transport due to their ability to carry heavy loads over long distances with very high speeds. Furthermore, trains are more energy efficient than other transport systems and their carbon emissions are relatively low, also they are punctual and safe compared to other mass transit systems. A significant number of challenges are to be faced as the service providers improve the quality of services to ensure customer satisfaction. Communication to trains as well as inside trains are critical issues. Current high-speed rail (HSR) communication systems have a predictable end to their working lives, and the assessment of future of HSR mobile communications began a few years ago. Fourth generation (4G) broad-band systems are one of the possible replacements of current HSR communication systems. These, compared to second-generation (2G) and third-generation (3G) systems, have greater capabilities as they offer higher data transfer rates [1]. Fifth generation (5G) systems are also being discussed as a potential option [1, 2].Because of their known performance and high level of reliability, over a long period of evolution for use with rail systems, 4G LTE-railway (LTE-R), is highly recommended as a reliable technology for the next generation of HSR communication systems [2, 3].

Overhead line equipment (OLE) contains the wires found along electrified railways that are used to transmit electricity to trains, long considered the most efficient method for providing trains with electrical energy [4]. The supply of electrical power to trains is divided into four main steps. First, power generation at the power stations then the transmission stage via the overhead transmission lines of the National Grid at very high voltage (400 kV). After that, the power is delivered to the feeder substations which convert it to 25 kV to be transmitted to the OLE [4]. The electric current is then collected from the contact wire by the panto-graph which is attached to the roof of the train. In the train, current is used to drive the motors with the aid of on-board controllers. The electrical power is something that trains must have access to at all times, but the contact wires come in fixed lengths so the panto-graph should overlap from one length of wire to the next, the panto-graph must slide smoothly from one to the other maintaining contact [4].

Carrying current at 25 kV the OLE is considered a medium-voltage (MV) transmission line. Several studies have discussed using MV power lines as a means of communication and showed that medium-voltage power line communication (MV-PLC) can provide reliable transmission services and can be regarded as a key technology for last-mile communication [5, 6]. Its main advantage is that it uses pre-installed MV power lines which means that a communication system is readily available. Because it could be a cost-effective solution for a range of communication problems MV-PLC has attracted a remarkable degree of research interest [7]. Monitoring of systems,

network management optimization and operational services are common applications of MV-PLC technology [8].

The non-negligible time that people spend commuting on trains can be used for preparing and/or reading reports, studying by reading electronic books, watching live and/or recorded programmes, listening to music and playing video games. However, communication within the train is another issue as the electromagnetic waves can be severely attenuated by the metal outer skin of the train coaches [9]. Connecting the train to a public network then distributing signals within and between coaches using an effective distribution system might be one scenario for communication inside the train [9]. A wireless local area network (WLAN) is an option as most of modern communication systems have WLAN interface [10]. WLAN is a relatively inexpensive distribution system and easy to install inside a train. Wireless Access Points (WAPs) can be installed in the train's coaches which can help increase network coverage with the train. The WAPs are connected to public networks, which support WiFi functions. However, as the train moves, commuters might experience a variation in signal strength as the train passes through different areas, some where the network coverage is weak, such as rural areas and tunnels.

Using a pre-installed infrastructure such as the existing low-voltage power-line communications (LV-PLCs) provides a competitive means of broad-band communication. This technology has been around for some decades, but it has been only used for limited applications such as, home automation, public lighting, and narrow band tele-remote relay applications. Due to associated problems such as electromagnetic compatibility (EMC), noise and attenuation, there are several practical issues that need to be overcome in order to ensure reliable transmission. Recent studies have shown promising results when using LV-PLC technology on-board vehicles (automotive and aircraft) suggesting it could be used to achieve broadband services between interconnected locomotive coaches, playing an important role in communication within the train [11].

Commuters can also enjoy broadband services using Optical Wireless Communication (OWC) technology which is predicted to play a crucial role in indoor wireless applications. Infra-red communication and visible light communication (VLC) are the two main technologies of indoor OWC. However, the use of light emitting diodes (LEDs) in VLC systems due to their economic consumption of energy has attracted significant attention and LEDs are considered one of the most important green communication technologies [12]. OWC can provide a wide range of benefits to the railway industry not only within trains but also inside stations with every source of light a possible wireless hot-spot [12]. Some light sources have properties that allow them to be used as part of VLC technologies both indoor and outdoor, LEDs are one such source that have the added advantage of energy efficiency, long life expectancy and low maintenance costs [13]. Nevertheless, there are a number of challenges to be investi-

gated and overcome before this technology can be fully employed [12]. Interference caused by the overlapping of adjacent LED light irradiated areas in the VLC link is one such technical problem, another is instability of signal reception caused by the frequent switching between areas covered by different LEDs, particularly as the area covered by each LED is small [14].

This thesis focuses on in/to train communication systems. The thesis investigates the use of the OLE as a train communication system. It also studies relay-based PLC/VLC systems as within train communication systems. The following are the research questions addressed:

- **1- In terms of to-train communication**:
- **Research question 1**: Can the two-port network model be developed to represent the transfer function of the OLE system?
- **Research question 2**: What is the channel capacity of OFDM-based OLE system for the given bandwidths and the given ranges of the SNR?
- **2- In terms of in-train signal distribution**:
- **Research question 3**: How can the statistical properties of PLC and VLC channels be exploited to develop mathematical models for an in-train hybrid PLC/VLC system, and be used to determine the capacity and outage probability of the entire system?
- **Research question 4**: Is the in-train relay-based PLC/VLC system a reliable communication system that can provide seamless transmission to the end user, what is the best configuration of the system that can provide best performance, and how do the parameters of the proposed systems affect their performance?
- **Research question 5**: How can the relay-based VLC system, the technology covering the last-meter access network to end-user in the proposed system, be made more energy-efficient and provide sufficient performance in terms of outage probability?

These research questions are answered in the course of this thesis. The first and second questions are addressed in Chapter 3, which investigates the OLE as a high data rate system that can be a communication medium between the in-train communication systems and the wayside and the results are published in [15]. The third and fourth questions address the performance of the in-train hybrid PLC/VLC system, which is discussed in Chapters 4 and the findings are published in [16, 17]. Question five is addressed in Chapter 5, which investigates the performance of a relay-based VLC system, which is the last-mile link, in terms of outage probability and energy consumption and the results are published in [18].

1.2 Research Aim and Objectives

1.2.1 Research Aims

This research aims to:

(i) Develop the ABCD model to represent the transfer function of the overhead line equipment channel, which in turns offers the opportunity to investigate the possibility of using the overhead line equipment as an access network to connect trains with the backbone communication networks.

(ii) Develop a cooperative of PLC and OWC services of the VLC systems to distribute the signal within the train after having it being received from an OLE communication system.

1.2.2 Research Objectives

To effectively accomplish these aims, the research objectives are:

1. To carry out comprehensive research on OLE system as a means of MV-PLC, and to conduct a study of PLC and VLC systems as last-mile communication systems.
2. To develop a channel model that can represent the transfer function of the OLE channel.
3. To investigate the channel capacity of the OFDM-based OLE communication system.
4. In order to increase the performance of onboard train communication, a combination of in-train broadband PLC and OWC services of the VLC systems is developed.
5. To derive analytical expressions for the overall capacity and outage probability of the cooperative relay-based systems, to help the author investigate the effect of certain system parameters on its performance.
6. To investigate the performance of a relay-based VLC system, as a last-metre of in-train communication technology, in terms of outage probability and energy consumption.

1.3 Research Contributions

In this thesis, several novel contributions have been made and are detailed below:

1.3.1 First Novel Contribution

Passenger demand for high-speed data access while travelling on a railway requires the provision of appropriate services. This contribution investigates the possibility of using the OLE as an access network to connect trains with core communication networks. The ABCD transfer line function model for the OLE channel is evaluated using computer simulations. In order to implement this model, an equivalent circuit for the whole system was derived using certain simplifying assumptions regarding the train electrification system. Equations that consider the acceleration and deceleration of the train are used to update the train position which represents the length of the transmission line. A simulation of OLE system using the actual channel response of the developed model is implemented using OFDM as the modulation scheme. The development of such a model can help in setting the basis for computer simulations which would help in any comprehensive study of the performance of a proposed system. It is worth pointing out that this model was not validated by practical measurements, which represents the major limitation of this contribution. This contribution is presented in Chapter 3 and has been reported in [15].

1.3.2 Second Novel Contribution

Reliable data transmissions offering better mobility to the end user can be achieved by integrating different communication systems. However, using the pre-installed infrastructure of in-train electrical wiring networks gives the opportunity to use PLC as a backbone for VLCs onboard the train. This contribution is the investigation of the performance of a cascaded in-train PLC/VLC system in the presence of amplify-and-forward (AF) and decode-and-forward (DF) relays. The major contribution resides in deriving analytical expressions for the ergodic capacity and the outage probability of the proposed hybrid PLC/VLC relay-based system. Formulating the overall capacity and outage probability of the proposed PLC/VLC system offers the opportunity to designers and engineers to examine the performance of such systems as well as to study the effect of the various system parameters on the system performance. However, the practical implementation of such a cooperative system is considered as one of the main limitations of this contribution. This contribution is introduced in Chapter 4 and has been reported in [16, 17].

1.3.3 Third Novel Contribution

VLC is a last-metre access technology that is predicted to play a crucial role in indoor applications including in-train communications. However, line-of-sight (LoS) is a requirement for efficient data transmission in VLC, but this cannot always be guaranteed

with in-train applications for a variety of reasons, such as moving commuters/train operators and the layout of the in-train environment. The relay-assisted VLC system is one of the techniques that can be used to address this issue and ensure seamless connectivity. This contribution investigates the performance of a half-duplex (HD) conventional DF relay system and cooperative systems (i.e., selective DF (SDF) and incremental DF (IDF)) over VLC channels in terms of outage probability and energy consumption. Analytical expressions for both outage probability and the minimum energy-per-bit performance of the aforementioned relay systems are derived. The derived expressions will allow designers and engineers to optimize VLC network parameters, including number of relays in the network, distances between relays, as well as the optimum relay protocol for specific systems. It should be highlighted that a key limitation of this contribution is the assumption of the perfect channel estimation. This work is presented in Chapter 5 and has been reported in [18].

1.4 Thesis Structure

This thesis is divided into six chapters. After the introduction, the chapters are focused to answer the research questions. The thesis is organised as follows:

Chapter 2 covers the key literature review and the relevant theoretical background regarding the concepts and challenges of to/in train communication.

Chapter 3 considers the OLE as an access network connecting trains to the public networks. The ABCD transmission model is used to represent the transfer function of the OLE channel. Furthermore, a simulation of OLE system is implemented using OFDM as a choice of modulation scheme.

Chapter 4 presents a comprehensive performance analysis of different in-train cooperative communication systems in the presence of AF and DF relays. The performance of the proposed in-train hybrid systems is evaluated in terms of the average capacity and the outage probability. Mathematical methods are developed for these networks to formulate the capacity and the outage probability by exploiting the statistical properties of the channels of the proposed systems.

Chapter 5 investigates the performance of HD conventional DF relay system and cooperative SDF and IDF over the last-metre access VLC channels in terms of outage probability and energy consumption. It also studies, analyses and compares the performance of single-hop and multi-hop scenarios. Analytical expressions for both outage probability and the minimum energy-per-bit performance of the aforementioned relay systems are derived.

Chapter 6 contains the conclusions which summarise the results achieved in this work. It also introduces possible future work.

Appendix A contains the Matlab codes which are used in this thesis. The road map of this thesis is shown in Figure 1.1.

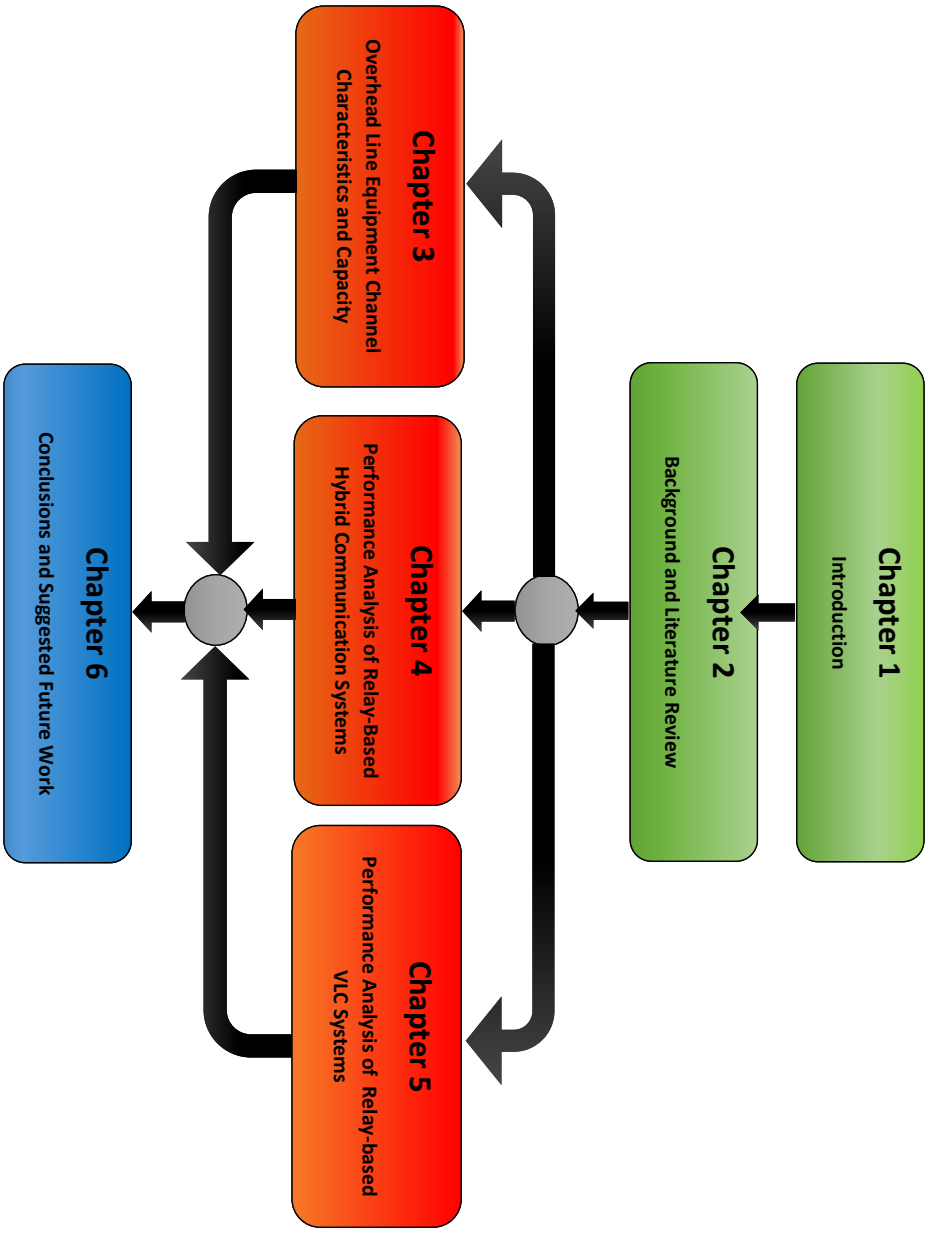

Figure 1.1 Structure of this thesis.

Chapter 2

Background and Literature Review

This chapter presents a brief history of railway communication and the existing communication systems and their challenges are analyzed. In addition, communication inside trains and how signals can be distributed on-board and between the train coaches are discussed. The chapter also reviews the relevant literature to provide an appropriate background to/in train the communication topics important for this thesis. It also presents an overview of relevant previous research areas.

2.1 Introduction

The quality of the railway services has been improving, especially since the use of high-speed trains started. However, a number of critical challenges associated with this highly efficient form of transport in terms of technology, industry; and environment still need to be overcome. For example, to ensure customer safety and satisfaction, and the efficient handling of the rapid increase in traffic, reliable communication systems to/inside trains are required. Railway operators have used different ways of communicating, such as the second-generation communication system, also known as the global system for mobile (GSM) communications, and the third generation mobile telecommunications (3G) [1].

These HSR communication systems have a foreseeable end to their working lives and the need for reliable communication that can meet the incredible growth in the railway system is unavoidable. Therefore, the service providers have started evaluating a best candidate to replace current HSR communication systems. Some issues that should be considered when selecting a suitable system to fulfil the requirements of HSR operations are: performance, service attributes, frequency band and industrial support. Different communication systems, such as 4G and 5G have been included in the assessment of the future HSR communication system. However, as the 5G system is currently not available, the established 4G network which has been subject to long term evolution (LTE) is likely to be the best candidate for the upcoming generation of HSRs [2, 3, 19].

A considerable number of UK workers and students spend an hour or more per day commuting by trains to and from work. Ther are different activities that commuters often do while travelling including listening to audiobooks and podcasts and watching TV and movies. This can be achieved using a reliable in-train communication system. Communications inside train coaches can be provided by connecting the train to a public network then a reliable distribution system can be used inboard for signal distribution within the train [9]. Different distribution systems can be adapted to distribute signals within the train. The wireless local area network (W-LAN) interface option popular with current communication devices is one of the best distribution systems available for inside trains [10]. This technology is inexpensive, and W-LAN, femtocells or repeaters of mobile communication standard can be easily installed inside the coaches to boost network coverage and improve the performance of the system [10].

PLC is another candidate for in train communication. This can be used to achieve broadband services between interconnected coaches. The principle of PLC is based on the use of the existing power lines in a buildings, utility grid or vehicles to carry data and electricity, simultaneously [20, 21]. This technology has been around for some decades, but it has only been used for limited applications as described in Chapter 1. However, only a limited number of studies have been carried out so far concerning

broad-band PLC (BB-PLC) inside trains, particularly on PLC channel characterization [11, 22, 23].

Mobile phone and laptop users can also enjoy broadband services using visible light communication (VLC) which has recently matured.Some light sources have advantages that have enabled VLC technology to be used in various indoor and outdoor applications [24–26]. LEDs are a light source that can enhance the energy efficiency, and life expectancy, and lower the maintenance costs when using VLC technology [13]. However, some technical issues are to be studied before the full deployment of this technology [12].

In this chapter, a brief history of railway signalling and communication based train control operation is provided. An overview of railway communication systems, including their limitations is also provided. Furthermore, comparisons between public networks and railway networks are made, with a survey of communication systems which can be used to distribute signals inside and between train coaches.

2.2 Research Gaps

This chapter has reviewed current railway communication systems and the candidates that might replace them together with their limitations. The chapter has also scrutinized the literature to obtain an insight into how signals can be distributed inside trains. In this regard, this chapter has provided an overview of the results of previous researchers and the gaps left by existing work.

- To Train Communications

  The demand for access to high-speed data and broadband internet as part of the railway infrastructure is increasing, and the need to find a suitable communication system that meet these requirements as part of HSR operation is necessary. This chapter suggests using the OLE as an access network to connect trains with backbone communication networks. However, the literature review did not find any study that has considered this as a medium for communication. Therefore, channel modelling and characterization is required to investigate the possibility of using the OLE as a communication medium. The development of an appropriate channel model of the OLE can help in setting the basis for computer simulations which would help in any comprehensive study of the performance of a proposed system.

- In Train Communications

  Providing reliable network coverage and seamless communication to the train commuters is essential for service providers. However, offering more reliable

data transmission and better mobility to the end user can be achieved by integrating different communication systems. Using the pre-installed electrical wiring infrastructure gives the opportunity to use PLC as a backbone for VLCs. Relays are normally implemented for better performance and to tackle the technical issues of improving both networks. It is believed that only few researchers have studied the performance of cascaded PLC/VLC links in the presence of AF and DF relaying protocols in terms of average capacity and outage probability, and a comprehensive study of the implementation of AF and DF relays to connect PLC and VLC links is required. However, such a study requires deriving analytical expressions for the ergodic capacity and the outage probability of the proposed hybrid PLC-VLC relay-based system. This will require investigating the performance of such systems as well as examining the effect of various system parameters on system performance.

LoS is a requirement for efficient data transmission in VLC, but this cannot always be guaranteed in indoor applications for a variety of reasons, such as moving objects and the layout of the indoor environment. The relay-assisted VLC system is one of the techniques that can be used to address this issue and ensure seamless connectivity. However, while relays can enhance the performance of communication systems increasing the number of relays increases total energy consumption of the system. Despite the considerable amount of published work in this area, it is believed that no work in the open literature has provided a comprehensive performance analysis of multi-hop VLC systems in terms of outage probability and energy-efficiency.

2.3 To Train Communications

2.3.1 Brief on Railway Communications

The survey of railway communication and its development starts from the first purpose-built passenger-carrying railway with haulage by locomotives on the Liverpool and Manchester Railway, opened in September 1830 [27]. The signalling systems were totally human-based. The guide-ways were divided into different sections, each section of about two miles, where a railway policeman was in position to give hand signals to train drivers. In the1890s, for single line track the electric token system was used instead of telegraphic orders [27] as a practical means of determining the presence of a train at a certain location. The demand for rail transport in Europe increased for many reasons including population growth, increased urbanisation, and trains being a more comfortable, faster and safer means of land transport, as well as being more energy-efficient and environmentally friendly [28–30]. This growth needs a more

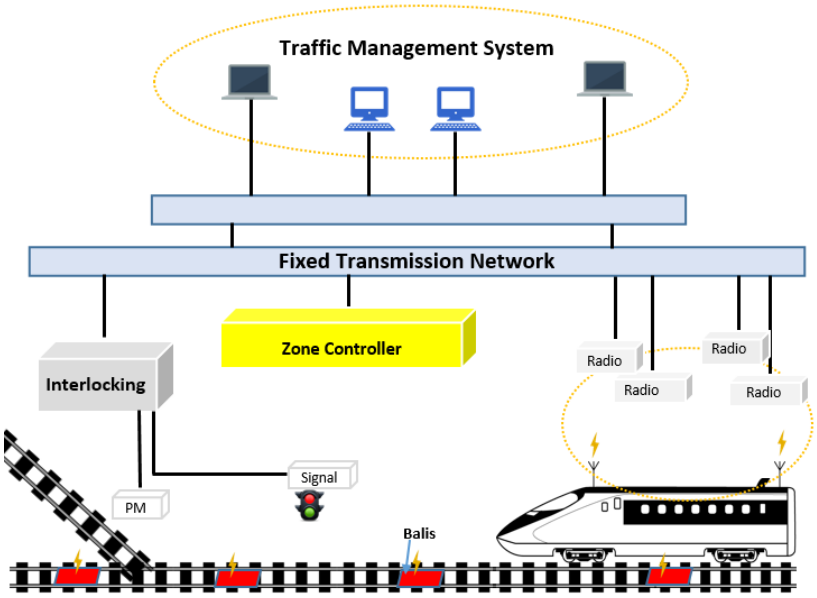

Figure 2.1 CBTC system overview.

modern communication-based signalling system to be installed compared to previous decades [31, 32]. Radio communication systems are the first choice of some operators as they offer high resolution and real-time train control information, while minimising the amount of track-side equipment and increasing the capacity of the track by reducing the safe distance between trains [33–35].

Communications-based train control (CBTC) operation uses high capacity radio communication for train control information exchange between train and wayside [36]. A combination of devices is used in CBTC systems to determine the train speed and location; including transponders ("balises"), tachometers, Doppler radar, speedometers, odometers, and geolocation systems such as GPS [37]. Figure 2.1 presents a CBTC system overview. Real-time information exchange, provided by CBTC systems, explains why these systems have replaced the conventional ones. Using this system reduces the headway distance between trains thus increases the capacity of the line while decreasing the amount of track-side equipment as required by the previous system, for instance, colour light signals and track circuits [32]. In contrast to the fixed blocks that were used to separate the trains in previous signalling systems, moving block operation is used in CBTC systems. As the location of the train is continuously corrected and updated, the occupancy block moves with the train with no fixed boundaries, and this permits trains to move in closer proximity. However, the main problem of using GPS is detecting the precise location of each when two trains are moving very close to each other. Also, CBTC suppliers cannot rely on satellite signals inside tunnels. Moreover, GPS is controlled by an external authority which makes the CBTC suppliers hesitant about relying on such a system and its use in CBTC systems is supplementary.

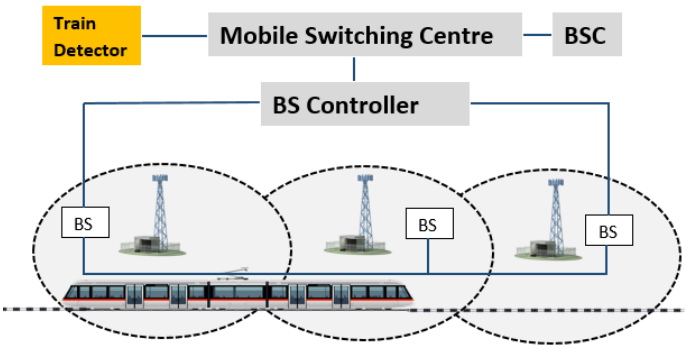

Figure 2.2 GSM-R system architecture.

GSM-R is an internationally agreed standard for wireless communication which has been introduced by European rail companies to replace the previous railway communication systems to ensure that trains can safely travel to different countries without any communications issues [38]. GSM-R mobile technology is a radio network which provides radio coverage for both passengers and train crews. In this system, the communication is secure as the coverage of the rail network is thorough, including deep cuttings and tunnels [39]. GSM-R and GSM systems are basically the same but GSM-R has railway specific functions based on European Standards [1]. Table 2.1 shows some parametric differences between GSM and GSM-R. Dedicated base stations (BSs) are installed beside the railway track to configure the GSM-R system. The BSs are linked together in groups and controlled by base station controllers (BSCs) which provide connections between the BSs and the mobile switching centres (MSCs) [40]. The GSM-R system architecture is shown in Figure 2.2. Handover is the most crucial issue that can affect the quality of service (QoS) in GSM-R systems [41]. The small area covered by each BS and the high mobility of the trains make the handover process in GSM-R systems different and more difficult than for GSM systems. This also increases the number of handovers during one voice call or data transmission [42, 40]. The growth of both GSM-R and public networks has increased the electromagnetic (EM) interference between the two networks [1]. The second source of conducted and radiated EM interference is caused by the arcing between contact wire and pantograph during the current collection process [43]. This is a common phenomenon in electrified railway systems that predominantly occurs at higher speeds and loads.

Capability is considered another challenge to the GSM-R system. An insufficient transmission rate and system delay can hardly support real-time applications and emergency communications [44]. Even though GSM-R continuity is ensured for the next few years, due to the above-mentioned limitations, the need to switch to another system which can overcome these limitations is necessary. At the current time LTE-R based on LTE standards might be the preferable candidate to replace the GSM-R system [45]. The deployment of LTE-R systems can improve the performance of the HSR communication

Table 2.1 GSM and GSM-R parameters.

Parameter	GSM	GSM-R
Up-link frequency	890-915 MHz	876–880 MHz
Down-link frequency	925-960 MHz	921–925 MHz
Bandwidth	850-1900 MHz	0.2 MHz
Modulation	GMSK	GMSK
Cell range	35 km	8 km
Data transmission	Requires voice call connection	Requires voice call connection
MIMO	No	No
Mobility	-	Max. 500 km/h

systems in terms of capacity and capabilities as it uses a fully packet-switched-based network [44]. Furthermore, LTE is a well established and off-the-shelf system that can coexist with the previous HRS communication systems, thus LTE-R is predicted to last for some time which strongly supports the move from GSM-R to LTE-R [1].

Compared to the GSM-R system, LTE-R system offers a high data rate of up to 50 Mbps for the down link, and 10 Mbps for the up-link. The optimal use of the frequency and spectrum of LTE-R is vital to provide a reliable and efficient communication system for HRS. Currently, 1 GHz, such as 1.8, 2.1, 2.3, and 2.6 GHz are the bands where most LTE system operate [1]. However, the first LTE-R network, which is based on LTE standards, is already scheduled to take place in some countries in the coming few years [1]. In this regard, some preliminary recommendations have been issued by the International Union of Railways, an industry-wide advisory body, on the feasibility of using standard LTE as the replacement for the current railway communication system [44]. Although the LTE capacity is less than the reliability in LTE-R, the LTE-R cell can serve 27 trains simultaneously at one of the main train stations and the capacity provided by the cell is enough to serve more trains at the same time [46]. Trains on the LTE-R network are supposed to be able to operate at a very high speeds, up to 500 km/h, sometimes in very complex railway environments. Table 2.2 shows some parametric differences between LTE and LTE-R.

The coexistence of the LTE public safety network and the LTE-R network is one of the problems associated with the deployment of LTE-R. Public safety networks, such as police, firefighters and the ambulance service, and LTE-R networks use the same frequency bands: 718-728 MHz for up-links and 773-783 for down-links [47]. Thus, a major challenge is how to eliminate radio interference between the networks in order to maintain reliability and safety [47]. The high speed of trains leads to a Doppler shift, which is a shift of the received frequency and, in some cases, this might lead to a phase shift of the signal which will impair reception of angle-modulated signals. Another major challenge is the handover process. LTE-R systems are meant to support

Table 2.2 LTE and LTE-R parameters.

Parameters	LTE	LTE-R
Frequency (uplink and downlink)	800 MHz, 1.8 GHz, 2.6 GHz	450 MHz, 800 MHz, 1.4 GHz, 1.8 GHz
Bandwidth	1.4–20 MHz	1.4–20 MHz
Modulation	QPSK/M-QAM/OFDM	QPSK/16-QAM
Cell range	1–5 km	4–12 km
Maximum mobility	350 km/h	500 km/h
MIMO	2x2 and 4x4	Only 2x2
Data transmission	Packet switching	Packet switching (UDP data)
Handover procedure	Hard and soft	Soft

high-speed trains, where the high speed and the small area covered by each base-station lead to increasing the number of handovers between the cells in LTE-R networks [42].

There are other challenges which should be taken in consideration when designing LTE-R systems such as a possible large Doppler spread which can cause signal-to-interference plus noise ratio degradation and corruption. Also, delay spread which can lead to a loss of orthogonality between the OFDM sub-carriers and a special category of guard interval. Linear coverage with directional antennas is used in railway communication systems [1] because this type of coverage consumes less power and generally provides better performance, however at some train locations outage probability can be high due to shadow fading [1]. Because of these limitations and the requirement of high-capacity communications for passengers travelling on the next generation of railways, it is necessary to find an alternative technology to current railway communication systems. Providing the required services means focusing on QoS, reliability and capacity as the principal issues of candidate technologies.

The extremely wide frequency bandwidths as have been well studied for 5G technology applications can solve the issue of shortage of available frequency bands. However, 5G technology is not yet in its final form which may not be finalized for sometime. This technology with its high-data transmission rate is expected to play a crucial role in applications that require more reliable and low-latency communication such as intelligent transportation systems. The 5G networks will be built upon the existing wireless systems including 2G, 3G and 4G and it aims to retrofit the architecture of the current communication systems (i.e., 4G) [48]. 5G networks can benefit from the current investment of the 4G networks and will expand their capabilities provided that 5G is interoperable with 4G and delivers the desired performance for railway communications.

Latency is one of the items that have been improved in 5G technology which can help enable functions that require a quick response, such as auto-driving trains. The new technologies that are implemented by 5G will reduce the 70 ms data transmission latency in 4G down to 1 ms. The millimeter wave technology used by 5G makes its spectrum bandwidth greater than those of existing technologies and enhances the speed of data transmission while offering better connectivity between train and wayside [48]. For example, the available bandwidth of the 5G networks is 9 GHz, while only 100 MHz of spectrum bandwidth is available in 4G-LTE networks. The targeted data rate of 5G technology is 20 Gbps, which is achievable with its recommended bandwidth and the implementation of massive multiple-input-multiple-output (massive-MIMO) [48].This makes 5G technology more reliable for use with railway communication than current communication systems.

Even though 5G technology seems to be the best candidate for upgrading existing railway communication systems, there are a number of challenges to consider. First, self-interference cancellation. Looking at the fundamental nature of 5G technology, self-interference can have a considerable effect on 5G networks [49]. Secondly, the power consumption of the overall system. As 5G networks utilize a larger bandwidth than current technologies, which means a higher data rate, more energy will be consumed for data transmission [50]. Furthermore, in multi-Gbps communication networks, data transmission is restricted by the characteristics of data propagation. It has been reported that a very-high path loss and attenuation are associated with high frequencies. This could be compensated by either increasing the transmit power or the gain of the receiving antenna [50]. Moreover, due to the nature of waves with a wavelength of millimeters in a railway environment, the transmission can be easily blocked or shadowed [51].

2.3.2 Overhead Line Equipment

With the greater accessibility and increase of video content on the internet, most people opt to use their smart gadgets while travelling. Most of the time, speed of internet plays the spoilsport and consumers demand an ever higher data rate and more reliable communication system from service providers. The drive to satisfy the demands pushes the entire industry towards finding a communication system that can deliver these requirements. The idea of utilizing power cables for both electricity and data transmission has been around for decades, and PLC is a key technology for the last-mile communication that enables sending data over existing low-, medium-, and high-voltage (LV, MV, HV) electricity cables. According to the frequencies used in the system, PLC technology is divided into narrowband PLC (NB-PLC) and broadband PLC (BB-PLC), where the former works at lower frequencies and the later at higher frequencies.

The distinct advantage of this technology is the widespread availability of electrical infrastructure that makes it very cost-effective [52].

OLE are considered as MV transmission lines and MV-PLC is used in several applications such as network management optimization and operational services [8]. Several studies have demonstrated that the signal sent over PLC can be transmitted over a long distance without causing any interference to the other communication technologies [53–55, 4]. In addition MV-PLC can provide reliable transmission and is a key technology that gives the opportunity for OLE systems to be used as an access network connecting trains to the backbone communication networks. The main superiority of the OLE system is that its use can save the cost of establishing a new channel because the OLE systems are already installed all over electrified railways. Furthermore, it can be installed as a complementary network to current railway communication systems to cover "holes" in their coverage, particularly in tunnels and remote areas.

2.3.2.1 Channel Modelling

For system implementation and performance evaluation purposes, the channel transfer characteristics of the OLE ought to be fully studied. One of the major challenges is that of developing an appropriate model of the OLE. Finding such a model that can represent the transfer characteristics of the main network in computer simulations can enable analysis of the performance of different network configurations and loads. However, several models are proposed in the literature, of these the multi-path and two-port network are the most relevant for PLC channels [56–58]. In contrast to these two models, the behaviour of the PLC network in most other models requires a large number of distributed components so their practical value is usually very limited. All network components (cables, joints, connected devices) should be known in detail in order to construct the models and obtain precise results. Practically, it is not possible for the required parameters to be determined with precision [59, 60].

Multi-path Model Multi-path Model The transmission function in the multi-path model is described by the delay portion of the path, the attenuation portion which increases as the length and frequency increase, and the weighting factor representing the transmissions and reflections that occur along the path, as presented in Equation (2.1):

$$\underline{H}(f) = \sum_{i=1}^{N} \underbrace{|g_i(f)|}_{\text{weighting factor}} e^{\varphi_{gi}(f)} \underbrace{e^{-(a_o + a_1 f^k) d_i}}_{\text{attenuation portion}} \underbrace{e^{-j2\pi f \tau_i}}_{\text{delay portion}} \tag{2.1}$$

where d_i is the path length, $|g_i(f)|\, e^{\varphi_{gi}(f)}$ represents the weighting factor, $e^{-(a_o + a_1 f^k) d_i}$ is the attenuation, and a_o and a_1 are the attenuation parameters with a typical value of

the attenuation exponent factor, (k), between 0,5 and 1. $e^{-j2\pi f\tau_i}$ represents the delay portion, with (τ_i the delay of the path. N is number of paths and i is the path number, where the path with lowest delay has i =1. Equation (2.1), is simplified in [60], to

$$\underline{H}(f) = \sum_{i=1}^{N} \underbrace{g_i}_{\text{weighting factor}} \underbrace{e^{-(a_o+a_1 f^k)d_i}}_{\text{attenuation portion}} \underbrace{e^{-j2\pi f(d_i/v_p)}}_{\text{delay portion}} \tag{2.2}$$

where v_p is the ratio between the speed of light and the square root of the dielectric constant of the insulating material.

In [60], the simulated results based on the given model in Equation (2.2), were compared to practical measurements for a specific network topology and well-known number of paths and geometric dimensions. The results were very promising as the simulation results matched the measured ones for a specific range of frequencies. However, the simulated results did not match the measurements at other frequencies, which is a major disadvantage of this model. Another disadvantage is that a large number of paths with particular weighting factors and lengths must be known for sufficiently precise results to be obtained.

Two-port Network Model The channel transfer functions of a two-port network can be conveniently represented by ABCD matrix theory [61]. The power line is a two-port network that connects a transmitter at the sending end to a receiver at the other end. This two-port network can be considered as a black box that has input and output related by a transfer function. The relation of output to input values for this network is highly dependent on the physical properties of the power line. The transmission over the power line is characterized by losses due to parameters which are assumed uniformly distributed along the power line. These primary parameters (i.e., resistance (R), capacitance (C), inductance (L), and conductance (G) are length-dependent parameters and can form a relation between the output and input voltages, and current through the power line in terms that represents the transfer function of its channel.

The two-port Network Model is widely used in PLC technology as it can represent the channel transfer function (CTF) of LV-PLC and MV-PLC systems [57, 62]. The authors in [57], calculated the transfer function for a PLC channel based on actual parameters, and results from a practical measurement were also provided. Calculated and measured results were in perfect agreement. The authors of [62] developed the two-port network model to calculate signal transmission characteristics over a PLC network where the PLC modems were installed at random locations. Measurement results were provided to evaluate the model-based results. They found that the ABCD matrix model can effectively represent the transfer function of the PLC channel. Considering the

transmission theory of the power line, the two port-network was used by [63] to study the transfer function of an in-home broadband PLC (BPLC) network. Different network configurations (i.e., different loads, different network branches, and different power line lengths) were considered. Measurements made on the actual PLC network were used to verify the simulated results. It was found that the two-port network theory can accurately reflect the effects of the physical parameters of the PLC.

2.3.2.2 Modulation Schemes for PLC

Although MV-PLC presents an interesting solution for higher bit rates, there are technical limitations and constraints to be considered [64]. Signal reflection due to impedance mismatching is recognized as one of the major technical limitations of MV-PLC systems. This occurs at locations of impedance change on the network. Noise over the MV-PLC is the second technical issue that affects data transmission [65]. This is strongly weather dependent and it is caused by the high voltage power line being subjected to switching and power-line faults [64]. The noise level varies and is most significant during very cold weather. Noise also can be caused by interference generated by adjacent electronic equipment operated in the same frequency domain and can destroy a set of transmitted data [64, 66].

The transmission over MV-PLC is significantly affected by weather conditions, such as, rain, fog, snow and ice [67]. Ice is the weather condition, which can most severely disturb the communication over MV-PLC. Attenuation is affected by the ice coating on the lines and it can increase or decrease depending on the operating frequency. Generally, MV-PLC is characterized by relatively low attenuation, which increases as the distance between the transmitter and receiver increases, and as frequency of the signal increases [67]. The high level of electromagnetic interference due to equipment near the PLC system, and which might cause a malfunction of electronic devices is another issue. However, various advanced modulation techniques, such as OFDM, code division multiplexing access (CDMA), and multi carrier-direct sequence-code division multiplexing have been used with PLC systems in order to tackle such technical issues [68].

While the CDMA technique is normally used to reduce Electro-magnetic interference (EMI), OFDM can be used to reduce the effect of noise over PLC and the frequency selectivity of the PLC channel. Earlier works have proved that PLC systems that are based on OFDM are less affected by noise [69–73]. In addition, OFDM is a very efficient and flexible method that is at the heart of PLC standards in use today. The main purpose of choosing this technique is due to its simplicity in implementation and its ability to provide a sufficient improvement in the performance of the PLC systems. Furthermore, it is less sensitive to noise compared to single carrier applications. This is due to the discrete Fourier transform (DFT) operation that is implemented at the receiver,

where the impact of noise is spread among multiple transmitted OFDM subcarriers, therefore, the longer the OFDM duration, the less the effect of noise [74]. However, when the amplitude of the noise is relatively high, noise mitigation techniques ought to be implemented [70].

Much work has been carried out to reduce the effect of noise using multicarrier modulation (MCM). For example, the effect of noise on OFDM systems in radio communications was first analyzed in [74] where a closed-form expression for the probability of error was derived for two different scenarios, namely, single-carrier (SC) and MCM. It was found that MCM outperforms SC systems, especially when the noise power is moderate, and the probability of occurrence of noise is not too high. This was explained as follows: the effect of impulsive noise gets spread over several data symbols in the case of MCM systems whereas in SC systems, the impulsive noise will affect only one symbol. However, this advantage can turn into a disadvantage if the energy of the impulsive noise exceeds a certain level, but this study did not consider the effect of the channel. In [75], the Bit-Error-Rate (BER) performance of OFDM systems and the effect of multi-path PLC channels were investigated by means of computer simulations. In [76], the BER performance of such systems under the effects of impulsive noise and multi-paths was analyzed theoretically and closed-form formulas were obtained. It was concluded that the adverse effects of multi-path over PLC channels can be more serious than just that of impulsive noise.

Another mitigation technique is proposed in [71] where a nonlinear device was placed at the front end of the OFDM receiver. This technique is simple and easy to implement and for these reasons is widely used in practice. There are three different types of nonlinear preprocessors: blanking, clipping and combined blanking and clipping (hybrid) whose basic principles are discussed below. These are also referred to as time domain mitigation techniques. Any OFDM sample that has an amplitude lower than a specific threshold passes without modification of its amplitudes as it is considered as a clear OFDM signal. On the other hand, OFDM samples with amplitudes above the threshold are clipped or replaced with zero depending on the technique used [69]. OFDM is also broadly used as the prime transmission method in most PLC applications for its capability to resolve the frequency selectivity of the PLC channel [77]. Furthermore, due to the long symbol duration in OFDM, inter-symbol interference caused by the multipath effect of the PLC channel is reduced and can be completely eliminated by utilizing a cyclic time guard. OFDM transmission over OLE channels is presented in Chapter 3.

2.4 Inside Train Communication

For inside train communication the required connection can be made in two different scenarios. In the first scenario, electronic devices can be connected to the communication network individually. In this scenario, transmission to the mobile devices is highly attenuated by the metallic coating of coaches, particularly modern ones. Furthermore, such communication suffers from the Doppler shift due to the high speed of the train and the high transmission frequency of the wireless networks [78]. In most of the cases, the second scenario is preferable. In this scenario, the train is connected to a public network then the signal is distributed inside the train coaches using a suitable distribution system [78].

Dedicated wireless networks, such as GSM-R and LTE-R, are used to provide trains with different communication services. These two networks are dedicated particularly to support HSR by providing specific information that can help monitor and control rail traffic and thus eliminate train accidents [78]. However, the public networks, such as GSM and LTE are designed with specific cells overlapping. This overlapping is large enough to permit a full handover procedure between two neighbouring cells in the HSR system. The main issue of the public networks is that they do not provide a network coverage for the entire railway system. Particular areas, such as remote areas and areas near to tunnels and bridges usually suffer from "holes" in the public network coverage. This is because of the lack of customers in such areas so that public operators do not install equipment there. Recently, HSR operators invited the public network operators to provide communication services in such places [78].

The reliability of in-train communication systems in the second scenario depends on two parameters, the receiving equipment and the distribution system inside the train. Generally, a roof-mounted antenna fixed on the train works well as a receiver. Various communication systems can be used for signal distribution within the train coaches. W-LAN can be installed in each coach to distribute signals to the passengers‘ user equipment (UE) [79]. Furthermore, the VLC technology that has recently matured is predicted to play a crucial role in the railway industry [12]. PLC systems have been used for many different indoor applications and can be used for distributing the signals inside the train using pre-installed power lines [11]. The main issue with PLC systems is that mobile users may not have access to the power lines. In such cases, cooperative PLC/wireless or PLC/VLC are options. The following section discusses how signal can be distributed within the train.

2.4.1 Wireless Access Point

As previously mentioned, electromagnetic waves are significantly attenuated by the metallic shielding provided by the mild steel outer surface of the coaches. For this reason, communication between UE on-board and the public networks outside the train can be improved by using a roof-mounted antenna to communicate with the public networks. Then a central distribution system can be installed inside train coaches to communicate between the UEs on-board and the roof-mounted antenna. Almost all modern electronic devices have a W-LAN interference so they can use this system for communication purposes [78]. This system has sufficient data rate to offer different services, such as internet access and entertainment services to HSR commuters [80].

The W-LAN system can be installed either in each coach of the train or as one system serving all coaches. However, if the former configuration is installed, then a receiving device (i.e a roof-mounted antenna) is needed in each coach to communicate with the on-board W-LAN and the base stations of the public networks. On the other hand, only one receiving device is needed if the latter configuration is installed. Then the connection between any two neighbouring coaches should be wireless to ease the assembling of coaches into a train at the terminus. As mentioned above, a receiving device is located in each coach or only in one coach depending on which way the WLAN system is installed [79]. This device will be responsible for connecting the W-LAN in the train with the outside communication systems. The receiving device should support LTE modem type of functionality and a wire-line to be able to communicate with both external and in-train systems, respectively [79]. Figure 2.3, shows W-LAN system inside a train coach.

Another installation design is to attach receiving devices to the roof of the first and the last coaches of the train. This installation offers commuters high-capacity access to public networks and reduces the fixed infrastructure requirements [81]. Furthermore, both of the receiving devices are able to distribute the signal inside all of the train coaches. If one of the receiving devices is outside public network coverage the other is still communicating between the UE on-board and the public network. This is particularly useful in areas that suffer from small “holes” in the public network coverage, such as short tunnels and bridges [81].]. For all of the above-mentioned installations, although the train can be moving at high speed and passenger equipment are similarly moving relative to the fixed base stations of the public networks, the user equipment is stationary relative to the in-coaches WLAN system [78]. Of course, different W-LAN types such as Wi-Fi and wireless gigabit (WiGi) can be installed inside train coaches for signal distribution.

The Wi-Fi is a well-known cost effective W-LAN technology with Wi-Fi IEEE 802.11 the main standard [82]. The allowed achievable throughput of this technology is

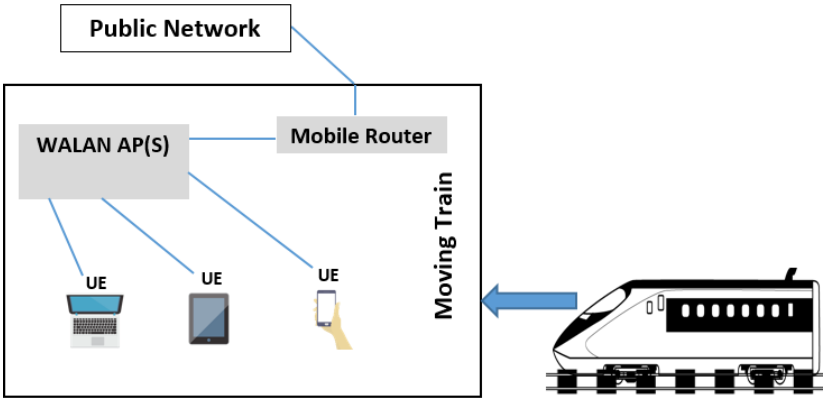

Figure 2.3 W-LAN system inside a train coach.

450 Mbps on both available frequency bands (2.4 and 5 GHz). However, amendment IEEE 802.11n refers to the use of multiple-input-multiple-output (MIMO) technology to increase transmission rates and the bandwidth, due to the aggregation of channels, is increased from 20 MHz to 40 MHz [82]. However, a more recent Wi-Fi standard which was first authorized in 2013 is Wi-Fi IEEE 802.11ac [83]. 500 Mbps is the achievable theoretical throughput of this standard and a 7 Gbps of throughput can be achieved by implementing the MIMO and multiplexing techniques [83]. Although the Wi-Fi technology has a larger transmission range than Wi-Gi, the latter provides better throughput.

Recently, millimeter wave technology, Wi-Gi, has gained researchers‘ attention due to the 6 Gbps of throughput it offers its users. Wi-Gi is commonly known as IEEE 802.11ad [84, 85]. Both bodies, the Wireless Gigabit Alliance and IEEE 802.11ad, have agreed an industrial standard for Wi-Gi which that was issued by IEEE in late 2012. The main aim of this technology is to transfer a high-volume of data with a throughput of around 7 Gbps over a relatively short range. It operates at 60 GHz frequency with 9 GHz bandwidth from 57 to 66 GHz which makes the 7 Gbps of throughput achievable [84]. In addition to the high-speed data rate offered by Wi-Gi, it also provides secure and protected transmission over short distances with low latency [83].

The main issue of this technology is its very limited transmission range, typically 1–10 m, due to its short wavelength, transmission is severely affected by the path loss, which can be as high as 28 dB [83, 85]. However, this loss can be compensated by increasing the gain of the antenna. This leads to a narrower antenna beam width, which will consequently require antenna beam forming. Omni-directional antennas were used by the previous IEEE 802.11 main standard as this was not considered an issue [83]. An extensive study was carried out by the authors of [85] on planning and formation of Wi-Gi networks. Two different network scenarios were investigated in order to extend the coverage of the Wi-Gi network. It was concluded that the performance of the Wi-Gi

network is affected by different parameters, such as network-load, and the percentage of intra-LAN and internet devoted network traffic.

2.4.2 Visible Light Communication (VLC)

One of the most significant current discussions in OWC technologies is light fidelity (Li-Fi) technology. This green technology is predicted to play an essential role in indoor communication applications. Instead of using radio frequencies, short-range Li-Fi technology is based on the implementation of VLC. However, this technology is seen as a complementary wireless technology to radio-frequency (RF) [86]. Light emitted from low-cost, energy-efficient LEDs is the transmission medium which makes its potential implementation complex, but this is compensated for by its cost being very low [16, 87, 26]. Li-Fi technology is better in terms of data exchange security compared to RF, because hackers cannot gain access from outside the line-of-sight (LoS) of the propagating light [87]. Furthermore, this technology offers better performance than that provided by the RF technology. This is because of no electromagnetic interference, high transmission power and the wide frequency spectrum available [88].

As other communication systems, VLC contains three main components, namely transmitter, transmission medium, and receiver. In general, any light source can be utilized as a transmitter. However, energy efficient LEDs are predicted to replace other light sources in future [12]. White LEDs (WLEDs) are one of the best light sources suited to VLC and can be used for illumination and data transmission simultaneously [89]. Typically, this light source has a longer lifespan compared to other sources such as incandescent bulbs [90].This short-range technology uses the portion of the electromagnetic spectrum, which can be seen by the human eye, with wavelengths from 390nm-to-750nm as the transmission medium [91]. At the receiver, a photo-diode detector, the received signal is converted from light into an electrical signal which is then demodulated to provide the desired information [12, 92].

This fast-growing technology can offer a wide range of support services to railway operations: internet facilities (inside trains and underground stations), smart lighting inside train stations, and improving railway safety [12]. In trains, LEDs can be equipped with transceivers to provide different multimedia facilities and internet services to train passengers [12]. Furthermore, using LEDs for providing internet services inside underground stations can help to tackle the lack of connectivity issue that faces passengers in such areas. Moreover, due to the distribution of light sources inside, for example, train stations, they can ensure seamless connectivity to the people who are on the move and they can be used for in-station positioning and venue navigation [12].

A number of technical issues need to be studied before this technology can be fully implemented by the railway industry. First, the area covered by each LoS of

an LED is relatively small. This is because of the rectilinear propagation of light requires frequent horizontal handovers when a passenger is moving, which might be a source of instability in data reception [16]. During the handover process, the user changes the information with a central unit (CU) which can take up to 3000 ms, this leads to a transmission loss [93]. Furthermore, there will be light interference due to overlapping with other neighbouring light sources and sunlight [12, 94]. However, different techniques are proposed in the literature for reduction of such interference [95–97]. For example, authors of [95] suggested choosing a suitable transmission band, which experiences relatively-less interference by other light-sources, to tackle the effect of this type of interference. The band can be chosen according to different factors, such as distance between the transmitter and receiver, irradiance angle, and incident angle. The results of this study have proven that the suggested technique works efficiently and can improve the performance of the VLC system by tackling the interference issue. Both communication and illumination practice standards should be considered for the deployment of the VLC technology. This is different from any other communication system and adds the issue of coordination between different regulatory bodies [98].

To resolve such shortcomings and to improve VLC system performance, research investigations have considered the implementation of hybrid communication systems [16, 99, 100]. Integrating communication systems such as free space optics with RF communication, VLC, PLC, etc., can offer a significant range of benefits in terms of security and performance of in-train communication [16, 17, 101]. For example, providing an up-link using VLC can be problematic, however, as Li-Fi technology does not interfere with RF, a cooperative VLC-RF system, where the VLC is used for down-linking and the RF for up-linking, can offer full connectivity and improve the QoS. Nevertheless, such cooperation leads to a vertical handover between the VLC and the RF systems which can cause instability and delay in data reception [98].

2.4.3 Power-line Communication (PLC)

In recent years, there has been an increasing interest in PLC technology. Simply, in this technology, the pre-installed wiring network of a building or utility grid is utilized for both carrying electricity and data to consumers[102]. This advantage makes PLCs a cost-effective and competitive technology for networking applications [100]. According to its operating frequency this technology is grouped into two different groups, low frequency PLC (NB-PLC) and high frequency PLC (BB-PLC). NB-PLC operates at frequencies from 3-to-500 kHz and it is characterized by its low-data rate and long range of transmission [103].

BB-PLC performs at frequencies from 1.8–250 MHz and it has a higher data rate but shorter transmission distance than NB-PLC. The PLCs can also be divided according

to the type of current carried by the power lines: PLC over lines carrying alternative current and PLC over lines carrying direct current.

In PLC systems, the transmitted data is first modulated by modem node then injected into the power lines, which represent the transmission medium, to be sent to its destination. At the receiver node, the information signal passes through a filtering process then demodulation to recover the original data [104]. Different modulation techniques can be used with this technology such as, frequency shift keying, OFDM, binary phase shift keying (BPSK) and spread-frequency shift keying. PLCs systems have been used for different applications such as, home automation, home networking, and narrow-band PLC - radio broadcasting [105, 103]. NB-PLC systems have been generating widespread attention amongst academia and industries owing to its applications in different fields such as: home-control, the smart-grid, smart energy generation and micro-inverters.

The BB-PLC was initially used for home applications only, but recent studies have proved that this technology can fulfil future requirements of smart-grid applications [106]. This technology has been recently used in vehicle applications where transmission of data between the electronic parts of the vehicle such as sensors and actuators is achieved by using its existing electrical wiring, reducing costs without adding extra weight [11, 107]. Inside trains, the BB-PLC technology can be used for many purposes, such as in-train entertainment for commuters on long-haul trips through the power line networks of the train. This technology can also distribute a high-speed internet to the commuters inside trains if the trains are connected to a suitable communication network [11]. For safety and security reasons, cameras and other safety devices can be connected by the BB-PLC to monitor the train coaches. Furthermore, the on-board electronic equipment can be inter-connected to share important data [107].

PLC is a harsh transmission medium and a number of technical issues remain to be solved. The power lines were installed for current transmission only. To assess their suitability for use for data transmission, analytical models describing their transfer functions including the huge variation in response between frequency, phase and amplitude of the signal need to be developed. The transmission over such channels can be attenuated by signal reflection due to the mismatching of electrical impedances caused by changes in topology and physical properties. Thus, one of the major issues is to study the transfer function of PLCs and to find an appropriate channel model which can accurately represent it in computer simulations [108]. However, there are number of channel models that can accurately model the transmission channel proposed in the literature such as multi-path and two-port network models, the latter is also known as ABCD matrix channel model [60, 109].

Transmission over PLCs is also affected by noise which is considered one of the most problematic issues in this technology. Noise over PLCs is categorized into two main

categories, coloured-background noise and impulsive noise. The former varies slowly with time and can remain stationary for minutes, sometime hours, the latter occurs randomly with short duration and high power spectral density (PSD) [69]. Although impulsive noise has a short duration, it can severely disturb and affect the transmission over PLC channels [60]. However, a number of mitigation techniques have been proposed in the literature. These include multi-carrier modulation (MCM), blanking nonlinearity, clipping non-linearity, hybrid blanking/clipping non-linearity, coding, multiple input multiple output (MIMO) and time and frequency domain techniques [69].

The power cables radiate electrical signals to the surroundings when signals travel along the PLC between the transmitter and the receiver [52, 110, 111]. These radiated signals can cause a malfunction in nearby electronic equipment, known as EMI. Thus, a number of official and industry bodies have agreed electromagnetic compatibility (EMC) standards to limit both inductive and conductive modes of EMI, to acceptable levels to ensure the reliability and safety of PLC systems [52, 112]. In addition, PLCs systems cannot provide services to the end users at mobility, when the end users are moving. Therefore, combining PLC systems with other communication systems such as RF and VLC can provide better mobility and performance to the end users [100, 16]. However, The implementation of such hybrid systems can also solve network coverage problems and increase the overall capacity of the systems [100, 16].

2.4.4 Hybrid Communication Systems

Reliable communication systems which can provide good network coverage, throughput and mobility to the train commuters is a critical issue in the design of onboard communication systems. This is due to the increase in multi-media users on trains, which means that a single network might not be able to provide reliable services to all the passengers. However, implementing hybrid communication systems, such as, PLC/VLC, PLC/RF and VLC/RF in indoor environments can improve the system performance and the user's QoS and provide better mobility to the end users [113, 16, 114–117]. Since each network does not affect the coverage of the other networks as there is no interference between them, the total capacity of the hybrid system is better than that of a single system [93]. Relays such as amplify-and-forward (AF) and decode-and-forward (DF) are often used with hybrid systems to increase transmission distances and offer greater system throughput [16, 100].

Integrating networks is one of the most significant current discussions in indoor applications and has attracted both academia and industry [100, 16, 93]. The study [93] discusses the implementation of hybrid Li-Fi/Wi-Fi networks in indoor environments. The authors believe that the 300 THz license-free frequency band used by Li-Fi

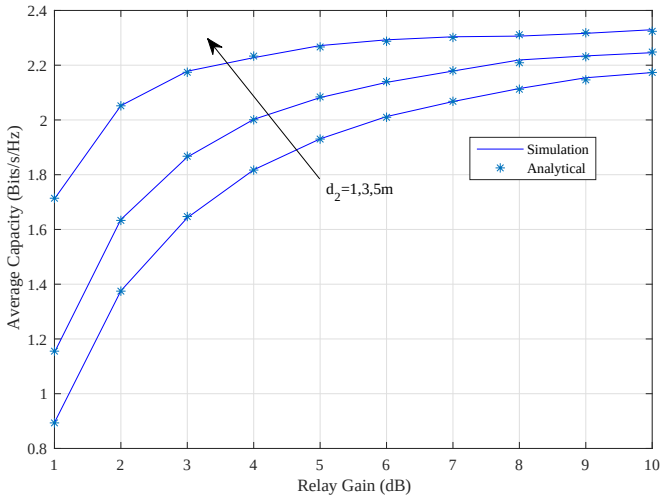

Figure 2.4 Average capacity versus the relay gain for different values of relay-destination distance.

technology can be considered as a solution to the problem of limited availability of the radio frequency (RF) spectrum. The electromagnetic spectrums used by these two technologies are totally different, so they do not interfere with each other which enables the implementation of a cooperative network [93]. The study proposed dynamic load balancing to tackle the issue of the frequent handover between the LoSs of the LEDs during the movement of end users. The Wi-Fi system provides services to the moving users and the static ones are served by the Li-Fi network. The authors concluded that the Li-Fi link provides higher data rate to the static users than that provided to the moving users by the Wi-Fi [93].

Using Li-Fi technology as a complementary network to RF was investigated in [118]. The authors considered a cooperative VLC/RF down-link where full coverage was provided by an RF network supported by the LoS of the LEDs. The authors indicated that the proposed cooperative system was able to provide a higher data rate than a single systems. It was also indicated that the system was able to overcome some of the issues associated with RF and Li-Fi networks such as limited availability of RF spectrum, the frequent handover of the Li-Fi due to its small-coverage area and the incapacity of the Li-Fi network in providing convenient up-link coverage [118]. Convinced that a hybrid Li-Fi/Wi-Fi system can enhance the robustness and increase throughput, the authors of [119] studied the cooperation between these two networks. The results showed that the hybrid system performed much better than WiFi alone, especially in crowded areas. It was also found that the VLC system could provide better performance than that provided by the Wi-Fi system when the transmission distance is relatively small.

The advantage of utilizing the existing electrical network in indoor environments offers the opportunity to use PLC systems as a frame for both RF and VLCs. The

discussion regarding implementing hybrid PLC/RF started in the last decade. The proposed hybrid system was considered for vehicular and home applications as well as for automated metering infrastructure [120–122]. The implementation of cascade links for such applications was discussed in [123, 124], which considered both networks as working simultaneously. The cooperative PLC/RF system was also discussed in different aspects and different system setups by [125–127]. Their conclusions can be summarized as, a hybrid PLC/RF system can increase throughput and enhance the performance of the system by offering a better data rate to end users. This was also confirmed by our work in [100] where we compared the performance of a relay-based PLC/RF with its counterpart in PLC only.

Several studies have investigated the use of relays with PLC, RF, and hybrid PLC/RF systems [122, 100, 128–132]. The studies involved different relaying protocols such as AF, DF, and included incremental DF (IDF) and selective DF (SDF). The authors in [133, 134] indicated that optimizing the relay position on the network can offer better performance and improve the system. They also concluded that the use of relays can be more beneficial to RF networks than PLC. We discussed the implementation of an AF relay in a hybrid PLC/RF network in [100]. The proposed system was investigated in terms of average capacity. The effect of some of the system parameters on its performance was studied. The results showed that the system could offer better performance and mobility to the end users. As can be seen from 2.4, the performance of the system can be improved by increasing the relay gain which justifies the use of the relay in the system.

Recently, PLC technology has been associated with cooperative PLC/VLC systems. Where the PLC is used as a basis for the VLC which, in turn, transforms the electrical signal into an optical signal then delivers it to the users [135]. This hybrid system was first presented and discussed in [136] with the authors using white LEDs positioned in the ceiling for the indoor sources of optical wireless signals. It was concluded that such integration will play a crucial role in both indoor and outdoor applications. The main reason being that no new installations are required for the implementation of such a cascaded system. Since then, aspects of this hybrid system have been investigated by many researchers [136–139]. A discussion on implementing a hybrid PLC/VLC system in the presence of AF and DF relays is presented in Chapter 4. The results of this study indicated that the performance of the system is negatively affected by the overall distance and can be improved by increased the relay gain. It also revealed that the proposed system performs better with increasing input power.

It is worth pointing out that although increasing the number of relays in the communication systems can improve performance in terms of outage probability this will be at the cost of reducing the energy efficiency of the system [140]. The energy efficiency of the communication systems in the presence of relays has been investigated in previous

studies [140–145]. The authors of [140] provided a comprehensive study of the energy consumption performance for different relay protocols (i.e., AF, DF, SDF, and IDF) over the PLC channel. It was found that the SDF and IDF scenarios were more energy-efficient compared to the single-hop and non-cooperative DF and AF configurations. Different techniques were discussed in [141, 146] to improve the energy consumption in relay-based PLC systems. A DF-based indoor PLC network was considered by [141] who showed that placing the DF relay at the mid-point between the source and destination with optimal timeshare gives the most energy efficient performance.

In [146], the authors proposed an energy harvesting (EH) technique at the AF relay to improve the energy-efficiency of a dual-hop relay-based PLC system. The relay node harvests the power of the unwanted impulsive noise from the first link, which then contributes to powering the system. For the sake of comparison and to quantify the achievable gains, the conventional AF relay configuration (i.e., with no EH) was also considered by the authors. They concluded that the proposed system can significantly improve the energy consumption of AF-based PLC networks. Harvesting energy from the first link and then using it as a relay to transmit power for the second link has been discussed in [143, 147] in which a cooperative relay-based VLC/RF communication system was considered. Besides collecting the information from the first link (i.e., VLC link), the relay harvests the energy of the direct current component of the received optical signal and then this power is used to transmit power to the second link (i.e., RF link). It was concluded that the considered system with the proposed EH technique can be energy efficient. An EH technique where the energy from the first link is harvested and utilized as an additional energy resource for the DF relay was proposed in [144]. A cooperative VLC/RF system with an EH relay was considered and the results showed that the energy harvested from the transmitted signals through the VLC link can be used to supply the DF relay with power that can improve the performance of the entire system.

Improving energy efficiency and achieving a better data rate by using hybrid RF/VLC links was investigated in [148]. It was shown that the performance of the proposed RF/VLC system is better than that of the RF network alone. An optimum EH time-switching protocol was proposed by the authors of [149, 150]wherein the relay harvested the power of the useful signal and co-channel interference signals and then utilized it to send the signal to its destination node. Two different techniques were adopted, namely time-switching (TS) and power-splitting (PS) schemes. In the first scheme, the relay switches between harvesting energy and decoding information while in the other scheme a portion of the received power is harvested, and the remaining power is used for processing the information. It was found that, at high SNR, the PS scheme outperforms the TS. On the other hand, when the SNR is relatively low, the TS scheme is superior to the PS. In contrast to previous work which was limited to direct

link and one relay analysis, the authors of [128] studied the energy performance of the PLC system in the presence of more than one relay in the network. They showed that increasing the number of relays on the network can considerably improve the system performance in terms of outage probability, but this will be at the expense of increased power consumption. A comprehensive study and analysis of outage probability and energy per bit consumption performance of multi-hop VLC networks is provided in Chapter 5.

2.5 Summary

The HSR has been developed rapidly in recent years and more development is expected to take place in the coming years. The number of commuters is expected to increase as trains are regarded as a fast, safe and green public transportation system. However, the growth of railway demand and its development require a reliable communication system to meet the railway users' demands. For this reason, in this chapter, a survey of HSR-communication systems was provided, and challenges to the current communication system were discussed. It was found that, currently, the LTE-R which is based on the LTE network is the available candidate for a GSM-R communication system and can fulfill the requirement of the existing railway system. While this research agrees on that no doubt the LTE-R is capable to meeting demand for this stage of railway development, it is clear in the near future the need to move to a more reliable communication system is inevitable. Therefore, this chapter also presented some of the expected networks for future railway communication. Also, an overview of inside train communication was provided. The advantages and disadvantages of the onboard distribution systems are discussed. It was clear that hybrid systems can provide more reliable services to train commuters compared to the services provided by single systems.

Chapter 3

Overhead Line Equipment Channel Characteristics and Capacity

This chapter investigates overhead line equipment as an access network connecting trains to backbone communication networks. The two-port network model is used to represent the transfer function of the OLE channel. Furthermore, a simulation of OLE systems is implemented using orthogonal frequency division multiplexing (OFDM) as a choice of modulation scheme. For performance evaluation, MATLAB simulation was used to implement the model of the OFDM-based OLE system and to compute the capacity and BER of the OFDM-based OLE system. The results showed that the two-port network model can be developed to represent the transfer function of the OLE channel. It was also revealed that the strength of the signal is negatively affected by the speed of the train, frequency and length of the OLE. It was also found that the achieved data rates from the simulated OFDM-based OLE system is promising for the given bandwidths and the given ranges of the SNR.

3.1 Introduction

The use of PLC has attracted plenty of research interests as a cost-effective means of communication [7, 20] because it uses pre-installed medium-voltage power lines which means that the basis of the communication system is already available. Monitoring systems, network management optimization and operational services are common applications of MV-PLC technology [8, 20]. For performance evaluation purposes, and to assist in the development of this technology, models that represent the transfer function of the PLC channel are required. Different channel models have been presented in the literature, with the multi-path and two-port network the most useful as they can accurately represent its transfer function for performance analysis [56, 57, 52].

OLE has always been considered as a means of railway electrification and, to the best of the authors' knowledge, no study in the literature has considered this medium for communication. Figure 3.1, shows the four stages of power generation and supply. The main aim of this chapter is to investigate the OLE as a medium of communication that can deliver data from public networks to inside trains. The signal is then distributed inside the train coaches using in-train communication systems, which is discussed in the following two chapters. However, in this chapter, the two-port network model is used to represent the CTF of the railway electrification system using transmission line theory (TLT). In order to implement this model, the chapter simplifies the train electrification system and derives an equivalent circuit for the whole system. The position, velocity, acceleration, and deceleration of the train are updated using simple dynamic equations, with the train position representing the length of the transmission line. In achieving the aims and objectives of this thesis, a simulation of OLE system using the actual channel response of the developed model is implemented utilising OFDM as a choice of modulation scheme.

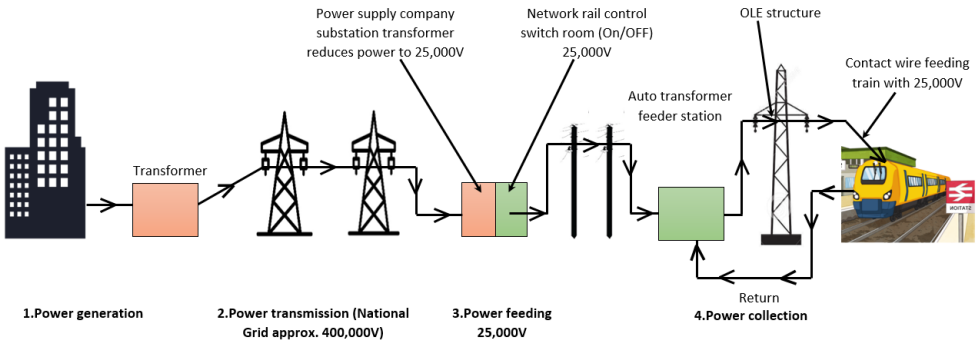

Figure 3.1 The four stages of the power generation and supply.

3.2 OLE Transfer Function

Channel modelling and characterization. Before the implementation of any communication system, the channel transfer characteristics have to be understood. The development of an accurate channel model of the OLE would provide engineers with a basis for computer simulations which would enable performance analysis of different network configurations and loads. Thus, the electrification system of the railway is simplified, and its equivalent circuit derived. The two-port network model is developed to represent the CTF of the OLE system.

3.2.1 Overhead Line Equipment System

In this subsection, the train electrification system is described, and the equivalent circuit of the catenary system is derived.

Over fifty years ago alternating current (AC) was established as the power supply for railway electrification. The single-phase 1x25 kV and the dual-phase 2x25 kV are the most common AC feed systems [151]. However, the former is the standard railway electrification system used in the UK and many other countries [152]. Each rail substation is fed by the utility grid through a power transformer where the primary of the transformer is connected to the utility grid and the secondary is connected to the feeder station [153]. Direct feeding, auto-transformer (AT) feeding, and booster transformer (BT) feeding are the three basic feeding configurations that are used to provide electricity to trains [154, 155]. In direct feeding, the secondary of the substation's transformer is connected directly to the catenary and rails. The main drawback of this form of connection is that a considerable amount of current leaks through the rails to the earth as these act as the return conductor to complete the catenary system circuit [156, 157]. This rail-to-earth leakage current is considered the main cause of electromagnetic interference to surrounding communication equipment. For this reason, and to improve the electrification process efficiency, BTs or ATs are added to the system [157]. In this study, the BT configuration is considered as it is the feeding method used in the UK electrification system.

3.2.1.1 General Structure of the BT Feeding

BTs are introduced to eliminate the interference with communication lines close to the track, caused by current leakage to ground [158]. The connection of the BTs is achieved by one of two approaches, either by connecting the primary to the contact wire of the catenary system and the secondary directly to the rails, or the secondary is connected to a return conductor [159]. In British railway electrification, the leakage current is reduced by connecting the BTs between the contact wire and a return conductor. These

BTs are normally located along the contact wire at approximately every 3 km. The current flows through the primary side of the BT that is connected in series with the contact wire of the catenary system. To have the same amount of current flowing on the secondary side as in the primary, the BTs have primary and secondary windings of unity turn-ratio. The return current flows through the return conductor which is connected to the secondary winding of the BT, and no current flows through the rails [159]. Fig 3.2 shows the classical single-phase 1x25kV feeding configuration with BT which is considered in this thesis.

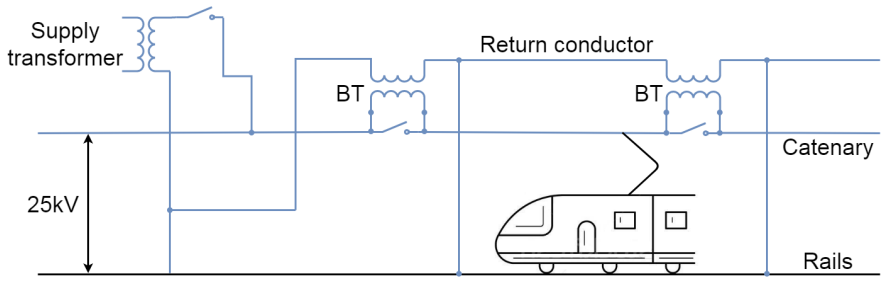

Figure 3.2 Classical single-phase 1x25kV feeding configuration with BT.

3.2.1.2 BT Feeding Equivalent Circuit

As stated above the catenary system considered here is equipped with one active conductor of 25 kV. Catenary systems usually contain multiple physical conductors, divided into, positive, negative, and ground [160].

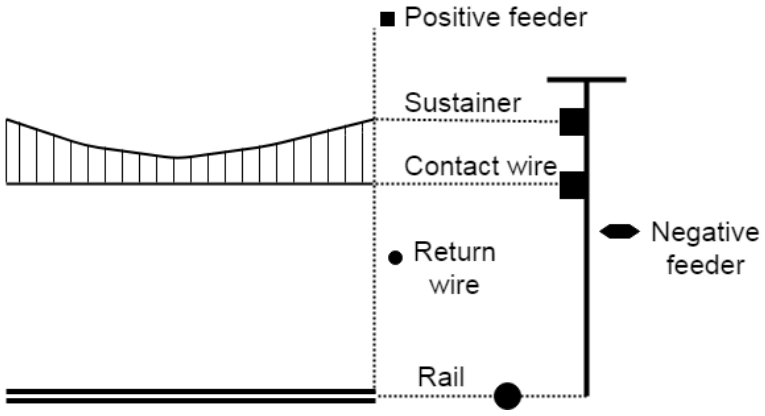

Figure 3.3 Typical conductor distribution.

Figure 3.3 shows the typical configuration of the mono-voltage catenary of an AC supply for a HSR line. While there is only one negative wire that represents the negative feeder, the positive group is represented by three wires, namely the contact wire, the sustainer wire, and the positive feeder. The ground group also contains three conductors the rail, the collector wire and the return conductor [160].

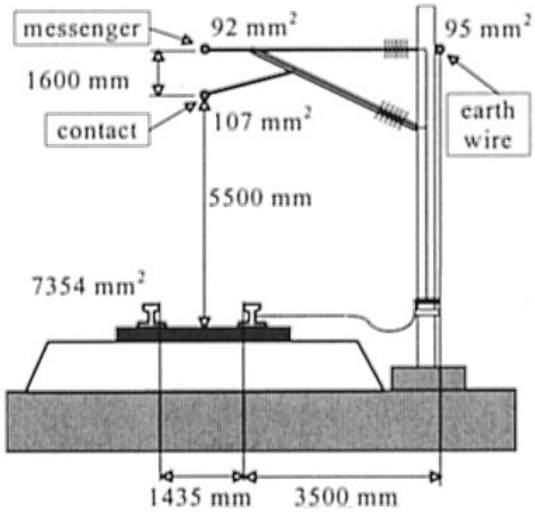

Figure 3.4 Typical cross section of (a) ac single track systems.

Figure 3.4 shows a typical cross-section of a catenary of a single-track system. The representation of the conductors of the same group can be reduced to one conductor by assuming that each conductor group has the same voltage. Furthermore, the current of the equivalent conductor for each group is equal to the sum of the currents of the physical conductors [159]. Figure 3.5 presents a simplified conductor distribution.

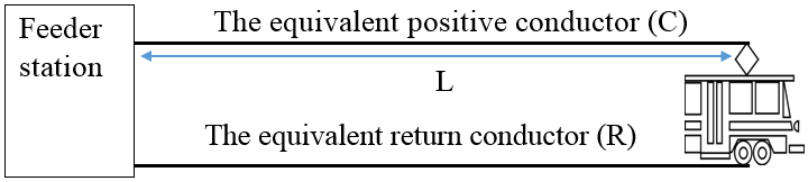

Figure 3.5 Simplified conductors distribution.

To implement TLT the BTs connected between the equivalent positive and return conductors must be considered. As mentioned above, the primary side of the BT is connected to the positive conductor and the secondary side is connected to the return conductor. The BT has a leakage flux at both of its windings that give leakage reactance X_1 and X_2. Furthermore, the windings possess resistances R_1 and R_2 as shown in Figure 3.6.

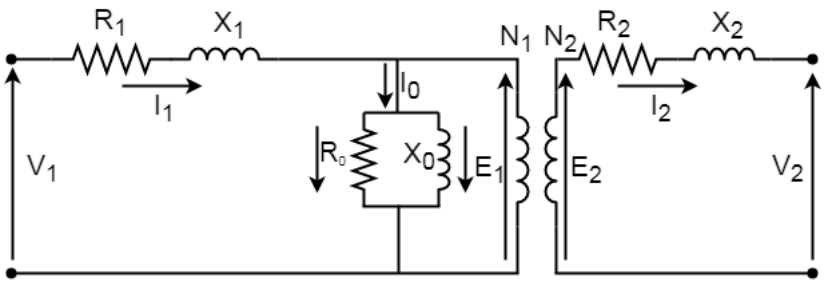

Figure 3.6 Equivalent Circuit of the BT.

The impedance at the primary and secondary windings can be represented by

$$Z_1 = R_1 + X_1. \tag{3.1}$$

$$Z_2 = R_2 + X_2. \tag{3.2}$$

To simplify the equivalent circuit of the BT, the secondary side parameters can be referred to the primary side using the following equation:

$$\grave{Z}_2 = Z_2 \times n^2, \tag{3.3}$$

where n is the ratio between the number of winding on the primary and secondary sides, which is equal to unity, as the BT is a 1:1 ratio transformer.
The exiting current I_0 , which is drawn by X_0 and R_0, is very small and thus the excitation of this parallel circuit, X_0 and R_0, can be neglected. This means that the impedance of the primary side can be defined by the following equation:

$$Z_{eq} = Z_1 + \grave{Z}_2. \tag{3.4}$$

Thus, the equivalent circuit of the BT becomes that shown in Figure 3.6:

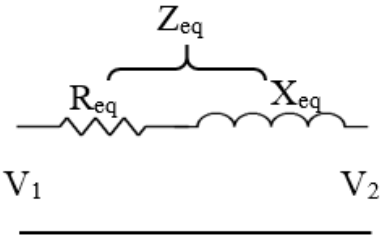

Figure 3.7 Simplified BT equivalent circuit.

The Z_{eq} of the BT is in series with the contact wire so it can be added to the contact wire impedance. Taking into consideration that trains can be represented by an impedance model [161] and assuming that only one train is fed by a substation, the equivalent circuit of this system can be simplified to the following:

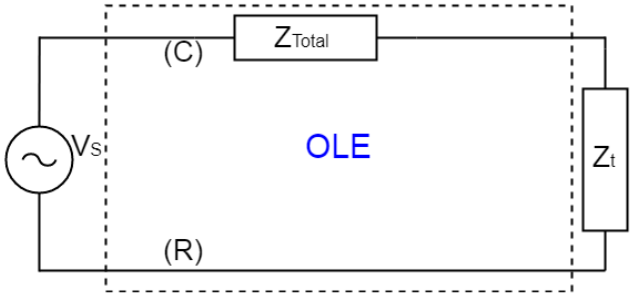

Figure 3.8 Feeding system equivalent circuit with one substation and one train.

Applying TLT to the OLE, where the OLE is represented by a distributed network, which is a per-length-unit network, using four parameters: resistance (R), inductance (L), capacitance (C) and conductance (G) as follows:

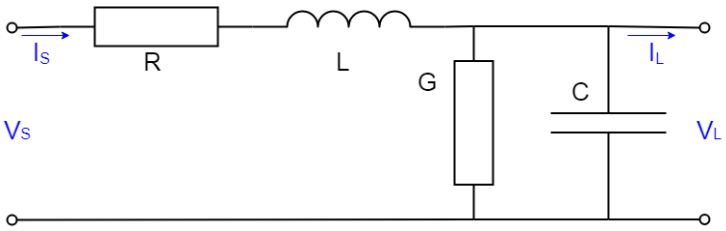

Figure 3.9 Transmission line per length unit network.

This network can be represented by a two-port network which is fully explained in the following subsection.

3.2.2 Two-port Network Model

This section studies the transfer function of the OLE channel by implementing the ABCD matrix based on theoretical considerations.

The ABCD matrix model is widely used in PLC technology to represent the CTF of a two-port network [57]. The main idea here is to apply TLT to the two-port network to define the relation between output and input values. Figure 3.10 shows a two-port network connecting a voltage source with a load.

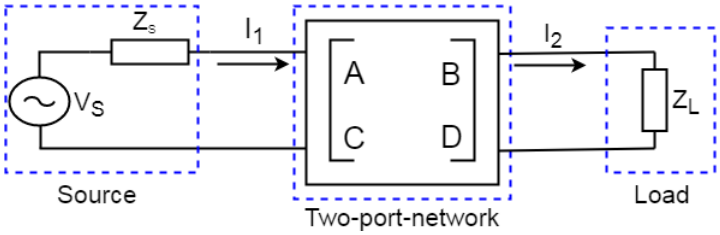

Figure 3.10 A two-port network connected to a voltage source and a load.

The lumped network shown in Figure 3.9 where the values of the primary parameters R, L, C and G of the OLE are lumped can be represented by a two-port network as: by a two-port network as following:

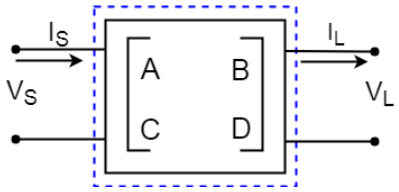

Figure 3.11 A two-port network for a lumped network.

The relation between the output and the input values for this two-port network is straightforward and generally expressed by:

$$V_S = A \times V_L + B \times I_L, \tag{3.5}$$

$$I_S = C \times V_L + D \times I_L, \tag{3.6}$$

where V_S, I_S are the voltage and current supplied by the source, respectively and V_L, I_L are the received voltage and current . A, B, C, and D aare the transmission parameters. These are constants and are used to analyse and study the performance of the electrical networks, and the output of the transmission networks. For simplicity, Equations (3.5) and (3.6) can be given in a form of a matrix:

$$\begin{bmatrix} V_S \\ I_S \end{bmatrix} = \begin{bmatrix} A & B \\ C & D \end{bmatrix} \begin{bmatrix} V_L \\ I_L \end{bmatrix}. \tag{3.7}$$

It is easy to derive the transfer function of the circuit of Figure 3.11 by using the ABCD matrix as:

$$H = \frac{V_L}{V_S} = \frac{Z_L}{AZ_L + B + CZ_LZ_S + DZ_S}. \tag{3.8}$$

Also, the input impedance can be easily evaluated from:

$$Z_S = \frac{V_S}{I_S} = \frac{AZ_L + B}{CZ_L + D}. \tag{3.9}$$

The ABCD matrix is based on the characteristics of the OLE as characterized by their propagation factor (γ) and characteristic impedance (Z_c) [57]. However, per unit-length calculations/measurements of R, L, C and G for the OLE are needed to calculate these two factors. The two secondary constants γ and Z_c of the OLE can be expressed as functions in the primary constants R, L, C and G of the OLE as:

$$Z_C = \sqrt{\frac{R + j\omega L}{G + j\omega C}}. \tag{3.10}$$

$$\gamma = \sqrt{(R + j\omega L)(G + j\omega C)}. \tag{3.11}$$

The effective resistance of the OLE is the resistance R for length l and cross-section area A of the conductor, and is equal to the direct-current resistance (R_{dc}) which can be calculated as:

$$R_{dc} = \rho l / A, \tag{3.12}$$

where ρ is the resistivity of the conductor material.

The per-unit-length of the OLE inductance (H/m) is a combination of internal and external inductances. The former is due to internal flux linkages and the latter is caused by external linkages and is given by:

$$L = L_{int} + L_{ext}. \tag{3.13}$$

$$L_{int} = \frac{\mu}{8\pi}. \tag{3.14}$$

$$L_{ext} = \frac{\mu}{2\pi} \times ln(\frac{D}{r}). \tag{3.15}$$

By substituting Equations (3.14) and 3.15 into Equation (3.13), the total inductance can be found as:

$$L = \frac{\mu}{2\pi} \times (\frac{1}{4} + ln(\frac{d}{r})), \tag{3.16}$$

where μ is the permittivity of the conductor, d is the distance between the conductors and r is the radius of the conductor.

The per-unit-length capacitance (F/m) can be calculated as:

$$C = \frac{2\pi\varepsilon_0\varepsilon_r}{ln\left(\frac{d}{r}\right)}, \tag{3.17}$$

where ε_0 represents free space permittivity and ε_r the relative permittivity of the medium.

As the parallel leakage of current is so small, the per unit length conductance (S/m) can be neglected. However, the shunt conductance G is given by:

$$G = A\delta/l, \tag{3.18}$$

where δ is the conductivity of the material.

However, the geometric mean distance (GMD) and geometric mean radius (GMR) of an irregular conductor are important for calculation of the primary parameters R, L, C and G [162].

The ABCD matrix for a known transmission line length l, characteristic impedance Z_C and propagation constant γ is given by:

$$\begin{bmatrix} A & B \\ C & D \end{bmatrix} = \begin{bmatrix} cosh(\gamma l) & Z_c.sinh(\gamma l) \\ \frac{1}{Z_c}.sinh(\gamma l) & cosh(\gamma l) \end{bmatrix}. \tag{3.19}$$

Substituting the values o A,B, C and D values from Equation (3.19) into Equation (3.8), the CTF of the OLE can be easily calculated.

The length of the transmission line changes according to the train's position. It increases if the train moves away from the substation and decreases when the train moves towards the substation. Therefore, equations that consider the movement of the train are needed to update the length of the transmission line by updating the position of the train in the model. The following equations are used in this model to update the train's speed and position:

$$v = \frac{d}{t}, \tag{3.20}$$

$$v_f = v_i + a \times dt, \tag{3.21}$$

$$a = \frac{v_f - v_i}{t}, \tag{3.22}$$

$$l_f = l_i + v_i + \left(0.5 \times a \times dt^2\right), \tag{3.23}$$

where v_i and v_f are the initial and final speeds of the train, a is the acceleration factor, dt represents the time-step, t denotes the duration of the acceleration, l_i and l_f are lengths of the transmission line before and after the update.

3.2.3 Analytical results

This section presents simulation results of the CTF of the proposed OLE.

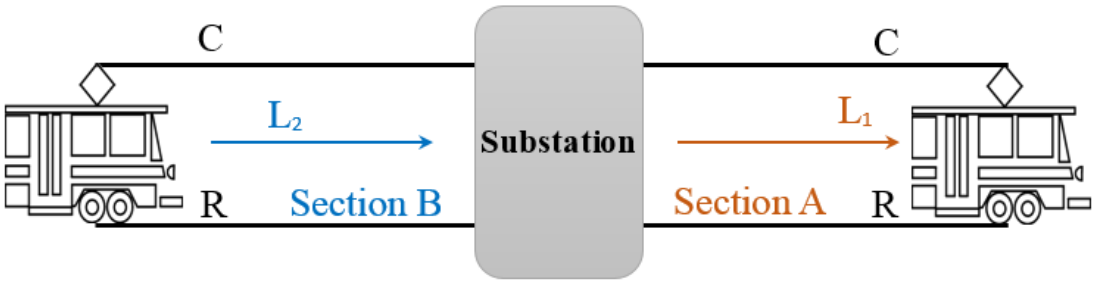

Figure 3.12 Sections A and B of the railway under considerations.

Different channel scenarios are included in this study of the CTF of the OLE to explore the effects of different channel parameters (channel length and transmission frequency) on transmission performance. It is assumed that a railway substation feeds two railway sections A and B. The transmitter device, installed at the substation, sends data to both sections with one train moving in each section as shown in Figure 3.12. The length of the OLE channel is defined as the distance between the transmitter which

is placed at the substation and the receivers which are installed on the trains. The length of each channel changes according to the movement of the train. The entire length of each railway section is 25 km. Frequencies from 1 to 30 MHz are considered in this analysis.

The start is with the train that moves within section A shown in Figure 3.12. It is assumed that this train moves away from the railway substation as appears in Figure 3.13. The train is moving with steady velocity of 80 km/h then after 15 minutes it decelerates to a standstill in 5 minutes. Movement equations are used to calculate the train acceleration and to update the train position which represents the length of the channel.

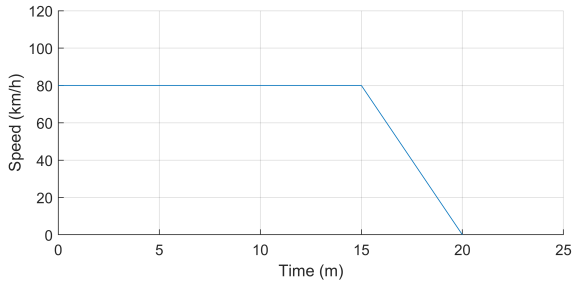

Figure 3.13 Speed line-graph of section A train.

In the second scenario, shown in Figure 3.14, the other train moves towards the substation in section B of the railway. It is assumed that this train begins from rest and accelerates to 80 km/h in five minutes, it continues at 80 km/h for ten minutes and then decelerates from 80 km/h to rest in 5 minutes. The duration of travel for both trains is 20 minutes. The train speed and position were updated every 0.25 second, i.e. dt = 0.25 s, in the movement equations.

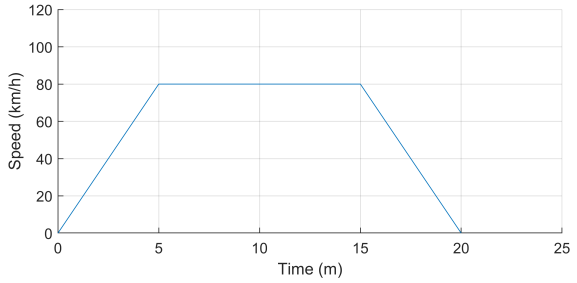

Figure 3.14 Speed line-graph of section B train.

Figure 3.15 shows a 3D surface of the channel response, H, of section A of the OLE shown in Figure 3.12 as a function of length, l, and frequency, f. In communication systems, it is known that the higher frequency corresponds to the higher attenuation and the attenuation is inversely proportional with distance. It can be seen from this figure that both increasing length of OLE and increasing frequency have a negative impact on the transmission, H increasing in value. This would prove that the ABCD model which was developed in this section can be used to represent the CTF of the OLE system. As would be expected, the transmission is less attenuated at lower frequencies and shorter distances. For example, the signal is attenuated by almost -12 dB at frequency of 10 MHz and distance of 10 km from the station, whereas there is nearly -25 dB of attenuation at 20 MHz and same distance from the data source.

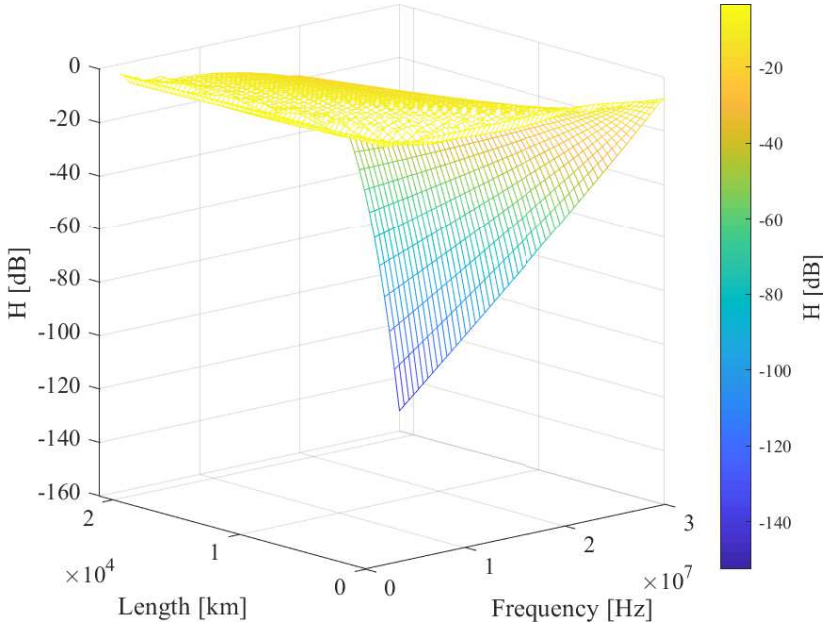

Figure 3.15 A 3D surface plot for the channel response as a function of frequency and line length.

It is also clear that the point of greatest attenuation -150 dB is for maximum frequency and greatest distance, 30 MHz and 25 km, respectively. In accordance to [163] , the attenuation constant for GSM signal propagate from base stations can be from 6.68 dB/km-to-17.8 dB/km. However, the attenuation constant for the OLE in this figure, when the operating frequency is 30 MHz, is about 6.5 dB/km.

To illustrate the nature of the OLE channel, the channel response is shown as a function of the train travel time, for different speeds in Figure 3.16. It can be clearly seen from this figure that the attenuation of the transmitted signal increases with train travel time, but not linearly. For example, when the speed of the train is 50 km/h, the signal attenuation is -30 dB after 10 minutes, but is -110 dB after 30 minutes.

It also can be seen that the higher the train speed the higher the attenuation of the transmission. For instance, after 20 minutes of the train travelling time, the signal is

attenuated by about -60, -54, and -50 dB for speeds 60, 50, and 40 km/h, respectively. However, the overall trend is for attenuation to increase towards the higher speeds and longer travelling time.

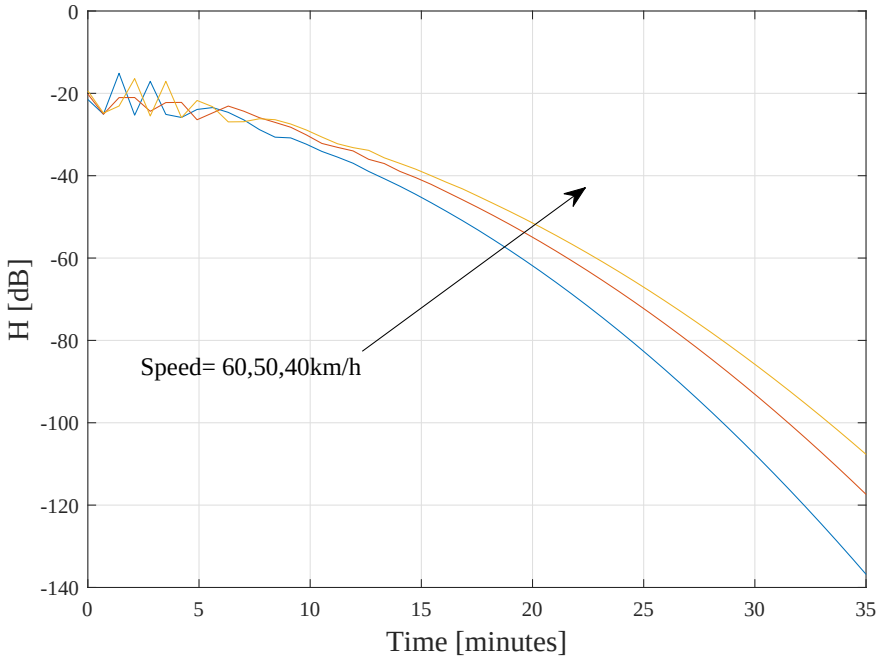

Figure 3.16 Channel transfer function with respect to time, for trains travelling at different speeds.

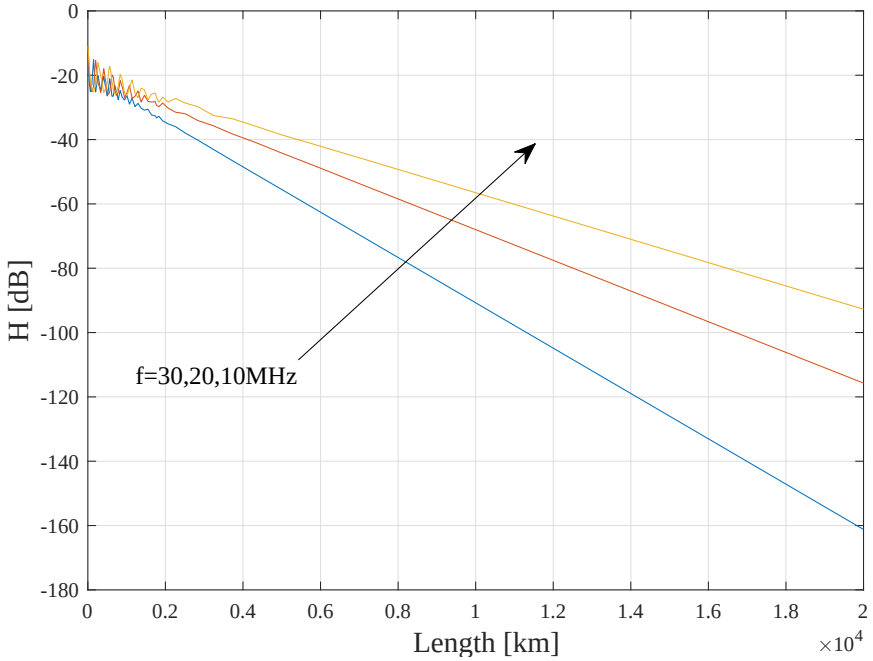

Figure 3.17 Channel response versus distance for three different frequencies.

Figure 3.17 shows the channel response of the OLE of section A as a function of the distance of the train for different values of frequency. It is clear that the attenuation of

the transmission increases the further the train is from the substation for all frequencies. For example, at operating frequency of 10 MHz, the attenuation is almost -25 dB when the train is 2 km from the substation and -60 dB when the train is 10 km for the same frequency. By looking at the three curves for the frequencies, we see that the lower the frequency the lower the attenuation. To illustrate this, when the train is 12 km from the transmitter, the signals are attenuated by approximately -100, -80, and -60 dB at operating frequencies 30, 20, and 10 MHz, respectively.

The channel response of section B of the railway is plotted versus OLE length for different frequencies in Figure 3.18. As anticipated, it can be seen that the signal strength increased when the train moved towards the substation. On the other hand, the transmission is highly attenuated at the beginning of the train movement when the train is far from the transmitter. For instance, at 20 MHz, the greatest signal attenuation is -118 dB, which occurs at the furthest distance of the train from substation and is only -10 dB when the train reaches the substation. The overall trend is for attenuation to decrease at lower frequencies and shorter distances.

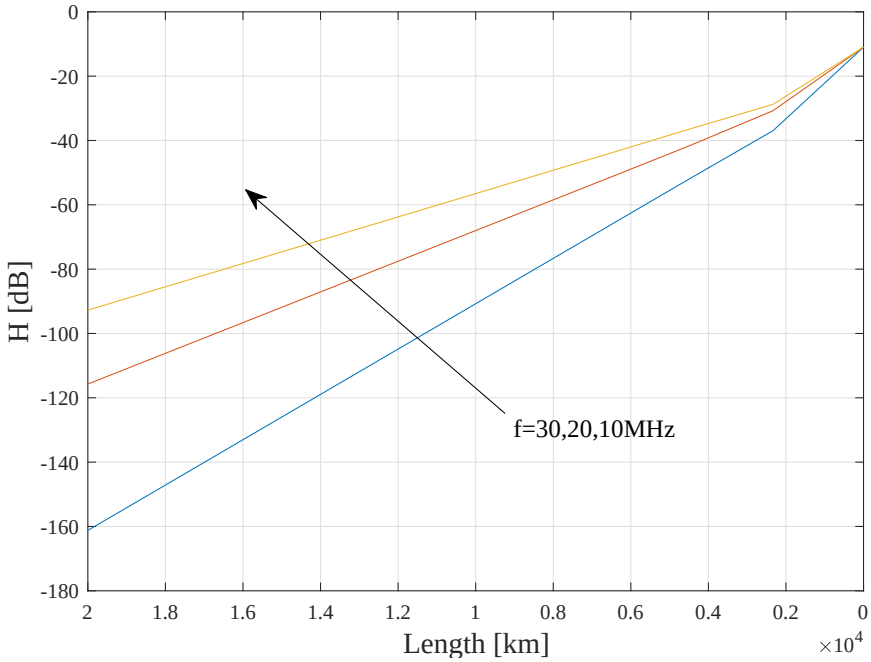

Figure 3.18 CTF of the OLE of section B with distance from source and frequency.

3.3 OFDM Transmission over OLE

A severe deterioration can easily occur in communication performance due to the frequency-selective channel of the PLC system and the presence of impulsive noise. Multi-carrier communications, such as OFDM, can be used for such a channel since it provides crucial advantages in tackling both frequency-selective fading and noise [69, 71, 72]. OFDM technology uses a large number of carriers, each one carries a

low bit rate of data, this means the OFDM is a convenient technique that can be used to reduce multipath effects, selective fading and interference as well providing a high degree of spectral efficiency [164]. Thus, a simulation of OFDM transmission over OLE is presented in this section. For performance evaluation, MATLAB simulation was used to implement the model of the OFDM-based OLE system and to compute the capacity and BER of the OFDM-based OLE system.

3.3.1 System Design

In the proposed OFDM transmission over the OLE channel, a high-speed serial bit stream is split into a number of parallel bit streams each at a lower rate. These streams are carried in multiple orthogonal sub-carriers by means of the Inverse Discrete Fourier Transform (IDFT). However, the OFDM process was performed after the data was modulated using a two-phase modulation scheme, Binary Phase Shift Keying (BPSK) which provided the input data stream to the OFDM. A serial-to-parallel converter (SPC) was applied at this point to convert the complex serial numbers into parallel data and the inverse fast Fourier transform (IFFT) transformed the date into the time domain. At this stage, a cyclic prefix (CP) was inserted in every block of data to protect the OFDM signals from inter-symbol interference and the data was reformed in a serial fashion using a parallel-to-serial converter (PSC). A digital-to-analog converter (DAC) was used to transform the time-domain digital data to time-domain analog data. The output of the DAC was a baseband OFDM signal which was ready to be sent through the OLE channel. Figure 3.19 shows a simple sketch diagram of the process to the OFDM transceiver.

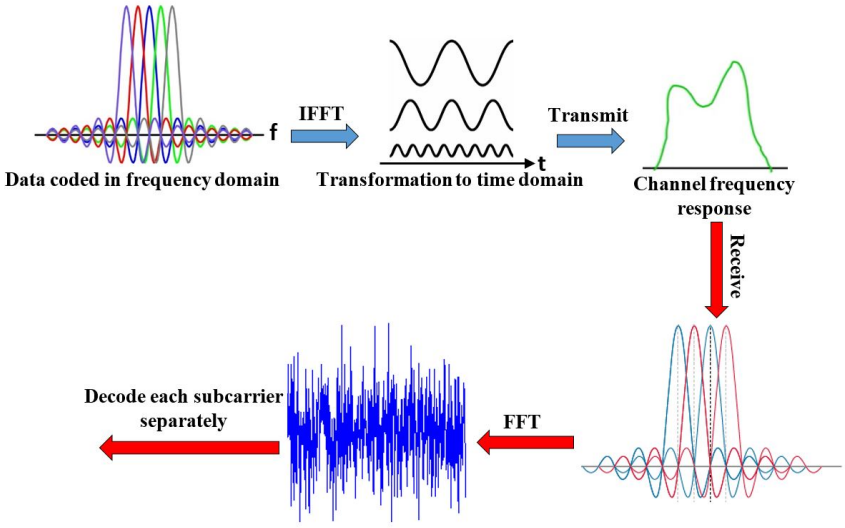

Figure 3.19 Sketch diagram of OFDM process.

The transmitted signal was convolved with one of the time-domain transfer functions of the derived OLE model. Then random noise which was a combination of impulsive

noise (n_i) and additive white Gaussian noise (AWGN), (n_g). The transmitted signal was recreated at the OFDM receiver by first passing the received signal through an analog-to-digital converter (ADC) to be converted into the digital domain. An SPC was used at this point to reformat the received vector into OFDM symbols. After that the CP, which was appended at the start of every OFDM symbol, was removed. Then a fast Fourier transform (FFT) was used by the OFDM demodulator to produce the frequency-domain signal. At this stage, to tackle the distortion incurred by the signal transmitted through the OLE channel, the frequency-domain transfer function of the derived OLE model was used for the equalization process. In the following, the parallel received signals were converted to serial data using the PSC. Finally, the signals were demodulated by BPSK demodulation and system performance was measured in terms of capacity and BER. A complete block diagram of the proposed OFDM-based OLE system is shown in Figure 3.20.

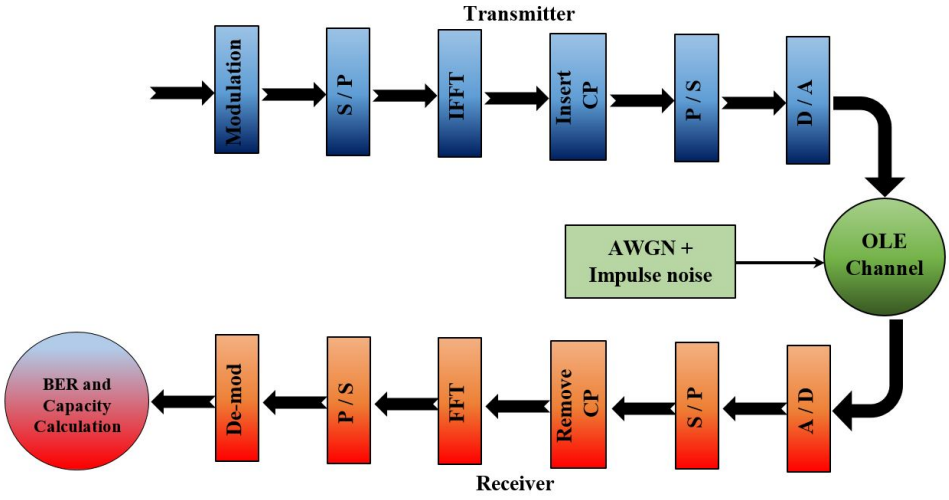

Figure 3.20 Block diagram of the proposed OFDM-based OLE system.

3.3.2 Simulation Results

In order to evaluate the performance of the system shown in Figure 3.20, MATLAB simulation was used to implement the model of the designed system and to analyse the capacity and BER of the proposed system. The following parameters were used for the proposed OFDM system design: the length of the FFT is 64, the number of sub-carriers is 52, the number of bits per OFDM symbol is 52 and the size of CP samples is 12. The channel response presented in Figure 3.15, which considers the first scenario of the train movement, see Section 3.2.3, is considered for the proposed OFDM system to represent the effect of the OLE channel on the transmitted signal.

3.3.2.1 Bit Error Rate

A MATLAB function is used at the receiver to compare the input data with the final output and to plot the BER graph. Figures 3.21 and 3.22 illustrate the performance analysis of the simulated OFDM-based OLE system in terms of BER as a function of SNR. Different OLE channel bandwidths are considered to ascertain the effect of channel bandwidth on the performance of the system. It is noticeable from both figures that as the SNR increases, the BER of the proposed OFDM-based OLE system decreases for all channel bandwidths. For example, in Figure 3.21, the BER decreases from almost $10^{-0.6}$ to 10^{-2} if the SNR increases from 0 to 35 dB when the bandwidth of the OLE channel is 10 MHz. This also applies to the other curves with different channel bandwidths.

It is also observed that, for the same SNR value, the system with higher channel bandwidth has greater BER value compared to that with lower bandwidth. For instance, in Figure 3.22, at a SNR of 30 dB, the values of BER are 0.26, 0.36, and 0.45 for channel bandwidths 20, 25, and 30 MHz, respectively. It is clear from both figures that the system with bandwidth 30 MHz has the highest BER and the system with 5 MHz has the lowest BER for a given SNR value.

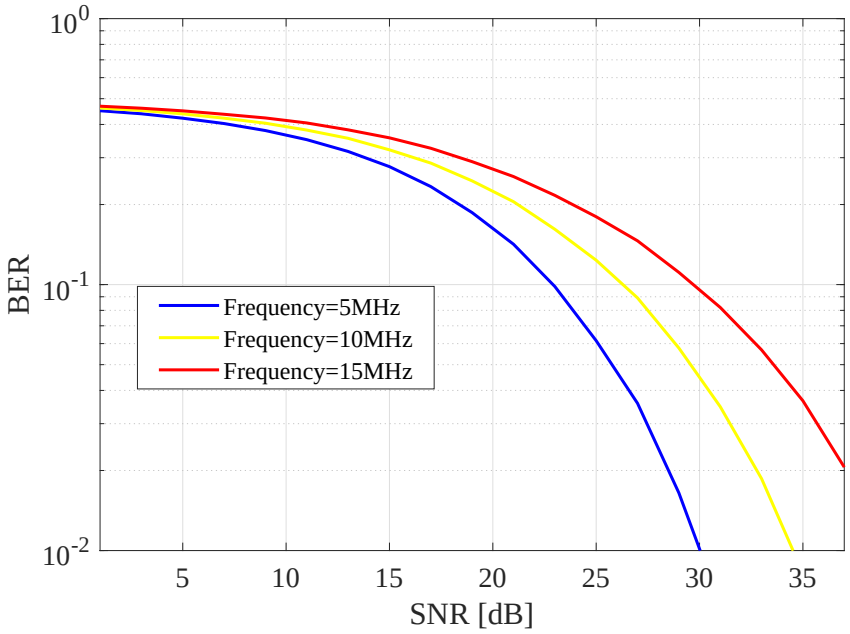

Figure 3.21 BER versus SNR per bit for 5, 10, and 15 MHz OLE channel bandwidths.

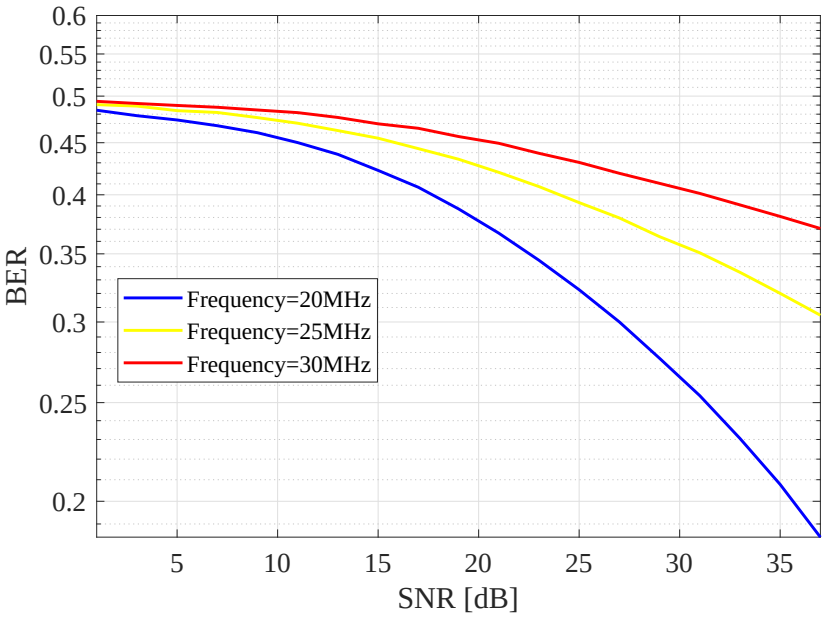

Figure 3.22 BER versus SNR for 20, 25, and 30 MHz of OLE channel bandwidths.

3.3.2.2 Capacity

The performance of the simulated OFDM-based OLE system is illustrated in Figures 3.23 and 3.24 in terms of achievable data rates computed at the receiver of the simulated system. In both figures, the capacity of the proposed system, measured in Bits/s/Hz, is plotted versus the SNR. Values of the OLE channel bandwidths considered are 5, 10, and 15 MHz, in Figure 3.23 and 20, 25, and 30 MHz in Figure 3.24.

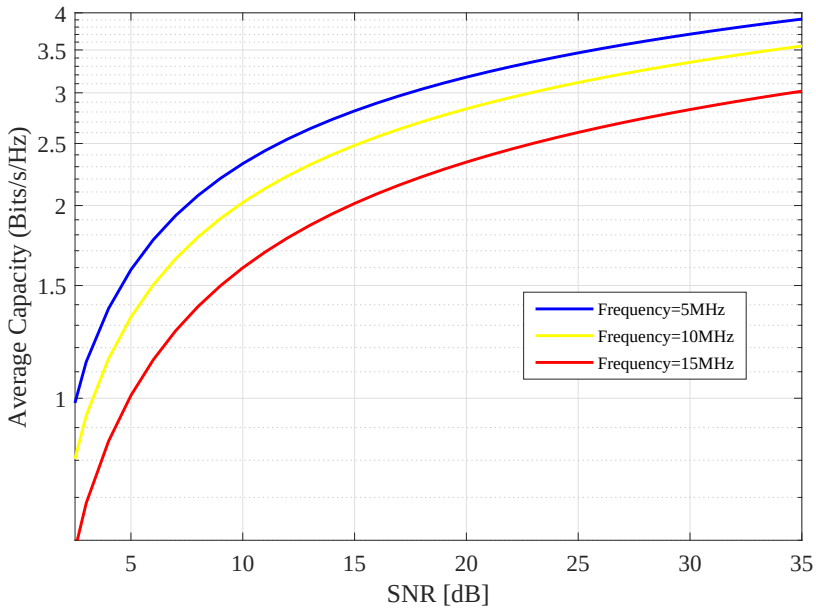

Figure 3.23 Average capacity in Bit/s/Hz versus SNR for 5, 10, and 15 MHz of OLE channel bandwidths.

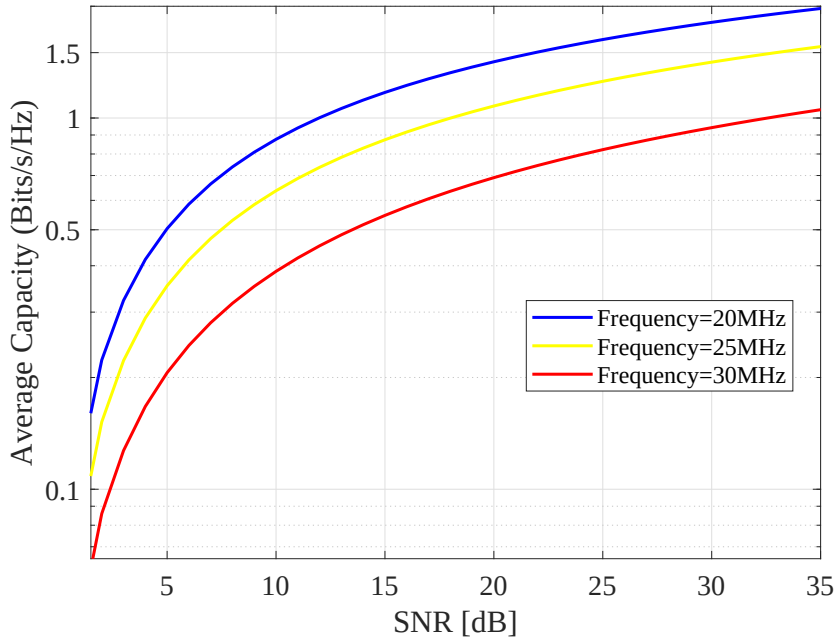

Figure 3.24 Average capacity in Bit/s/Hz versus SNR for 20, 25, and 30 MHz of OLE channel bandwidths.

The plots in Figures 3.23 and 3.24 clearly show that the greater the SNR, the better the achievable data rate of the simulated OLE system. For example, in Figure 3.23 at 10 MHz, the achieved data rate of the proposed OLE system increases from almost 0.5 to 3.5 Bits/s/Hz when the SNR rises from 0 to 35 dB. It is seen in both figures that the achievable data rate per s/Hz for the systems with lower OLE channel bandwidths is better than those with higher bandwidths. For instance, in Figure 3.24 we can see that at a SNR of 5 dB, the achievable data rates are 0.2, 0.35, and 0.5 Bits/s/Hz for the systems with channel bandwidths 30, 25, and 20 MHz, respectively. However, this is when the data rate is calculated per s/Hz, though the entire bandwidth should be considered when calculating the achieved bits per second. For example, when the SNR is 30 dB, the average capacity is 30 Mb/s for the channel bandwidth 30 MHz.

3.3.2.3 BER and Capacity Comparisons between Indoor PLC and OLE

Performance comparisons between broadband indoor PLC and the simulated OLE systems in terms of BER and average capacity are presented in Figures 3.25 and 3.26. The ABCD channel model which was provided in [57] to represent the CTF of the in-building PLC system is considered here to represent the effect of the indoor PLC channel on the transmitted signal. In-building PLC and OLE channel frequency responses and noise models in the 1–30 MHz range are considered. An SNR range from 0-to-35 dB is used in both performance comparisons.

The BERs of both systems are plotted against the given SNR values in Figure 3.25. It is clear from this figure that as the value of SNR increases, the BER of both systems

decreases. It is also observed that the proposed indoor PLC has less BER than that of the simulated OFDM-based OLE system for all given SNR values. For example, for SNR of 30 dB, the BER for the PLC and OLE are, respectively, 10^{-1} and $10^{-0.7}$.

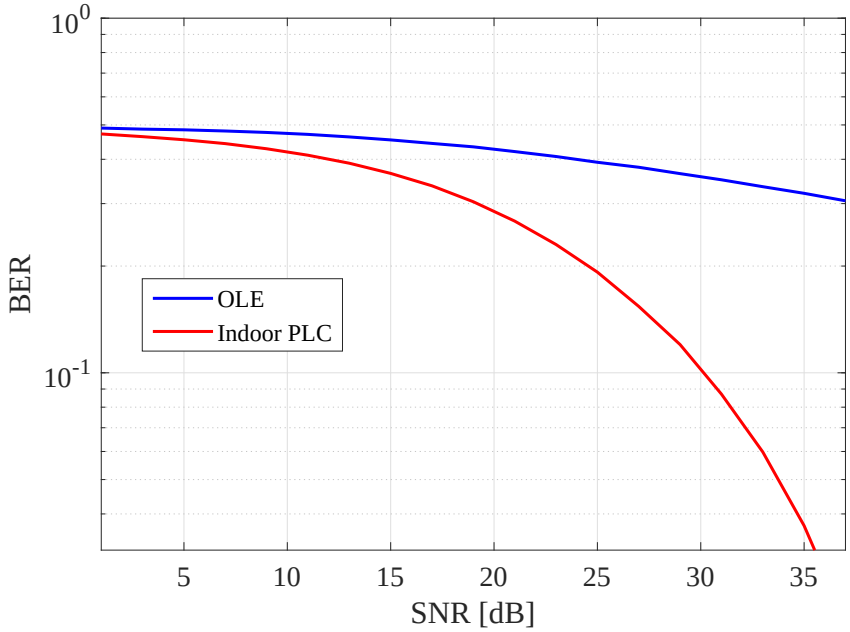

Figure 3.25 BER versus SNR for OLE and indoor PLC.

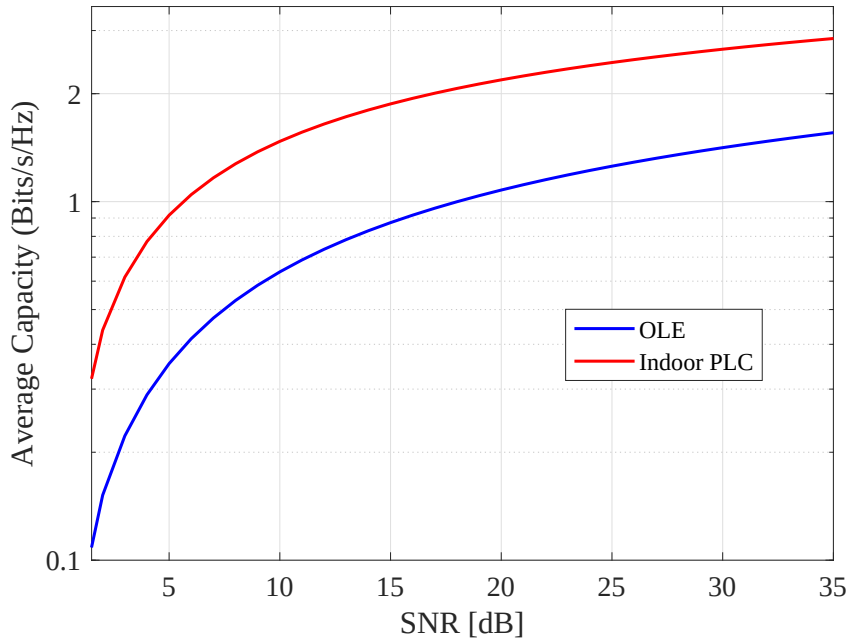

Figure 3.26 Average capacity versus SNR for OLE and indoor PLC.

In figure 3.26, the achievable average capacity of both systems are plotted as functions of SNR. It is noticeable that the performance of both systems improves as the SNR value increases. However, the achievable data rate of the indoor PLC is higher than that of the OLE.

It is observed from both figures that the performance of the indoor PLC system is better than the OLE, this is due to nature and the parameters of the OLE channel which make it a harsher transmitting medium. By looking at both figures one can notice that the BER and capacity curves of indoor PLC and OLE systems have the same pattern which would prove that the ABCD model can be used to represent the CTF of the OLE system.

3.4 Summary

In this chapter, a two-port network model was developed to characterize the transfer function of the OLE channel. The equivalent circuit of a simplified BT electrification system was derived. Dynamic equations of motion were used to determine the position of the train under constant acceleration and deceleration. A simulation of an OFDM-based OLE system was also presented in this chapter. The results showed that the strength of the signal is negatively affected by the speed and distance travelled by the train, frequency, and length of the OLE. It was also revealed that, when the operating frequency is 30 MHz, the attenuation constant is almost Compared to the 6.5 dB/km. These results are promising compared to the signal attenuation in wireless communication systems.

It was also found that the performance of the OFDM-based OLE system improves when the SNR value increases. However, the achieved data rates from the simulated OFDM-based OLE system is promising for the given bandwidths and the given ranges of the SNR. For instance, it was shown that data rate is 30 Mb/s when the OLE channel bandwidth is 30 MHz and the SNR is 30 dB. Based on these results, the OLE system can be used as a communication medium between public networks and in-train communication systems.

The following chapters discuss how the received signal from the OLE system can be effectively distributed inside the train and between the train coaches.

Chapter 4

Performance Analysis of Relay-Based Hybrid Communication Systems

The previous chapter investigated the possibility of using the OLE system as a communication medium between public networks and in-train communication systems. This chapter presents a comprehensive performance analysis of different in-train cooperative communication systems with amplify-and-forward (AF) and decode-and-forward (DF) relays. The performance of the proposed in-train hybrid systems is evaluated in terms of the average capacity and the outage probability. By exploiting known statistical properties of the channels of the proposed network systems the relative capacity and the outage probability are assessed. The results confirmed that the performance of the proposed hybrid system is affected by changes in: source power, source-to-relay distance, the transmit power relay, the height of the light source above the work plane, and the gain of the relay. A performance comparison was conducted between AF-based and DF-based PLC/VLC systems. The outcomes of the comparison showed that the performance of a cooperative PLC/VLC system with DF relay was better than that of the AF-based system.

4.1 Introduction

Exploiting pre-installed infrastructures of wired networks in buildings, vehicles, and utility grids makes power line communication (PLC) a competitive means of broadband communication in indoor applications. However, integrating PLC with other communication systems, such as visible light communication (VLC) or with wireless communication systems, to ensure more reliable transmission and better mobility to end users is being considered by many researchers [122, 113, 114, 116]. Thanks to its cost-efficiency and low-complexity of implementation VLC technology is predicted to be a useful last-mile solution for indoor applications including in-train applications. Hybrid PLC/VLC can provide advantages in terms of capacity, security and data rate improvement [165, 117, 166, 114].

Recently, the adoption of other communication technologies for hybrid systems has motivated many researchers to implement different relaying protocols to further enhance the communication systems' performance [115, 99, 167, 131, 132], the most common of which remain the half-duplex/full-duplex DF and AF relaying protocols. The former decodes the received signal and re-encodes it before forwarding it to the intended destination, the received signal at the AF relay is amplified and then re-transmitted to its destination [130]. Other relay protocols over PLC channels recently studied have included incremental DF and selective DF relaying, see e.g., [128, 168, 140]. While the capacity achieved by the full-duplex relaying protocol can be as twice that of the half-duplex, the practical implementation of the former is more difficult due to the considerable amount of self-interference.

In this chapter, a comprehensive performance analysis of a cooperative PLC/VLC system in the presence of AF and DF relays is presented. The performance of the proposed hybrid systems is evaluated in terms of the average capacity and outage probability using mathematical techniques developed for determining capacity and outage probability based on the statistical properties of the channels of the proposed systems. Formulating the overall capacity and outage probability of the proposed systems offers the opportunity to study the performance of in-train cascade systems and to examine the effect of the different system parameters such as relay location and relay-to-destination distance on the performance of the proposed systems. The outage probability is defined as the probability that the instantaneous SNR of system is less than a certain threshold value.

4.2 System Model

This section presents a proposed model for the hybrid PLC/VLC system in the presence of AF/DF relays. The system model under consideration is shown in Figure 4.1 where

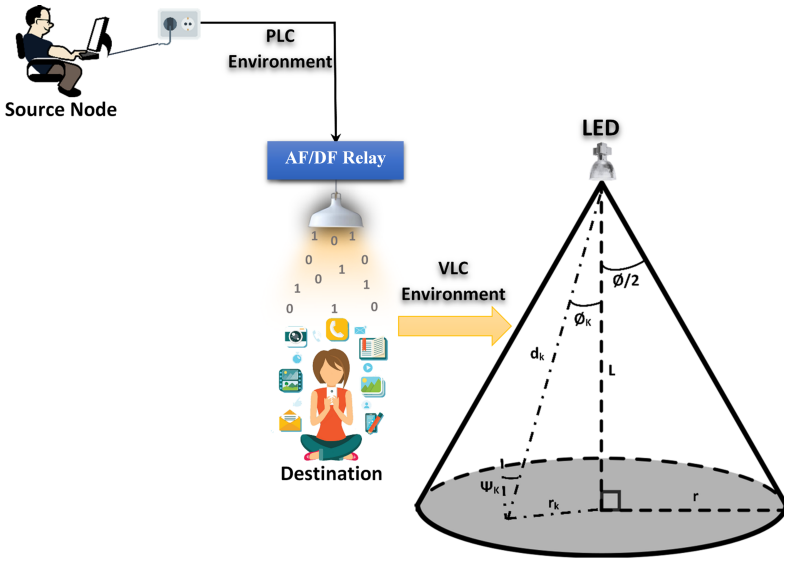

Figure 4.1 System model for the hybrid PLC/VLC network for in-train communication applications.

the data that are delivered from the wayside by the OLE system is initially connected to the PLC link. In the case of the AF-based PLC/VL system, the data sent by the source node through the PLC link is amplified by the AF relay and then retransmitted to the destination through the VLC link. While in the DF-based PLC/VLC system, the DF relay receives the data from the source node via the PLC link. The data is then decoded and re-transmitted by the DF relay to the end user through the VLC link. The complex channel gains h_P and h_v represent the source-to-relay channel gain, (i.e., the PLC link) and the channel gain of the VLC link (i.e., the relay-to-destination channel), respectively. Both channels are assumed to be independent and identically distributed. The amplitude of the channel coefficients of the PLC channel is log-normal [169]. Although, the down-link transmission of the VLC link consists of line-of-sight (LoS) and non- line-of-sight (NLoS) components, the LoS link only is considered in this study as it represents more than 90% of the total received signal [170]. The LED is located on the ceiling of the train coaches with a vertical distance to the user plane L and Euclidean distance to the destination d_k. The VLC channel is subjected to a random distribution which is affected by the uniform distribution of the users' location [170]. Because of the nature of the network structure adopted here, it is logical to assume that there is no direct link between the source and destination nodes. It is worth mentioning, for simplicity and without loss of generality, that noise over the two links is assumed to be AWGN.

4.3 Performance of Power-Line/Visible-Light Communication Systems

4.3.1 Performance analysis of AF-Based PLC/VLC System

Analytical expressions of the average capacity and outage probability of the hybrid PLC/VLC system in presence of AF relay are derived in this subsection.

4.3.1.1 Average Capacity

The average capacity of a communication system can be defined as the maximum data rate that can be achieved over the channel of the system within a certain bandwidth, considering the noise effect. However, for the proposed system, the whole communication process is divided into two phases. The signal received during the first segment at the AF relay is given by:

$$y_r(t) = \sqrt{P_s} e^{-\alpha d_1} h_P s + n_r, \tag{4.1}$$

where P_s represents the source transmit power, d_1 is the source-to-relay distance which represents the length of the PLC link, s is the information signal with $E[s]$ =1, n_r is the noise at the relay which is assumed to be complex Gaussian with zero mean and variance σ_r^2, and α is the PLC channel attenuation factor and is given by $\alpha = a_0 + a_1 f^k$, where a_0 and a_1 are constants determined by measurement, f is the system operating frequency and k denotes the exponent of the attenuation factor.

The received signal at the VLC user can be described by the following formula

$$y_d(t) = h_v G \sqrt{P_r} \left(\sqrt{P_s} e^{-\alpha d_1} h_P s + n_r \right) + n_d, \tag{4.2}$$

where G is the relay gain, P_r is the relay transmit power and n_d represents the destination noise with zero mean and variance σ_d^2.

Using Equation (4.2), and grouping the information signal and noise signal terms, the signal-to-noise ratio (SNR) at destination can be written as:

$$\gamma_{AF} = \frac{G^2 P_r P_s e^{-2\alpha d_1} |h_P|^2 |h_v|^2}{G^2 P_r |h_v|^2 \sigma_r^2 + \sigma_d^2}. \tag{4.3}$$

The instantaneous capacity for this hybrid system can be calculated as:

$$C = \frac{1}{2} E\left[\log(1+\gamma)\right], \tag{4.4}$$

where γ_{AF} is the SNR at the destination and the factor $\frac{1}{2}$ is due to the fact that communication between the transmitter and receiver is performed in two stages.

To begin with, Equation (4.3) is rewritten as

$$\gamma_{AF} = \frac{P_s e^{-2\alpha d_1} |h_P|^2}{\sigma_r^2 + \frac{\sigma_d^2}{P_r G^2 |h_v|^2}}. \tag{4.5}$$

To make the analysis easier to follow, the following substitutions is used $A = P_s e^{-\alpha d_1} |h_P|^2$, $b = \sigma_r^2$ and $C = \frac{\sigma_d^2}{P_r G^2 |h_v|^2}$. Now Equation (4.5) can be written as:

$$\gamma_{AF} = \frac{A}{b+C}. \tag{4.6}$$

Substituting Equation (4.6) into (4.4), the hybrid system average capacity can be expressed as:

$$C_H = \frac{1}{2} E\left[\log\left(1 + \frac{A}{b+C}\right)\right], \tag{4.7}$$

where the superscript H denotes the hybrid system. According to [171, Eq (5)], for any non-negative random variables u and v, the average capacity can be calculated as:

$$E\left[\ln(1+\frac{u}{v})\right] = \int_0^\infty \frac{1}{z}(1 - M_u(z))\,\mathscr{M}_v(z)dz, \tag{4.8}$$

where $M_u(z)$ and $M_v(z)$ denote the moment generation functions (MGFs) of the random variables u and v, respectively. Using this definition, Equation (4.7) can be rewritten as:

$$E\left[\ln(1+\frac{A}{b+C})\right] = \frac{1}{2}\int_0^\infty \frac{1}{z}(1 - M_A(z))\,M_{C+b}(z)dz, \tag{4.9}$$

where $\mathscr{M}_A(z)$ denotes the MGF of the random variable A given by:

$$\mathscr{M}_A(z) = M_{|h_P|^2} P_s e^{-2\alpha d_1}, \tag{4.10}$$

and $\mathscr{M}_{C+b}(z)$ is the MGF of $C+b$.

As previously mentioned, the PLC channel is affected by log-normal fading and according to [172, Eq (2.54)] the MGF of the log-normal distribution is given by:

$$\mathscr{M}_h(z) \backsimeq \frac{1}{\sqrt{\pi}} \sum_{n=1}^{N_p} H_{x_n} \exp\left(10^{\frac{-\sqrt{2}\sigma_h x_n + (-2\mu_h)}{10}} z\right), \tag{4.11}$$

where H_{x_n} and x_n represent the weight factors and zeros respectively of the N_p order Hermite polynomial. By using this for $|h_P|^2$ with parameters $(2\mu_{h_P}, 4\sigma_{h_P}^2)$, the MGF of A can be expressed as

$$\mathscr{M}_A(z) \backsimeq \frac{1}{\sqrt{\pi}} \sum_{n=1}^{N_p} H_{x_n} \exp\left(10^{\frac{-\sqrt{2}2\sigma_{h_P} x_n + (-2\mu_{h_P})}{10}} P_s \mathrm{e}^{-2\alpha d_1} z\right). \tag{4.12}$$

On the other hand, considering the random distribution mentioned above for the VLC link and the Lambertian radiation pattern for LED light emission, the VLC channel gain h_v can be written as[99]

$$h_v = \frac{m_k + 1}{2\pi d_k^2} A_d \cos^{m_k}(\phi) \cos(\Psi_K) U(\Psi_K) g(\Psi_K) R_p, \tag{4.13}$$

where A_d is the detection area of the detector, $d_k = \sqrt{r_k^2 + L^2}$, $U(\Psi_K)$ represents the optical filter gain, $g(\Psi_K)$ denotes the optical concentration gain, the responsivity of the photo-detector is represented by R_p, ϕ is the total angle of the LED, $\cos^{m_k}(\phi) = \cos(\Psi_K) = \frac{L}{\sqrt{r_k^2+L^2}}$, and m_k is the order of the Lambertian radiation pattern which is given by

$$m_k = \frac{-1}{\log(\cos(\phi/2))}, \tag{4.14}$$

where $\phi/2$ denotes the semi-angle of the LED, see Figure 4.1.

To simplify our analysis, let us assume that $Q = \frac{1}{2\pi} A_d U(\Psi_K) g(\Psi_K) R_p$. In light of this, Equation (4.13) can be rewritten as:

$$h_v = \frac{Q(m_k+1)L^{m+1}}{(r_k^2 + L^2)^{\frac{m+3}{2}}}. \tag{4.15}$$

It is assumed that the location of the users is uniformly distributed with probability density function (PDF):

$$f_{r_k}(r) = \frac{2r}{r^2}. \tag{4.16}$$

The PDF of the un-ordered channel gain of the VLC link can be resolved using the change-of-variable method used in [99] as follows:

$$f_{h_k}(h) = \mid \frac{\mathfrak{d}}{\mathfrak{d}h} u^{-1}(h) \mid f_{h_k}(u^{-1}(h)). \tag{4.17}$$

In this respect, the PDF of the VLC channel gain can be expressed as [99]:

$$f_{h_k} = \frac{2Q^{\frac{2}{2+m}} \left((m_k+1)L^{m_k+1}\right)^{\frac{2}{m+3}} h^{-\frac{2}{m_k+3}-1}}{(m_k+3)r^2}, \tag{4.18}$$

where r is the maximum cell radius of the LOS.

Consequently, the PDF of h_k^2 can be obtained as follows:

$$f_{h_k^2} = \frac{-Q^{\frac{2}{2+m}} \left((m_k+1) L^{m_k+1}\right)^{\frac{2}{m+3}} h^{-\frac{m_k+5}{m_k+3}}}{(m_k+3) r^2}. \tag{4.19}$$

In order to obtain the MGF for $C+b$, we have to find the PDF of $\frac{1}{|h_v|^2}$ as $C = \frac{\sigma_d^2}{P_r G^2 |h_v|^2}$. Using the change-of-variable method the PDF of $\frac{1}{|h_v|^2}$ can be written as:

$$f_{\frac{1}{h_v^2}} = \frac{\left(Q\,(m_k+1)\,L^{m_k+1}\right)^{\frac{2}{m+3}} h^{-\frac{2}{m_k+3}-1}}{(m_k+3) r^2}. \tag{4.20}$$

By using Equation (4.20) the MGF of $\frac{1}{|h_v|^2}$ can be obtained as:

$$\mathscr{M}_{\frac{1}{h_v^2}}(z) = \int_{t_{min}}^{t_{max}} f_{\frac{1}{h_v^2}}(z) \exp(-zh)\, dz, \tag{4.21}$$

where $t_{min} = \frac{\left(Q(m_k+1)L^{m_k+1}\right)^2}{(r^2+L^2)^{m_k+3}}$ and $t_{max} = \frac{\left(Q(m_k+1)L^{m_k+1}\right)^2}{L^{2(m_k+3)}}$.

Substituting Equation (4.20) in (4.21), the Equation (4.22) is obtained:

$$\begin{aligned}\mathscr{M}_{\frac{1}{h_v^2}}(z) = \frac{\left(Q\,(m_k+1)\,L^{m_k+1}\right)^{\frac{2}{m+3}}}{(m_k+3) r^2} \Bigg(& z^{-\frac{1}{m_k+3}} \Gamma\left(\frac{1}{m_k+3}, \frac{L^4 z}{Q^2 (1+m_k)^2}\right) \\ & - z^{-\frac{1}{m_k+3}} \Gamma\left(\frac{1}{m_k+3}, \frac{L^{-2(m_k+1)} (L^2+r^2)^{m_k+3} z}{Q^2 (1+m_k)^2}\right)\Bigg).\end{aligned} \tag{4.22}$$

Finally, $\mathscr{M}_{C+b}(z)$ can be written as Equation (4.23):

$$\begin{aligned}\mathscr{M}_{C+b}(z) = \frac{\left(\frac{\sigma_d^2}{P_r G^2} z\right)^{-\frac{1}{m_k+3}}}{(m_k+3) r^2} \left(Q\,(m_k+1)\,L^{m_k+1}\right)^{\frac{2}{m+3}} \Bigg(& \Gamma\left(\frac{1}{m_k+3}, \frac{L^4 \sigma_d^2 z}{Q^2 (1+m_k)^2 P_r G^2}\right) \\ & - \Gamma\left(\frac{1}{m_k+3}, \frac{L^{-2(m_k+1)} (L^2+r^2)^{m_k+3} \sigma_d^2 z}{Q^2 (1+m_k)^2 P_r G^2}\right)\Bigg).\end{aligned} \tag{4.23}$$

4.3.1.2 Outage Probability

The outage probability is simply defined as the probability that the instantaneous capacity C of a communication system is less than the required threshold R_{th} of the information rate, and it is given as:

$$P_{outage} = Pr\left[C < R_{th}\right]. \tag{4.24}$$

The end-to-end outage probability for the proposed system can be written as:

$$P_{outage}^{AF} = Pr\{\gamma_{AF} < R_{th}\}. \tag{4.25}$$

Substituting Equation (4.5) into (4.25), the end-to-end outage probability can be rewritten as:

$$P_{outage}^{AF} = Pr\left\{\frac{G^2 P_r P_s e^{-2\alpha d_1} h_p^2 h_v^2}{G^2 P_r h_v^2 \sigma_r^2 + \sigma_d^2} < R_{th}\right\}. \tag{4.26}$$

To make the analysis easier to follow, use the following substitutions $k_1 = G^2 P_r P_s e^{-2\alpha d_1}$, $k_2 = G^2 P_r \sigma_r^2$ and $k_3 = \sigma_d^2$. Now, Equation (5.5) can be written as:

$$P_{outage}^{AF} = Pr\left\{\frac{k_1 h_p^2 h_v^2}{k_2 h_v^2 + k_3} < R_{th}\right\} \tag{4.27}$$

$$= Pr\left\{h_v^2 < \frac{k_3 R_{th}}{k_1 h_P^2 - k_2 R_{th}}\right\}. \tag{4.28}$$

Since h_v^2 always greater than or equal to zero, the above outage probability can be calculated as:

$$P_{outage}^{AF} = \begin{Bmatrix} Pr\left(h_v^2 < \frac{k_3 R_{th}}{k_1 h_P^2 - k_2 R_{th}}\right), & h_P^2 < \frac{k_2 R_{th}}{k_1} \\ Pr\left(h_v^2 > \frac{k_3 R_{th}}{k_1 h_P^2 - k_2 R_{th}}\right) = 1, & h_P^2 > \frac{k_2 R_{th}}{k_1} \end{Bmatrix}. \tag{4.29}$$

The outage probability can now be expressed as:

$$P_{outage}^{AF} = \int_0^{\frac{k_2 R_{th}}{k_1}} f_{h_P^2}(z)dz + \int_{\frac{k_2 R_{th}}{k_1}}^{\infty} f_{h_P^2}(z) \underbrace{Pr\left(h_v^2 < \frac{k_3 R_{th}}{k_1 z - k_2 R_{th}}\right)}_{F_{h_v^2}(.)} dz, \tag{4.30}$$

where $f_{h_P^2}(.)$ is the PDF of the first link (i.e., the PLC channel). The probability in the second part of the second integral is the Cumulative Density Function (CDF) of h_v^2(i.e., the VLC link). The PDF and the CDF of the first and the second links are given respectively as:

$$f_{h_P^2}(z) = \frac{\zeta}{z\sqrt{8\pi}\sigma_{h_p}} \exp\left(-\frac{(\zeta \ln(z) - (2\mu + \zeta \ln(c_1)))^2}{8\sigma_{h_p}^2}\right), \tag{4.31}$$

and

$$F_{h_v^2}(\Gamma) = \frac{-1}{r^2}\left((m_k+1)QL^{m_k+1}\right)^{\frac{2}{m_k+3}} h^{\frac{-1}{m_k+3}} + \left(1 + \frac{L^2}{r^2}\right), \tag{4.32}$$

where ζ is a scaling constant and it is equal to $10/\ln(10)$ and $c_1 = \frac{P_s e^{-2\alpha d_1}}{\sigma_r^2}$. Hermite–Gauss quadrature is used to obtain an accurate approximation for Equation (4.31). Finally, by substituting Equations (4.31) and (4.32) into Equation (4.30), the outage probability of the proposed system can be determined.

4.3.1.3 Numerical Results

This subsection presents some numerical results of the derived expressions with Monte Carlo simulations. Monte Carlo simulation is a model widely used to predict the probability of different outcomes when deadline with random variables which is common when studying in communication channel fading. The system parameters which are considered in our evaluations are, unless indicated otherwise, as in Table 4.1. These parameters represent practical PLC and VLC environments [140, 99].

Table 4.1 Parameters of the hybrid PLC/VLC system.

Parameter	Value
Operating frequency	500 kHz
Exponent of the attenuation factor of PLC	0.7
a_0	2.03×10^{-3}
a_1	3.75×10^{-7}
d_1	30 m
P_s	1 W
P_r	1 W
G	10 dB
SNR	10 dB
A_d	0.001 cm
$U(\Psi_K) = g(\Psi_K)$	1 dB
R_p	0.4 A/W
r_e	3.6 m
L	2.15 m
$\phi/2$	60°
FoV	60°

Average Capacity

To demonstrate the impact of the source-to-relay distance on the system performance, the average capacity is plotted in Figure 4.2 which shows that the average capacity of the system significantly improves when the relay gain increases and this justifies the use of a relay in the system. As seen in the figure, the average capacity is low when the relay gain is 0 dB compared to its values for higher gains. It is clear that the system

becomes more efficient when the relay gain increases and the vertical distance between the relay and the user plane decreases.

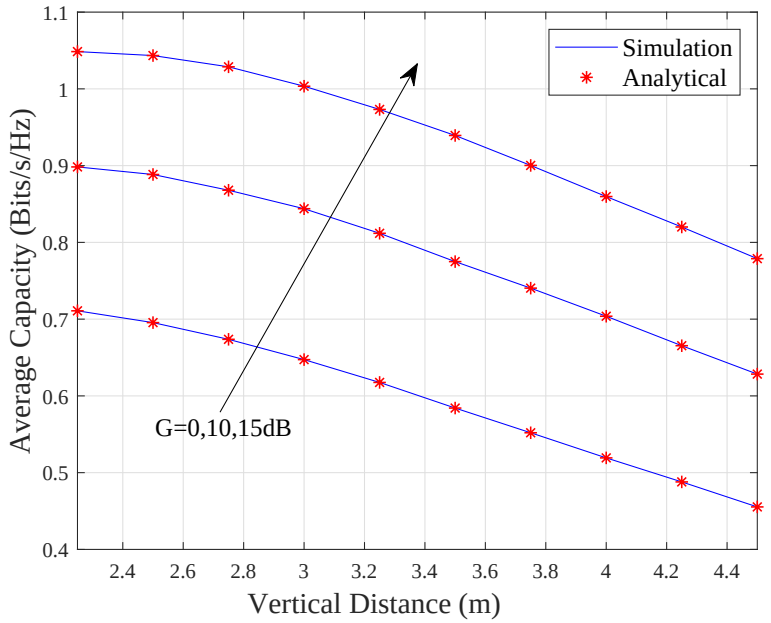

Figure 4.2 Average capacity with respect to the vertical distance to the user plane for three values of relay gain.

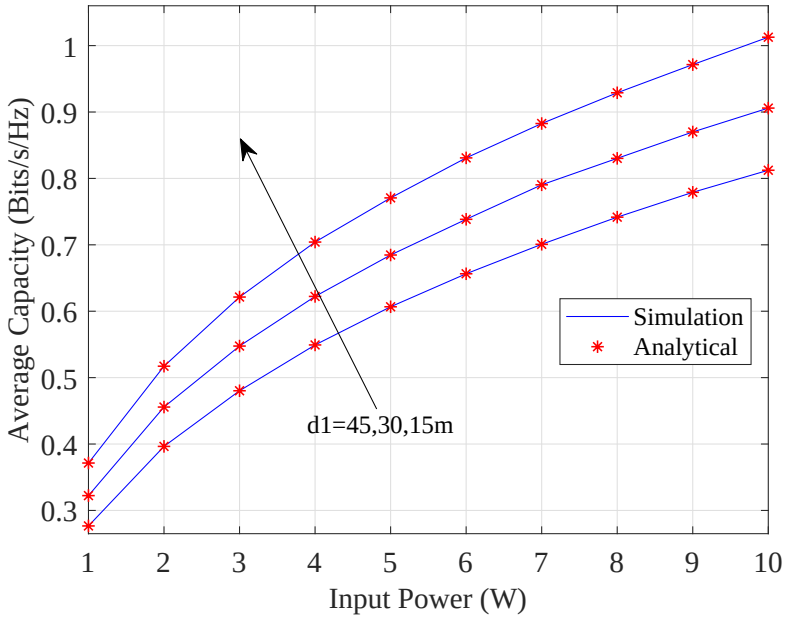

Figure 4.3 Average capacity versus input power for different values of source-relay distance.

To demonstrate the impact of the source-to-relay distance on the system performance, the average capacity is plotted in Figure 4.3 versus input power for different link lengths.

It is obvious that there is a near-perfect agreement between the simulated and the analytical results, obtained from Equation (4.9). It is also clear that the capacity improves as the input power increases. On the other hand, a performance degradation can be clearly seen when the distance between the source and relay increases.

Outage Probability

The calculated outage probability of the proposed system is presented in Figures 4.4 and 4.5. The outage probability is plotted versus the vertical LED distance to the user plane for different values of the AF relay gain in Figure 4.4. It can be seen that the relay gain has a positive effect on the performance of the system under consideration, the outage probability increases when the relay gain decreases. On the other hand, the height of the LED has a negative impact on the system performance as the outage probability becomes higher when the vertical distance increases.

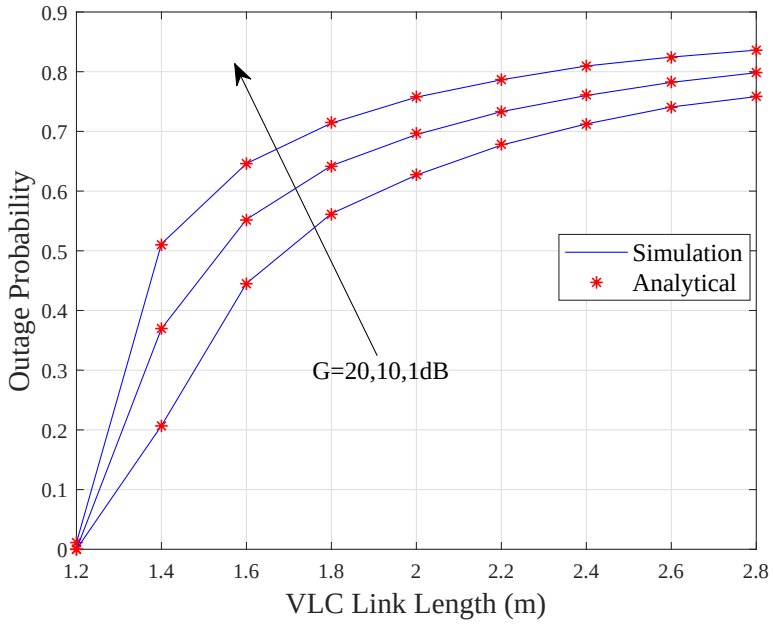

Figure 4.4 Outage probability versus VLC link length for different values of relay gain.

In Figure 4.5 the outage probability of the AF-relay based PLC/VLC system is plotted with respect to the threshold for different values of the relay transmit power. Looking at the figure, it is clear that the outage probability lessens as the relay transmit power increases. However, the outage probability increases with increase in threshold value. A closer look at Figures 4.4 and 4.5, shows that both relay gain and transmit power can significantly enhance the performance of the proposed system.

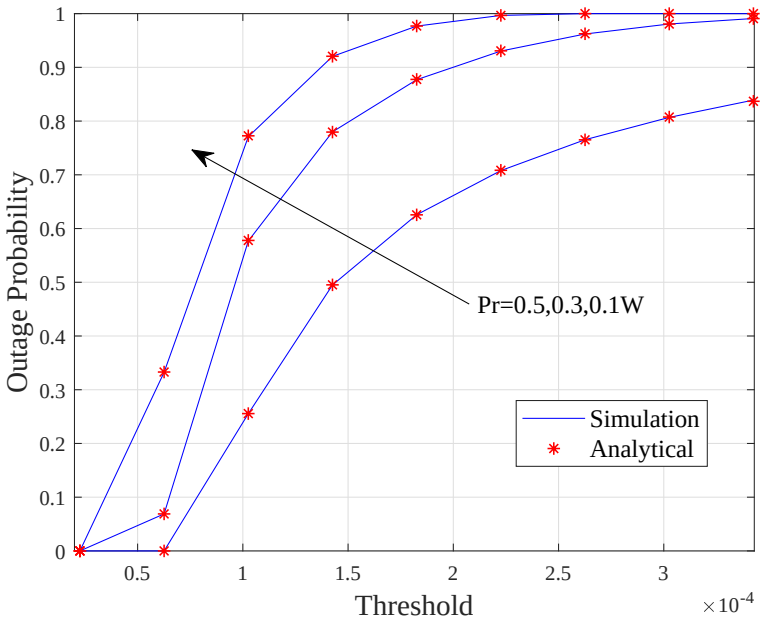

Figure 4.5 Outage probability with respect to threshold for different values of relay transmit power.

4.3.2 Performance analysis of DF-Based PLC/VLC System

In this subsection, analytical expressions of the average capacity and outage probability of the hybrid PLC/VLC system in the presence of a DF relay are derived.

4.3.2.1 Average Capacity

As with the AF-based system, communication over the DF-based PLAC/VLC system is divided into two phases. In the first, the signal is sent to the DF relay through the PLC link, then it is decoded and forwarded by the DF relay through the VLC link to its destination. The instantaneous capacity of this hybrid system is given by:

$$C = \min(C_{PLC}, C_{VLC}), \tag{4.33}$$

where C_{PLC} and C_{VLC} are the instantaneous capacities of the PLC and VLC links.

Thus, the capacity of each link should be derived to find the overall capacity. The start is with the PLC link which connects the transmitter with the DF relay and acts as a backhaul to the VLC link. The signal at the relay can be given by:

$$y_r(t) = \sqrt{P_s} e^{-\alpha d_1} h_{PS}(t) + n_r, \tag{4.34}$$

The SNR at the DF relay can be written as:

$$\gamma_r = \frac{P_s e^{-2\alpha d_1} |h_P|^2}{\sigma_r^2}. \tag{4.35}$$

Mathematically, the average capacity of this system can be calculated as:

$$C_P = \int_0^\infty \log_2(1+\gamma_r) f_\gamma(\gamma_r) d\gamma, \tag{4.36}$$

where $f_\gamma(\gamma_r)$ is the PDF of γ_r given by:

$$f_\gamma(\gamma) = \frac{\zeta}{z\sqrt{8\pi}\sigma} \exp\left(-\frac{(\zeta \ln(\gamma) - (2\mu + \zeta \ln(a_1)))^2}{8\sigma^2}\right), \tag{4.37}$$

where ζ is the scaling constant and it is equal to $10/\ln(10)$ and $a_1 = \frac{P_s e^{-2\alpha d}}{\sigma_{d2}^2}$. Hermite–Gauss quadrature is used to obtain an accurate approximation for Equation (4.36). It is assumed:

$$x = \frac{\zeta \ln(\gamma) - 2\mu + \zeta \ln(a_m)}{8\sigma^2}. \tag{4.38}$$

Now, Equation (4.36) is written as:

$$C_P = \int_\infty^\infty \frac{1}{\pi} h(x) \exp[-x^2] dx. \tag{4.39}$$

Using Hermite–Gauss quadrature Equation (4.39) can be expressed as:

$$C_P = \frac{1}{\sqrt{\pi}} \sum_{n=1}^{N_p} H_{x_n} h(x_n), \tag{4.40}$$

where

$$h(x_n) = \log_2\left(1 + \exp\left(\frac{\sqrt{8}\sigma x_n + 2\mu + \zeta ln\phi/2(a_1)}{\zeta}\right)\right). \tag{4.41}$$

Now the calculation of the average capacity of the VLC link. The received signal at the VLC user can be expressed as:

$$y_d(t) = s_2(t) h_v \sqrt{P_r} + n_d, \tag{4.42}$$

where $s_2(t)$ is the information signal with E[s]=1, P_r is the relay transmit power and n_d represents the destination noise with zero mean and variance σ_d^2.

The SNR at the destination can be written as:

$$\gamma_d = \frac{G^2 P_r |h_v|^2}{\sigma_d^2}. \tag{4.43}$$

The average capacity of the VLC link can be calculated from:

$$\mathrm{E}[C_{VLC}] = \int_{t_{min}}^{t_{max}} \log_2(1+\gamma_d)\, f_\gamma(\gamma_d) d\gamma, \tag{4.44}$$

where $f_\gamma(\gamma_d)$ is the PDF of γ_d, $t_{min} = \frac{\left(Q(m_k+1)L^{m_k+1}\right)^2}{(r^2+L^2)^{m_k+3}}$ and $t_{max} = \frac{\left(Q(m_k+1)L^{m_k+1}\right)^2}{L^{2(m_k+3)}}$. The PDF of h_k^2 is given by Equation (4.19) as:

$$f_{h_k^2} = \frac{-Q^{\frac{2}{2+m}}\left((m_k+1)L^{m_k+1}\right)^{\frac{2}{m+3}} h^{-\frac{m_k+4}{m_k+3}} h^{\frac{1}{m_k+3}}}{(m_k+3)r^2}. \tag{4.45}$$

Substituting Equations(4.43) and (4.45) in Equation (4.44), Equation (4.46) is obtained:

$$\mathrm{E}[C_{VLC}] = \frac{1}{2\log[2]} \int_{t_{min}}^{t_{max}} \log\left[1+\frac{P_r}{\sigma_d^2}h\right] \left(\frac{-Q^{\frac{2}{2+m}}\left((m_k+1)L^{m_k+1}\right)^{\frac{2}{m+3}} h^{-\frac{m_k+4}{m_k+3}} h^{\frac{1}{m_k+3}}}{(m_k+3)r^2}\right). \tag{4.46}$$

Substituting t_{min}, t_{max} values in Equation (4.46), Equation (4.47) can be obtained:

$$\begin{aligned} E[C_{VLC}] = \frac{\frac{1}{(m_k+3)r^2}\left(Q(m_k+1)L^{m_k+1}\right)^{\frac{2}{m+3}}}{2\log[2]}(m_k+3)\Bigg(t_{max}^{-\frac{1}{m_k+3}}\Bigg(-3-m_k+(3+m_k)_2 \\ F_1\left[1,-\frac{1}{m_k+3},\frac{m_k+2}{m_k+3},-t_{max}\frac{P_r}{\sigma_d^2}\right]-log\left[1+t_{max}\frac{P_r}{\sigma_d^2}\right]\Bigg) \\ -t_{min}^{-\frac{1}{m_k+3}}\Bigg(-3-m_k+(3+m_k)_2 F_1\left[1,-\frac{1}{m_k+3},\frac{m_k+2}{m_k+3},-t_{min}\frac{P_r}{\sigma_d^2}\right] \\ -log\left[1+t_{min}\frac{P_r}{\sigma_d^2}\right]\Bigg)\Bigg). \end{aligned} \tag{4.47}$$

4.3.2.2 Outage Probability

The outage probability, O_{outage} is given as:

$$O_{outage} = P_r\left[C < R_{th}\right]. \tag{4.48}$$

The end-to-end outage probability for the proposed system can be written as:

$$O_{outage} = O_{out}^{PLC} + \left(1 - O_{out}^{PLC}\right) O_{out}^{VLC}, \tag{4.49}$$

where $O_{out}^{PLC}$is outage probability of the first segment (PLC link) and O_{out}^{VLC} is the outage probability of the second segment (VLC link).

The CDF of each link represents the outage probability of that link. Therefore, the outage probability of the PLC and VLC links can be respectively calculated as:

$$O_{out}^{PLC} = \int_0^{\infty} \frac{\zeta}{z\sqrt{8\pi}\sigma} \exp\left(-\frac{(\zeta \ln(\gamma) - (2\mu + \zeta \ln(a_1)))^2}{8\sigma^2}\right) d_z, \tag{4.50}$$

and

$$O_{out}^{VLC} = \frac{-1}{r^2}\left((m_k+1)\,QL^{m_k+1}\right)^{\frac{2}{m_k+3}} h^{\frac{-1}{m_k+3}} + \left(1 + \frac{L^2}{r^2}\right). \tag{4.51}$$

The total outage probability of the DF-based PLC/VLC can be found by substituting Equations (4.50) and (4.51) into Equation (4.49).

4.3.2.3 Numerical Results

This sub-subsection presents some of the numerical results of the analytical expressions of both average capacity and outage probability of the cooperative DF-based PLC/VLC system. The analytical results of these expressions are validated with Monte Carlo simulations. The system parameters which are considered in our evaluations are, unless indicated otherwise, as in Table 4.1.

Average Capacity

The effect of different system parameters on the average capacity of the hybrid PLC/VLC system is assessed in this sub-section. For example, in Figure 4.6, the average capacity is plotted with respect to the source-to-relay distance for different values of source power. This is to demonstrate the impact of both the length of PLC link (distance from source to relay) and the source transmit power on the performance of the system. The results confirmed the previous studies as they showed that the performance of the system is inversely proportional with distance and the system performs better when the relay transmit power increases. It is clear from this figure that the hybrid PLC/VLC system performs better with shorter source-to-relay distances (PLC link length) than longer distances. The figure also shows that the source transmit power has a positive effect on system performance.

Figure 4.7 illustrates the effect of relay transmit power and vertical distance of the LED from the working plane, on the performance (average capacity) of the DF-based PLC/VLC system. It is noticeable from this figure that the average capacity of the system noticeably improves when the relay transmit power increases. It also shows that increasing the vertical distance between relay and user plane has a negative impact on the performance of the system, the average capacity of the system degrades when the

vertical height of the LED increases. However, it is clear from both Figures 4.6 and 4.7 that there is near-perfect agreement between the simulated and the analytical results, obtained from Equation (4.33).

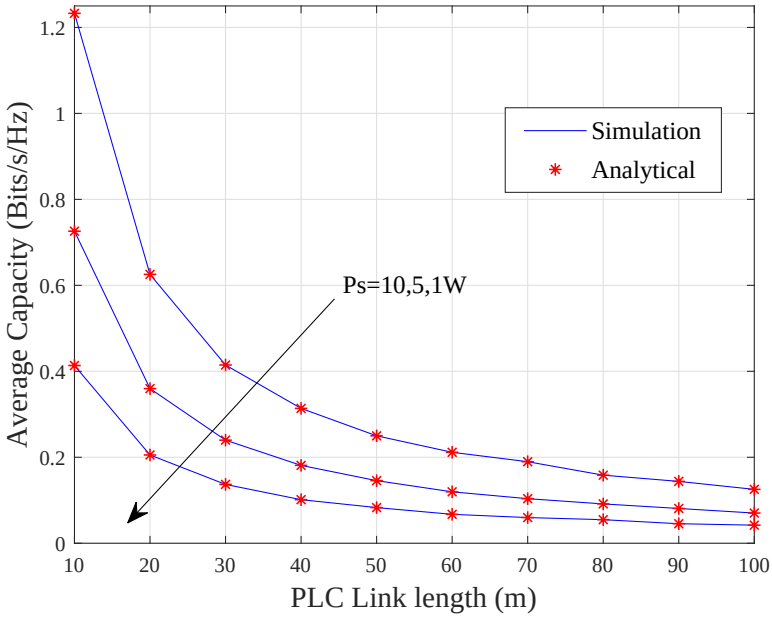

Figure 4.6 Average capacity with respect to source-to-relay distance for different values of source transmit power.

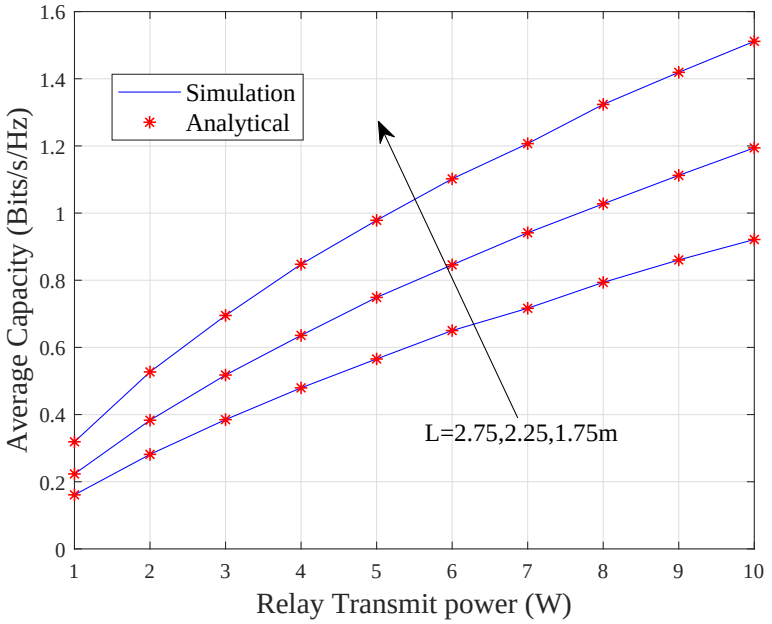

Figure 4.7 Average capacity versus relay transmit power for three values of the vertical height of the LED.

Outage Probability

The outage probability of the proposed DF-based PLC/VLC system is presented in Figures 4.8 and 4.9. Figure 4.8 illustrates the outage probability of the system with source-to-relay distance for three values of source transmit power, 1, 5 and 10 W. It is noticeable that the proposed system has lower outage probability for higher values of the source transmit power. However, the outage probability increases with increase of distance between source and relay. For example, the outage probability of the system is less than 0.2 when the PLC link length is less than 3 m for all three transmit powers, but is greater than 0.7 for all three transmit powers when source-to-relay distance is more than 7 m.

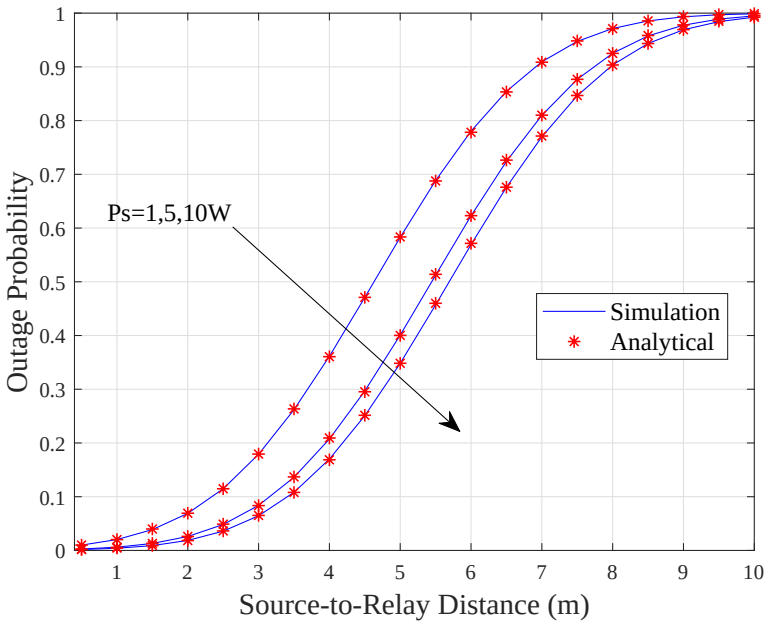

Figure 4.8 Outage probability with source-to-relay distance for three values of relay transmit power.

In Figure 4.9, to show the effect of height of the LED above the working plane on the system performance, the outage probability is plotted with respect to the threshold for three different values of LED height. As it can be seen, the vertical distance has a negative impact on the performance of the proposed system. The outage probability increases as the vertical height of the LED increases. It is also shown that the threshold values can considerably degrade the performance of the system, outage probability increases as the threshold value increases. It is worth mentioning that one of the important achievements of this chapter is that there were near-perfect agreements between the analytical results and the simulation ones which would prove the accuracy of derived expressions.

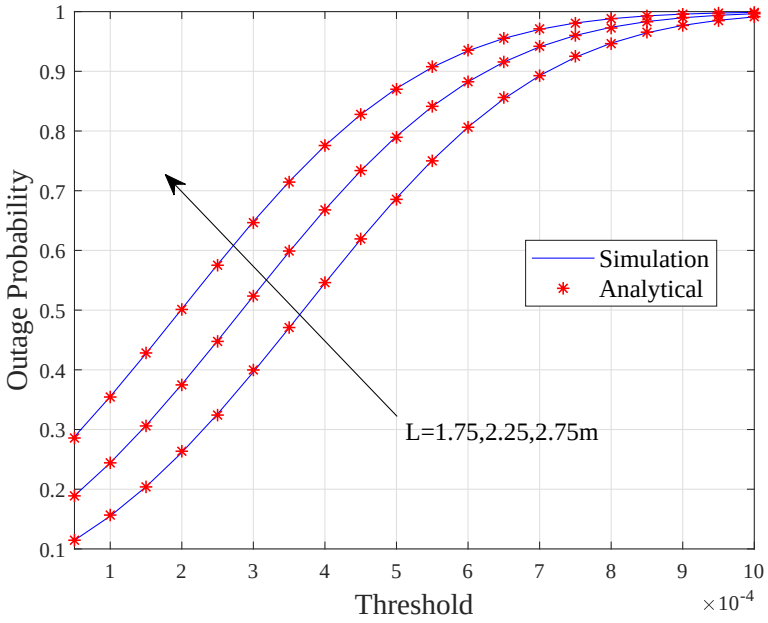

Figure 4.9 Outage probability versus the threshold value for three values of vertical distance of LED from user plane..

4.3.3 Performance comparison between AF-Based and DF-Based PLC/VLC Systems

In this subsection, a comparison in the performance of the AF-based PLC/VLC and DF-based PLC/VLC is presented by comparing the average capacity and the outage probability of each system with the other. The system parameters which are considered in this comparison are, unless indicated otherwise, as in Table 4.1. However, the gain of the AF relay is taken as 0dB. Figures 4.10 and 4.11 show the comparative performances of both systems.

The results of the performance comparison confirmed that the DF-based cooperative system outperforms the AF-based one. This can easily be explained, with the AF-based system the relay amplifies the received signal then forwards it through the second link. This causes amplification of the noise and thus reduces the signal-to-noise ratio, which leads to a noticeable performance degradation. On the other hand, in the DF-based system, the relay decodes the received signal before forwarding it to the destination node. In Figure 4.10 the average capacity of both systems is plotted with respect to the source power. It is clear from this figure that the average capacity of the DF-based system is greater than that of the AF-based system for all values of source power. For additional performance analysis, the outage probability of AF-based and DF-based systems are presented against source-to-relay distance in Figure 4.11. It is obvious that the performance of the system with the DF relay is better than that of the system with AF.

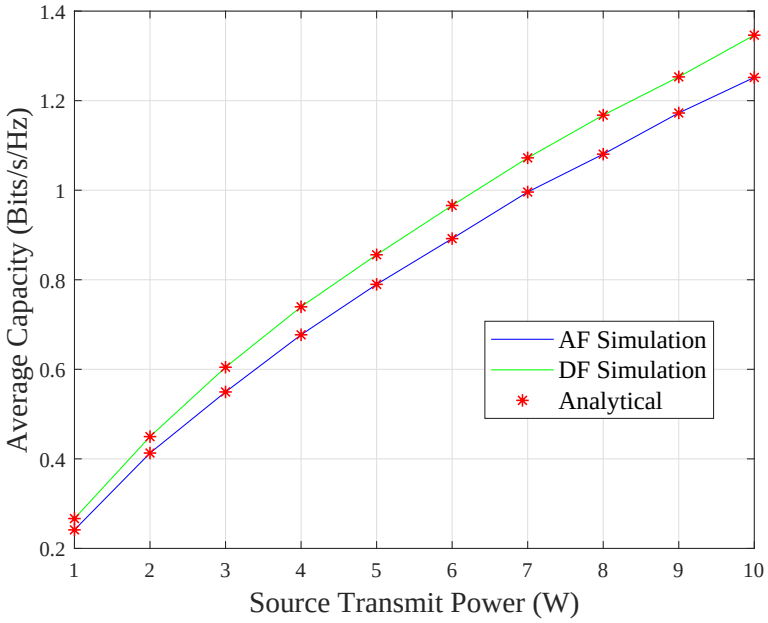

Figure 4.10 Average capacity for AF and DF based systems with respect to source transmit power for different values of PLC link length

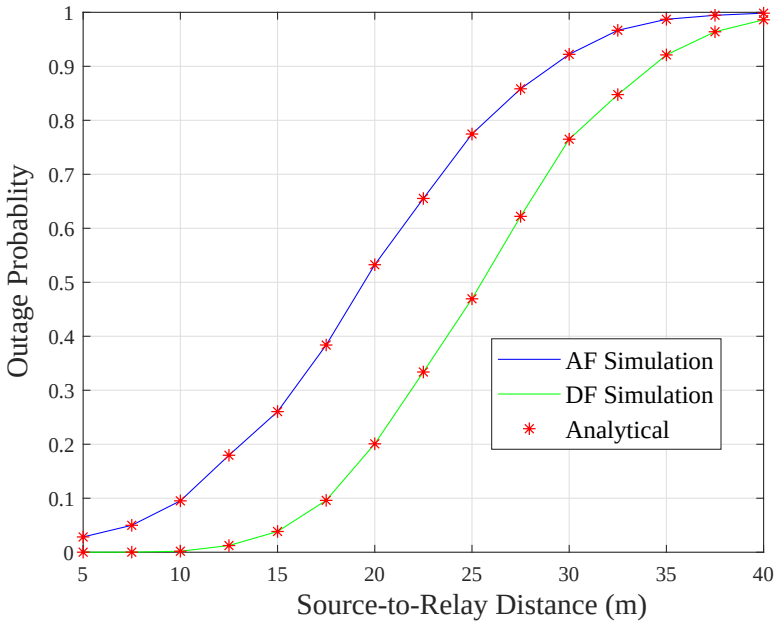

Figure 4.11 Outage probability for AF and DF based systems with respect to threshold for different values of vertical distance to user plane.

4.4 Summary

Relay-based cooperative communication systems are used to increase the coverage range and the channel capacity, which in turns enhances the performance. In this thesis, the hybrid system is not only implemented to improve the performance but to connect the VLC systems with the source of the information as VLC systems cannot be connected to it directly. In this chapter, the performance of the proposed in-train hybrid PLC/VLC system was discussed in terms of average capacity and outage probability with DF and AF relay protocols. Analytical expressions for these performance metrics were derived and then verified by Monte Carlo simulations. The effects of several system parameters were investigated. The results confirmed that the performance of the proposed hybrid system is affected by changes in: source power, source-to-relay distance, the transmit power relay, the height of the light source above the work plane, and the gain of the relay.

The results showed that increasing the gain of the AF relay has a positive effect on the performance of the AF-based system. The performance of both AF and DF systems is also affected by the vertical distance between the LED and the user plane. It was confirmed that increasing the source-to-relay distance negatively affected performance. It was also demonstrated that increasing both source and relay transmit power can significantly enhance the performance of a relay-based hybrid system. A performance comparison was conducted between AF-based and DF-based PLC/VLC systems. The outcomes of the comparison showed that the performance of a cooperative PLC/VLC system with DF relay was better than that of the AF-based system. However, it is worth pointing out that implementing relays with communication systems can considerably enhance the performance and reliability, but the system will consume more power. Power consumption of the entire system is discussed in the next chapter.

Chapter 5

Performance Analysis of Relay-based VLC Systems

Chapter 3 discussed the OLE system as communication medium between public networks and in-train communication systems (i.e., PLC and VLC). Chapter 4 Chapter 4 discussed the performance of in-train PLC/VLC systems in the presence of relays between both links. However, it was pointed out that implementing relays with communication systems can increase the overall energy consumption of the system. Thus, this chapter investigates the performance of relay-based VLC systems, as a last-metre access technology of in-train applications, in terms of outage probability and energy consumption. Accurate analytical expressions for the overall outage probability and energy-per-bit consumption of the proposed system configurations, including single-hop and multi-hop approaches are derived.

It was shown that the SDF and IDF protocols have superiority over the single-hop and multi-hop DF approaches in terms of outage probability and energy efficiency. However, the IDF configuration has the best energy consumption performance compared to the other VLC system configurations which were considered in this work. The analyses also revealed that increasing the relay number on the network can dramatically improve the outage probability of the system but it contributes more to the energy consumption; thus, the system is less energy efficient.

5.1 Introduction

Visible light communication (VLC) access technology, which uses light-producing devices for the dual purpose of lighting and data transmission, can complement radio frequency (RF) technology as a last-metre indoor application. This technology can provide network access in offices, homes, trains, shopping centres, etc. [173–176]. Despite the advantages, connectivity disruption during the movement of the end-user is a major challenge to VLC technology. This is because the short cell size of VLC links requires frequent handovers between VLC cells. Furthermore, light interference caused by the overlapping of neighboring LEDs in the VLC environment can negatively affect transmission over a VLC network [14, 177, 94]. Transmission failure can also happen due to shadowing, caused by moving objects, blocking VLC links.

For better reliability and greater coverage, different light sources in in-train environments, such as ceiling and wall lights could be deployed as relay nodes to provide better mobility to end users [16, 178, 179]. Different relaying protocols, generally categorized into cooperative and non-cooperative, are often used in communication systems to ensure high performance and reliability. These protocols include amplify and-forward (AF), compress-and-forward (CF), decode-and-forward (DF), selective DF (SDF), and incremental DF (IDF) relaying protocols. However, increasing the number of VLC modems increases the total power consumption of the entire system.

This chapter studies the outage probability and energy per bit consumption performance of a half-duplex (HD) conventional DF relay system and cooperative systems (SDF and IDF) over VLC channels. The single-hop scenario is also considered and investigated as a benchmark against which to compare the cooperative systems. Accurate analytical expressions for the overall outage probability and energy-per-bit consumption of the proposed system configurations, including single-hop and multi-hop approaches are derived. This chapter also measures and studies the effect of number of relays on the network, source power, and vertical distance of the VLC environment, on the performance of the system. Monte Carlo simulations, which is an efficient method to model and simulation communication systems both wired and wireless, are used to validate the theoretical results of the derived expressions.

5.2 System Model

The system model of the proposed in-train, multi-hop relaying VLC system is presented in Figure 5.1. The assumption is that LEDs which are the data sources send the information directly to the destination through the VLC link. In case of transmission failure due to LED fault or shadowing, data is forwarded by relay nodes (i.e., intermediate light sources) to the destinations. In our case, link C between the VLC source and end-user

is disconnected due to shadowing. Therefore, the destination node is connected to the source node through intermediate relay node. For example, is route A-B via a relay node situated on the carriage wall above the seated passenger.

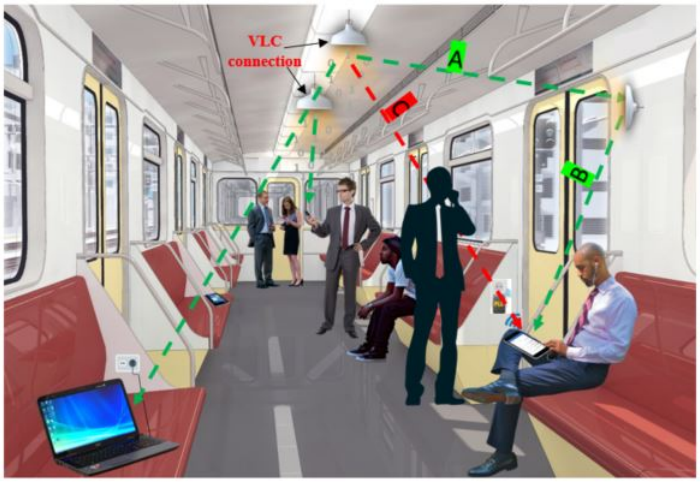

Figure 5.1 The proposed system model which consists of direct and relay nodes.

As specified previously, in this analysis, only the line-of-sight (LoS) VLC channel is considered, as it typically represents more than 90% of the total received signal [170, 18]. The source nodes (the LEDs) are situated on the ceiling with Euclidean distances d to the destinations/relays and vertical distances L to the users/relay plane, as shown in Figure 5.2. It is assumed that the VLC links between the nodes are randomly distributed, and the user locations are uniformly distributed [180, 181]. For simplicity and without loss of generality, it is assumed that the noise over the VLC and RF channels is AWGN.

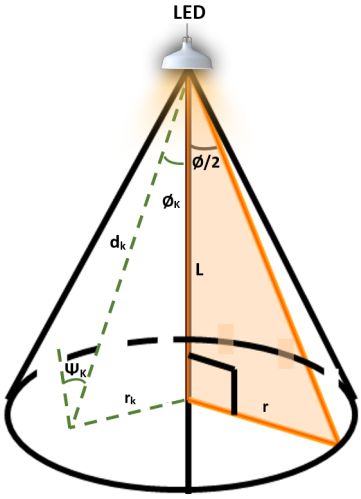

Figure 5.2 LoS channels for the VLC environment.

5.3 Performance Analysis

The outage probability and energy efficiency performance of all the proposed VLC system configurations are analyzed in this section. Each configuration contains two nodes: a source (S) and a destination (D). The communication between these two VLC nodes is achieved either via N intermediate relays, as shown in 5.3a, or through a direct VLC link, as in Figure 5.3b. In the former configuration, the nth relay is denoted as R_n where $n \in [1, N]$. On the other hand, in the single-phase configuration, end-to-end communication is accomplished without relaying.

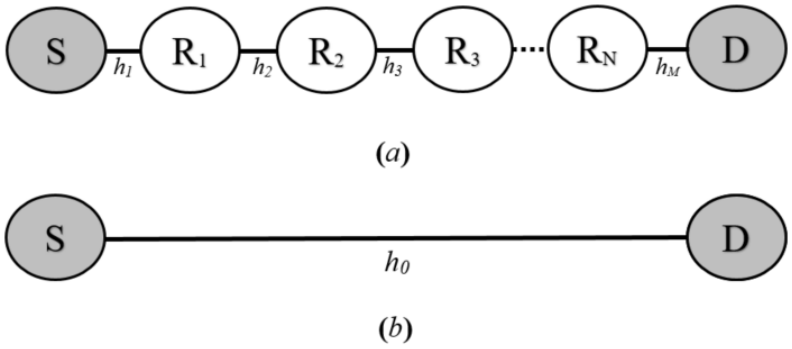

Figure 5.3 Basic block diagrams of the proposed VLC systems, (**a**) with N intermediate VLC relays, and (**b**) with a direct VLC link.

5.3.1 Single-Hop VLC System

This system is a one-phase system where only two nodes, source and destination modems, are involved in the overall communication process. The energy per-bit consumption for a single-hop VCL system can be expressed as [140]:

$$E_{b,SH} = \frac{P_{t,SH}}{R_b}, \tag{5.1}$$

where $E_{b,SH}$ is the energy-per-bit consumption of the single-hop system, $P_{t,SH}$ denotes the average optimal source power which is required to achieve the desired outage probability for the single-phase approach. R_b represents the data rate, calculated by multiplying the bandwidth (B) and spectral efficiency (ε).

The overall outage probability of the direct link needs to be derived in order to determine $P_{t,SH}$. The received signal of a direct-link VLC link at the destination node y_d is:

$$y_d = \sqrt{P_{t,SH}} h_0 s(t) + n, \tag{5.2}$$

where h_0 is the gain of direct channel, $s(t)$ denotes the useful sent signal with E[s]=1, and n represents the destination noise with variance σ^2 and zero mean.

The SNR at the destination node is given by:

$$\gamma = \frac{P_{t,SH}\,|h_0|^2}{\sigma^2}. \tag{5.3}$$

Using Equation (5.3), the probability of the direct-link that is below the desired threshold ω, can be expressed as:

$$O_{SH} = \Pr\left\{\log_2\left(1+\gamma\right) < \omega\right\}. \tag{5.4}$$

This equation can be mathematically manipulated to give:

$$O_{SH} = \Pr\left\{\gamma < \left(2^{\omega}-1\right)\right\}. \tag{5.5}$$

Here, Equation (5.5) indicates the CDF of the VLC link which can be written as:

$$O_{SH} = F_{\gamma}(2^{\omega}-1), \tag{5.6}$$

where $F_{\gamma}(\cdot)$ is the CDF of γ.

Furthermore, according to [16] the PDF of the instantaneous SNR of the VLC channel gain can be written as:

$$f_{h_k^2}(t) = \frac{-Q^{\frac{2}{2+m_k}}\left((m_k+1)L^{m_k+1}\right)^{\frac{2}{(m_k+3)}}\,t^{-\frac{m_k+5}{(m_k+3)}}}{(m_k+1)r^2}, \tag{5.7}$$

$$Q = \frac{1}{2\pi}AU\left(\phi_K\right)g\left(\phi_K\right)R_{ph}, \tag{5.8}$$

where $t \in [C_{min}, C_{max}]$, $C_{min} = \frac{\left(Q(m_k+1)L^{m_k+1}\right)^2}{(r^2+L^2)^{m_k+3}}$ and $C_{max} = \frac{\left(Q(m_k+1)L^{m_k+1}\right)^2}{L^{2(m_k+3)}}$, as indicated in [180, 16], A is the effective area of detector, $U\left(\phi_K\right)$ and $g\left(\phi_K\right)$ are the optical filter and concentration gains, respectively. R_{ph} is the responsivity of the photo-detector, L is the direct distance from the LED to the user plane, r represents the maximum cell radius of the VLC environment, see Figure 5.2, and m_k is the order of the Lambertian radiation pattern which is given by:

$$m_k = \frac{-1}{\log_2(cos(\phi/2))}, \tag{5.9}$$

where $\phi/2$ represents the semi-angle of the LoS, again ee Figure 5.2,.

Hence, the CDF of the direct VLC link can be calculated by integrating Equation (5.7) over $[C_{min}, C_{max}]$, which represents the overall outage probability of the VLC link, O_{VLC}.

$$O_{VLC} = \frac{-1}{r^2}\left(\alpha Q L^{\alpha}\right)^{\frac{2}{\beta}}h^{-\frac{1}{\beta}} + \left(1+\frac{L^2}{r^2}\right), \tag{5.10}$$

where $\beta = m_k + 3$ and $\alpha = m_k + 1$.

using Equation (5.10), the end-to-end outage probability of the proposed single-hop approach can be calculated as:

$$O_{SH} = \frac{-1}{r^2} \left(\alpha Q L_{SH}^{\alpha}\right)^{\frac{2}{\beta}} \left(|h_0|^2\right)^{-\frac{1}{\beta}} + \left(1 + \frac{L_{SH}^2}{r^2}\right). \tag{5.11}$$

where Ł$_{SH}$ is the vertical distance of the direct link.

We now obtain $f_{(h_0)^2} F\left(\frac{\delta\sigma^2}{P_{t,SH}}\right)$.

$$O_{SH} = \frac{-1}{r^2} \left(\alpha Q L_{SH}^{\alpha}\right)^{\frac{2}{\beta}} \left(\frac{\delta\sigma^2}{P_{t,SH}}\right)^{\frac{-1}{\beta}} + \left(1 + \frac{L_{SH}^2}{r^2}\right), \tag{5.12}$$

where $\delta = (2^{\omega} - 1)$.

By rearranging Equation (5.12) and solving for $P_{t,SH}$, we get

$$P_{t,SH} = \left(\frac{\left(\delta\sigma^2\right)^{\frac{-1}{\beta}} \left(\alpha Q L_{SH}^{\alpha}\right)^{\frac{2}{\beta}}}{-r^2 O_{SH} + r^2 + L_{SH}^2}\right)^{-\beta}. \tag{5.13}$$

Finally, by substituting Equation (5.13) into Equation (5.1), the energy consumed per bit of the configuration being considered is obtained:

$$E_{SH} = \frac{1}{R_b} \left(\frac{\left(\delta\sigma^2\right)^{\frac{-1}{\beta}} \left(\alpha Q L_{SH}^{\alpha}\right)^{\frac{2}{\beta}}}{-r^2 O_{SH} + r^2 + L_{SH}^2}\right)^{-\beta}. \tag{5.14}$$

5.3.2 Multi-Hop VLC System

In this subsection, both outage probability and energy efficiency of the different multi-hop relay protocols are analyzed.

5.3.2.1 Decode-and-Forward Relaying Protocol

The non-cooperative DF configuration is where there is no direct link between the destination and source nodes, they communicate only through the DF relay which receives the data from the source then decodes and forwards it to the end-users. It is presumed that the DF nodes are positioned equal-distant from source and destination nodes. First, the expressions for the cases when M=2, and 3 are derived. These expressions are crucial parts in the analysis because they allow us to determine the pattern of the generalized expression of the multi-hop scenario.

- Performance Analysis for a Two-Link Scenario $M = 2$

In such a configuration, the consumed energy is calculated as follows [140]

$$E_{MH2} = \frac{P_{MH2}}{R_b}\left(O_{SR_1} + 2O^c_{SR_1}\right), \tag{5.15}$$

where P_{MH-2} is the transmit power of the two-link system, O_{SR_1} denotes the outage probability of the source-to-relay link and $O^c_{SR_1}$ is its complementary which is equal to $1 - O_{SR_1}$.

For a two-link scenario, , it is considered that the relay is placed half-way between both end-nodes (i.e., $L_{SR_1} = L_{R_1D}$), the overall outage probability of this system can be expressed as [140]:

$$O_2 = O_{SR_1} + O^c_{SR_1} O_{R_1D}, \tag{5.16}$$

where O_{R_1D} is the outage probability of the relay-to-destination link.

Now, assuming that source transmit power is equal to that of the DF relay (i.e., $P_{SR_1} = P_{R_1D}$) then following the same steps of subsection 5.3.1, O_{SR_1} and O_{R_1D} can be defined as:

$$O_{SR_1} = \frac{-1}{r^2}\left(\alpha Q L^{\alpha}_{SR_1}\right)^{\frac{2}{\beta}} \left(\frac{\delta\sigma^2_{r_1}}{P_{SR_1}}\right)^{\frac{-1}{\beta}} + \left(1 + \frac{L^2_{SR_1}}{r^2}\right), \tag{5.17}$$

$$O_{R_1D} = \frac{-1}{r^2}\left(\alpha Q L^{\alpha}_{R_1D}\right)^{\frac{2}{\beta}} \left(\frac{\delta\sigma^2}{P_{R_1D}}\right)^{\frac{-1}{\beta}} + \left(1 + \frac{L^2_{R_1D}}{r^2}\right), \tag{5.18}$$

where $\sigma^2_{r_1}$ represents the variance of additive white Gaussian noise at the DF relay node. As both links of the DF-based system are identical, the outage probabilities of both links will be the same (i.e., $O_{SR_1} = O_{R_1D}$), then the outage probability of the entire system can be given as:

$$O_2 = O^*\left(2 - (O^*)\right), \tag{5.19}$$

where $O^* = O_{SR_1} = O_{R_1D}$.

Substituting Equations(5.17) and (5.18) into Equation (5.19), the outage probability of the link can expressed as:

$$O_2 = \left(\frac{-1}{r^2}\left(\alpha Q L^{\alpha}_2\right)^{\frac{2}{\beta}} \left(\frac{\delta\sigma^2_2}{P_{MH2}}\right)^{\frac{-1}{\beta}} + \left(1 + \frac{L^2_2}{r^2}\right)\right) \left(2 - \left(\frac{-1}{r^2}\left(\alpha Q L^{\alpha}_2\right)^{\frac{2}{\beta}} \left(\frac{\delta\sigma^2_2}{P_{MH2}}\right)^{\frac{-1}{\beta}} + \left(1 + \frac{L^2_2}{r^2}\right)\right)\right), \tag{5.20}$$

where $P_{MH2} = P_{SR_1} = P_{R_1D}$, $L_2 = L_{SR_1} = L_{R_1D}$ and $\sigma_2^2 = \sigma_{r_1}^2 = \sigma^2$.

Rearranging Equation (5.20) and solving for P_{MH2}, the optimal transmit power for the two-hop scenario can be obtained as:

$$P_{MH2} = \delta\sigma_2^2 \left(\frac{(1-(1-O_2)^{0.5}) - \left(1+\frac{L_2^2}{r^2}\right)}{\frac{-1}{r^2}\left(\alpha Q L_2^{\alpha}\right)^{\frac{2}{\beta}}} \right)^{\beta}. \tag{5.21}$$

Finally, by substituting Equation (5.21) into Equation (5.15), the energy consumption of the two-hop configuration can be obtained as:

$$E_{MH2} = \frac{1}{R_b} \left(\delta\sigma_2^2 \left(\frac{(1-(1-O_2)^{0.5}) - \left(1+\frac{L_2^2}{r^2}\right)}{\frac{-1}{r^2}\left(\alpha Q L_2^{\alpha}\right)^{\frac{2}{\beta}}} \right)^{\beta} \right) \left(O_{SR_1} + 2O_{SR_1}^c \right). \tag{5.22}$$

- Performance Analysis for Three Links Scenario $M = 3$

In such scenarios, the energy consumption performance is calculated as follows:

$$E_{MH3} = \frac{P_{MH3}}{R_b} \left(O_{SR_1} + 2O_{SR_1}^c O_{R_1R_2} + 3O_{SR_1}^c O_{R_1R_2}^c \right), \tag{5.23}$$

where $O_{R_1R_2}$ denotes the second link outage probability (i.e., relay$_1$-to-relay$_2$ link) and $O_{R_1R_2}^c$ is its complementary.

Assuming that relays are spaced equally between both end-nodes, the end-to-end outage probability can be expressed as:

$$O_3 = O_{SR_1} + O_{SR_1}^c (O_{R_1R_2} + O_{R_1R_2}^c O_{R_2D}), \tag{5.24}$$

where O_{R_2D} represents the outage probability of relay$_2$-to-destination link. The outage probabilities of the links can be calculated as:

$$O_{SR_1} = \frac{-1}{r^2}\left(\alpha Q L_{SR_1}^{\alpha}\right)^{\frac{2}{\beta}} \left(\frac{\delta\sigma_{r_1}^2}{P_{SR_1}} \right)^{\frac{-1}{\beta}} + \left(1 + \frac{L_{SR_1}^2}{r^2}\right). \tag{5.25}$$

$$O_{R_1R_2} = \frac{-1}{r^2}\left(\alpha Q L_{R_1R_2}^{\alpha}\right)^{\frac{2}{\beta}} \left(\frac{\delta\sigma_{r_2}^2}{P_{R_1R_2}} \right)^{\frac{-1}{\beta}} + \left(1 + \frac{L_{R_1R_2}^2}{r^2}\right). \tag{5.26}$$

$$O_{R_2D} = \frac{-1}{r^2}\left(\alpha Q L_{R_2D}^{\alpha}\right)^{\frac{2}{\beta}}\left(\frac{\delta\sigma^2}{P_{R_2D}}\right)^{\frac{-1}{\beta}} + \left(1+\frac{L_{R_2D}^2}{r^2}\right). \tag{5.27}$$

The overall outage probability of this configuration can be calculated by substituting Equations (5.25), (5.26) and (5.27) into Equation (5.24). Rearranging Equation (5.24) and solving for P_{MH-3}:

$$P_{MH3} = \delta\sigma_3^2\left(\frac{(1-(1-O_3)^{0.3}) - \left(1+\frac{L_3^2}{r^2}\right)}{\frac{-1}{r^2}\left(\alpha Q L_3^{\alpha}\right)^{\frac{2}{\beta}}}\right)^{\beta}. \tag{5.28}$$

The energy consumed per bit for the 3-hop approach can be obtained by substituting Equation (5.28) into Equation (5.23), and is expressed as:

$$E_{MH3} = \frac{1}{R_b}\left(\delta\sigma_3^2\left(\frac{(1-(1-O_3)^{0.3}) - \left(1+\frac{L_3^2}{r^2}\right)}{\frac{-1}{r^2}\left(\alpha Q L_3^{\alpha}\right)^{\frac{2}{\beta}}}\right)^{\beta}\right)$$
$$\left(O_{SR_1} + 2O_{SR_1}^c O_{R_1R_2} + 3O_{SR_1}^c O_{R_1R_2}^c\right). \tag{5.29}$$

- Performance Analysis with M Hops

The overall outage probability of a VLC system with M hops can be found as follows:

$$O_{MH} = O_{SR_1} + \left[\sum_{n=1}^{N-1}\left(O_{R_nR_{n+1}} \times \prod_{j=1}^{n-1} O_{R_jR_{j+1}}^c\right)\right.$$
$$\left. + O_{R_ND} \times \prod_{n=1}^{N-1} O_{R_nR_{n+1}}^c\right] \times O_{SR_1}^c, \tag{5.30}$$

where

$$O_{SR_1} = \frac{-1}{r^2}\left(\alpha Q L_{SR_1}^{\alpha}\right)^{\frac{2}{\beta}}\left(\frac{\delta\sigma_{r_1}^2}{P_{SR_1}}\right)^{\frac{-1}{\beta}} + \left(1+\frac{L_{SR_1}^2}{r^2}\right), \tag{5.31}$$

$$O_{R_nR_{n+1}} = \frac{-1}{r^2}\left(\alpha Q L^{\alpha}_{R_nR_{n+1}}\right)^{\frac{2}{\beta}}\left(\frac{\delta\sigma^2_{r_1}}{P_{R_nR_{n+1}}}\right)^{\frac{-1}{\beta}} + \left(1+\frac{L^2_{R_nR_{n+1}}}{r^2}\right), \tag{5.32}$$

$$O_{R_ND} = \frac{-1}{r^2}\left(\alpha Q L^{\alpha}_{R_ND}\right)^{\frac{2}{\beta}}\left(\frac{\delta\sigma^2}{P_{R_ND}}\right)^{\frac{-1}{\beta}} + \left(1+\frac{L^2_{RD}}{r^2}\right), \tag{5.33}$$

where N represents the number of relays on the network and $n \in \{1, 2, ..., N\}$. The optimal transmission power for a known outage probability is given by:

$$P_{MH} = \delta\sigma^2_M\left(\frac{(1-(1-O_M)^{\frac{1}{M}}) - \left(1+\frac{L^2_M}{r^2}\right)}{\frac{-1}{r^2}\left(\alpha Q L^{\alpha}_M\right)^{\frac{2}{\beta}}}\right)^{\beta}. \tag{5.34}$$

The energy per bit consumption of the M hope VLC system can be expressed as:

$$E_{MH} = \frac{P_{MH}}{R_b}\left(O_{SR_1} + O^c_{SR_1}\left[\sum_{n=1}^{N-1}\left((n+1)\,O_{R_nR_{n+1}}\prod_{j=1}^{n-1}O^c_{R_jR_{j+1}}\right) + O_{R_ND}\prod_{n=1}^{N-1}(N+1)\,O^c_{R_nR_{n+1}}\right]\right). \tag{5.35}$$

5.3.3 Cooperative relaying protocols

The selective DF and the incremental DF are two cooperative strategies for relay systems. In the first configuration the relay is always in a cooperative mode, in the latter mode it only cooperates if the direct link communication fails.

5.3.3.1 Selective DF Relaying Protocol

Two-time slots are involved in this relaying system. During the first time slot, the source sends the data to the cooperative relay and the destination nodes. During the second time slot, the DF relay decodes the received signal and forwards it to the destination node. However, in this protocol, both received signals at the destination (i.e, source signal and relay signal) are combined, in a process called spatial diversity, which can considerably improve the performance of the communication system [182]. In such scenarios, the consumed energy-per-bit is written as:

$$E_{SDF} = O_{SR_n} \frac{P_{SDF}}{R_b} + (1 - O_{SR_n}) \frac{2P_{SDF}}{R_b}, \tag{5.36}$$

where E_{SDF} denotes the energy-per-bit consumption for this SDF relaying, P_{SDF} is the optimal transmit power. To begin with, in order to define the consumed energy in this configuration, the overall outage probability is obtained as:

$$O_{SDF} = O_{SH} \left(O_{SR_n} + (1 - O_{SR_n}) O_{R_nD} \right), \tag{5.37}$$

where O_{SH} is the outage probability of the direct link given by Equation (5.12), O_{SR_n} and O_{R_nD} are the outage probabilities of the first and second links, respectively, which can be written as:

$$O_{SR_n} = \frac{-1}{r^2} \left(\alpha Q L_{SR_n}^{\alpha} \right)^{\frac{2}{\beta}} \left(\frac{\delta \sigma_{r_n}^2}{P_{SR_n}} \right)^{\frac{-1}{\beta}} + \left(1 + \frac{L_{SR_n}^2}{r^2} \right), \tag{5.38}$$

$$O_{R_nD} = \frac{-1}{r^2} \left(\alpha Q L_{R_nD}^{\alpha} \right)^{\frac{2}{\beta}} \left(\frac{\delta \sigma^2}{P_{R_nD}} \right)^{\frac{-1}{\beta}} + \left(1 + \frac{L_{R_nD}^2}{r^2} \right), \tag{5.39}$$

where L_{SR_n} is the length of the first link, P_{SR_n} represents the minimum source power which is needed to accomplish O_{SR_n}, L_{R_nD} indicates the second link length (i.e, relay-to-destination link) and P_{R_nD} the optimum SDF relay power required to achieve O_{R_nD}.

Maintaining the assumption that the relay R_n is placed at the mid-point between the source and the destination nodes, which provides the best performance of the SDF relay, the overall outage probability of the cooperative SDF relaying VLC system simplifies to:

$$O_{SDF} = O_{SH} \left(O^* \left(2 - O^* \right) \right), \tag{5.40}$$

where $O^* = O_{SR_n} = O_{R_nD}$.

Substituting Equations (5.12), (5.38) and (5.39) into Equation (5.40), the outage probability of the SDF relay is given in Equation (5.41):

$$O_{SDF} = \left(\frac{-1}{r^2} (\alpha Q L_1^{\alpha})^{\frac{2}{\beta}} \left(\frac{\delta \sigma_d^2}{P_{SDF}} \right)^{\frac{-1}{\beta}} + \left(1 + \frac{L_1^2}{r^2} \right) \right) \left(\frac{-1}{r^2} (\alpha Q L_2^{\alpha})^{\frac{2}{\beta}} \left(\frac{\delta \sigma_d^2}{P_{SDF}} \right)^{\frac{-1}{\beta}} + \left(1 + \frac{L_2^2}{r^2} \right) \left(2 - \left(\frac{-1}{r^2} (\alpha Q L_2^{\alpha})^{\frac{2}{\beta}} \left(\frac{\delta \sigma_d^2}{P_{SDF}} \right)^{\frac{-1}{\beta}} + \left(1 + \frac{L_2^2}{r^2} \right) \right) \right) \right) \tag{5.41}$$

where $P_{SDF} = P_{SH} = P_{SR_n} = P_{R_nD}$, $L_1 = L_{SH} = 2L_2 = 2L_{SR_n} = 2L_{R_nD}$ and $\sigma_d^2 = \sigma_r^2 = \sigma^2$.

Numerical results for P_{SDF} in Equation (5.41), which is required to achieve the O_{SDF}, can be found by utilizing a software tool (specifically the Solve function in the Mathematica software). Finally, by substituting the numerical results of P_{SDF} into Equation (5.36), the consumed energy per bit performance of the proposed configuration can be obtained.

5.3.3.2 Incremental DF Relaying Protocol

As previously mentioned, compared to the SDF protocol where the relay is always in cooperative mode, the IDF cooperates only if the direct link between the source and destination does not meet the link quality requirement. This means that the relay does not participate in the communication process while the destination node receives the desired information from the source through the direct link. This can decrease the consumed power and improve energy efficiency [183]. In this scenario, the consumed energy-per-bit is written as [140]:

$$E_{IDF} = (1 - O_{SD}) \frac{P_{IDF}}{R_b} + O_{SD} O_{SR_n} \frac{P_{IDF}}{R_b} + O_{SD} (1 - O_{SR_n}) \frac{2P_{IDF}}{R_b}, \tag{5.42}$$

where E_{IDF} represents the energy consumption performance for the IDF configuration, O_{SD} denotes the outage probability of the direct link which is equal to that of the single-hop one expressed in Equation (5.12) and P_{IDF} is the optimal transmit power which is required to meet the outage probability required of this approach. Each term of Equation (5.42) refers to a distinct scenario. $(1 - O_{SD}) \frac{P_{IDF}}{R_b}$ represents the energy consumed when the IDF relay does not cooperate in the communication process. The second, $O_{SD} O_{SR_n} \frac{P_{IDF}}{R_b}$ depicts the energy consumption when the information contained

in the signal cannot be correctly decoded by both destination and IDF nodes. The third term $O_{SD}\left(1-O_{SR_n}\right)\frac{2P_{IDF}}{R_b}$ refers to the energy consumed when communication through the direct link fails and the IDF relay is in active mode.

As with the outage probability of the SDF-based VLC system, the outage probability of the IDF consists of three outage probability terms as [140]:

$$O_{IDF} = O_{SD}\left(O_{SR_n} + \left(1-O_{SR_n}\right)O_{R_nD}\right). \tag{5.43}$$

Substituting Equations (5.12), (5.38) and (5.39) into Equation (5.43), the outage probability of the IDF relaying VLC system can be obtained in closed form, which is equal to that of the SDF protocol represented in Equation (5.41). However, the numerical results for the P_{IDF} can be straightforwardly determined using the same software tools that were used to calculate the P_{SDF} in the previous subsection. Finally, substitute the values of P_{IDF} into Equation (5.42) to determine the energy-per-bit consumption of the IDF relaying protocol.

5.4 Numerical Results and Discussions

The numerical results of the overall outage probabilities and the energy consumption for the different VLC systems are presented and discussed in this section. Again, Monte Carlo simulations were used to validate the numerical results. The parameters of the proposed VLC system, unless specified otherwise, were as shown in Table 5.1. These parameters represent practical VLC environment [99].

Table 5.1 Parameters of the VLC system..

Parameter	Value
L_{SH}	4 m
$L_{SR_1} = L_{R_1R_2} = L_{R_nR_{n+1}} = L_{R_ND} =$	$\frac{L_{SH}}{M}$
P_s	0.33 W
A_d	$A = 0.0001$ m^2
$U\left(\Psi_K\right) = g\left(\Psi_K\right)$	10 dB
R_p	1 A/W
r_e	3.6 m
$\phi/2$	60°

5.4.1 Average Outage Probability

The performance of the different VLC system configurations is discussed in this subsection in terms of outage probability. The effect of changes in system parameters on

performance is also considered. The discussion can be started with Figure 5.4, where the analytical predictions from Equations (5.12) and (5.20) for both the direct link and the non-cooperative DF are plotted with respect to vertical distance between source and working plane, with two different values of the source transmit power 0.4 W and 0.3 W.

It is noticeable, for both scenarios, that the numerical results for the outage probability for single-hop and two-hop links match nearly perfectly with the simulation results. When the transmit power was 0.3 W and the vertical distance was less than 2.6 m, the single-hop approach outperforms the DF. This is because the DF relay operates in half-duplex (HD) mode, which leads to a substantial loss in spectral efficiency and thus increases the outage probability of the system [184]. This implies that for short distances, when a direct link is available (i.e., direct transmission is not affected by shadowing/blocking), using DF-assisted VLC systems is relatively inefficient in terms of spectral efficiency. On the other hand, when the vertical separation is 3.6 m for the same 0.3 W transmit power, the outage probability of the DF configuration is 0.15% less than the single-hop approach. This is because of the inverse relationship between system capacity and the source-to-destination distance in the direct link system.

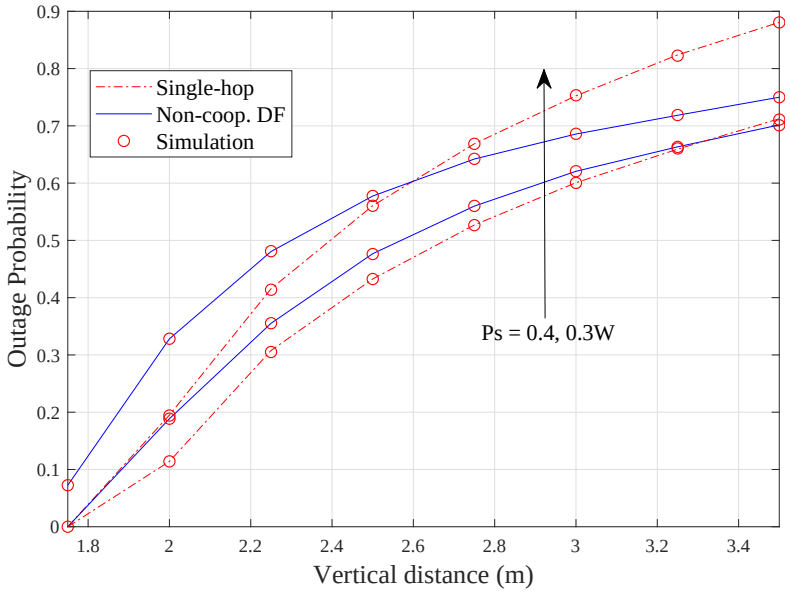

Figure 5.4 Outage probability of single-hop and non-cooperative DF relay configurations for vertical distance between source and work plane, for two transmit powers.

It is also noticeable from Figure 5.4 that the transmit power has a positive impact on the performance of both systems, while vertical separation negatively affected the performance of both configurations. For example, in the single-hop scenario, the outage probability increases from effectively zero to 0.7 as the vertical distance changes from 1.6 to 3.6 m when the transmit power is 0.4 W. However, for a transmit power of 0.3 W, we see an outage probability of almost 0.9 when the vertical distance is 3.6 m.

The analytical results of Equations (5.20), (5.24) and (5.30) are presented in Figure 5.5 along with the Monte Carlo simulated results. The result show that increasing the vertical distance between the LED and the user plan always results in performance degradation for all system configurations. The results also show that the performance of this DF-based VLC system is adversely affected by increasing the number of DF relays in the VLC system. For example, when the vertical distance is 3 m, the outage probabilities for N=3, N=2, and N=1 are 0.77, 0.90, and 0.98, respectively.

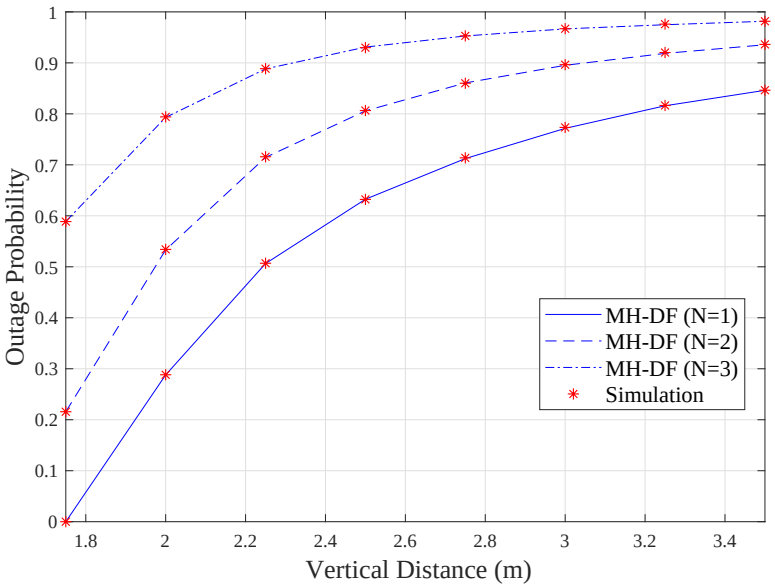

Figure 5.5 Outage probability of DF multi-hop scenarios.

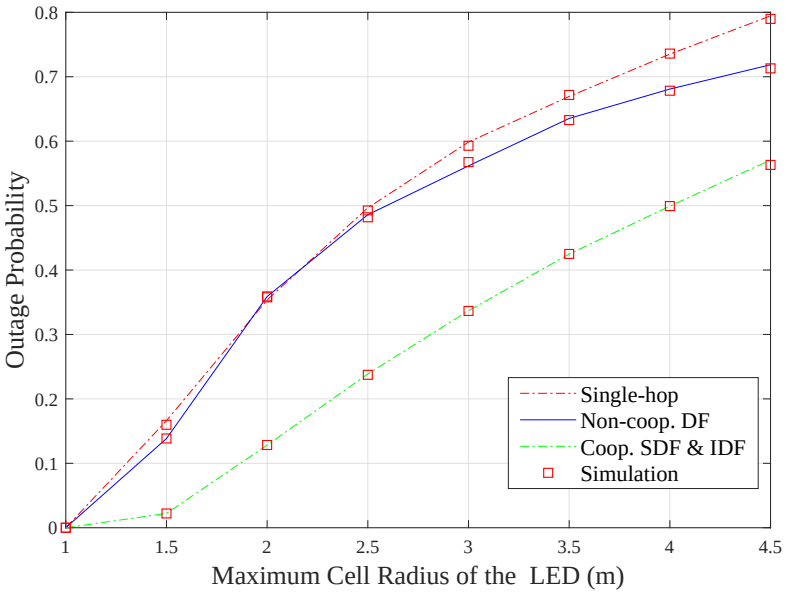

Figure 5.6 Performance comparison between the different VLC system setups as a function of VLC cell radius.

For the sake of performance comparison, the outage probabilities of the different configurations (i.e, the numerical predictions of Equations (5.12), (5.20) and (5.41)) are presented in Figure 5.6 as functions of the maximum cell radius of the LoS. The results show that the performance of every VLC configurations degrades as the size of the cell radius increases. It can be seen from the figure that the cooperative DF setups (SDF and IDF) outperform the other two configurations (single-hop and DF-based). This is because, in cooperative protocols, the capacity of the communication system is substantially improved by the spatial diversity accomplished at the destination node by combining the signals received from the source node and the relay node [185].When the maximum cell radius is 2 m, the outage probability of the cooperative DF relay scheme is 0.12 while it is almost 0.38 for both single-hop and DF approaches. However, the DF setup has a marginally superior performance over the single-hop, for values of the maximum cell radius of the LoS greater than 2.5 m, the superiority increasing with increase in distance.

To illustrate the impact of the position of the cooperative DF relay on the performance of the system, the outage probability of this configuration is plotted against threshold in Figure 5.7. It is clear from this figure that the system with the relay placed at the mid-point between the source and the destination nodes (i.e, $L_{RD} = L_{SR} = \frac{L_{SH}}{2} = 2$ m) offers performance better than the other system setups. This is because relays perform better in symmetric systems. However, placing the cooperative relay closer to the source modem (i.e, $L_{SR} = 0.25L_{SH} = 1$ m) provides better performance than placing it after the mid-point between both nodes (i.e, $L_{SR} = 3$ m).

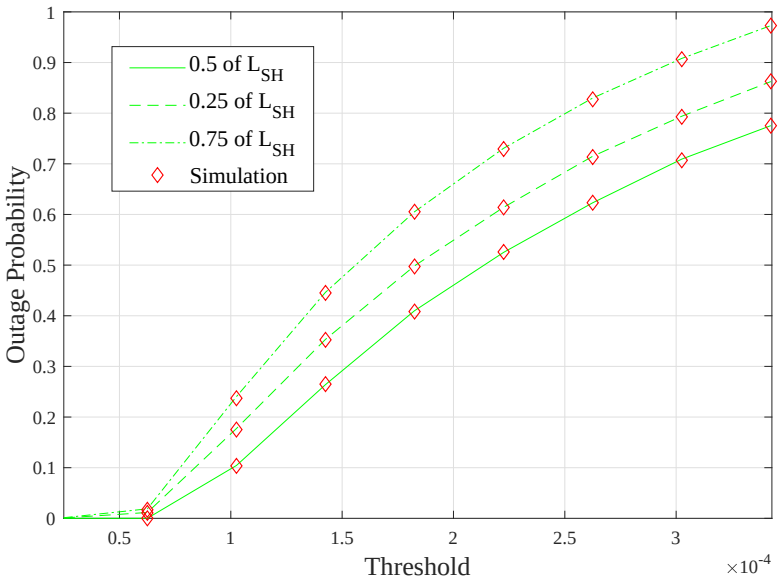

Figure 5.7 Average outage probability performance of the cooperative configurations as a function of threshold values.

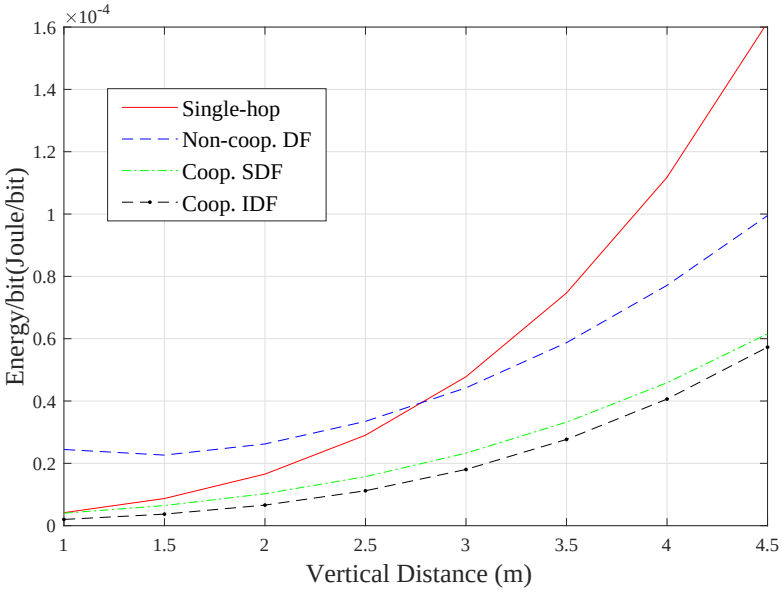

Figure 5.8 Energy performances of the different VLC system setups (Single-hop, Non-cooperative, Cooperative SDF, and Cooperative IDF) as a function of vertical distance between LED and working plane.

5.4.2 Energy-Per-Bit Performance

The energy consumption of the proposed scenarios is discussed in this sub-section. First, for the sake of comparison, the predicted energy consumptions of four different system configurations considered in this paper, single-hop, non-cooperative, cooperative SDF, and cooperative IDF, are plotted as a function of the vertical distance between LED and working plane in Figure 5.8.

It is obvious from this figure that the Cooperative IDF approach has superior performance compared to the other relaying protocols in terms of energy consumption. For example, when the vertical distance is 4.5 m, it consumes almost 3%, 60%, and 120% less energy compared to the SDF, non-cooperative DF, and single-hop approaches, respectively. This can be simply explained by the fact that the DF relay in this system only cooperates when the communication through the direct link fails. However, the SDF scheme consumes less energy compared to either single-hop or DF-based systems. It is also noticeable that, for shorter distances (vertical distances less than 2.7 m), the single-hop approach is more energy-efficient than the DF. The direct-link approach consumes about 10% and 1% less energy relative to the DF for vertical distances 1 m and 2.6 m, respectively. However, this configuration has the worst energy performance when the vertical distance is greater than 2.7 m. Another observation is that the energy consumed by all the configurations increases as vertical distance increases. This is because the energy consumption of the communication systems is inversely proportional to end-to-end distance.

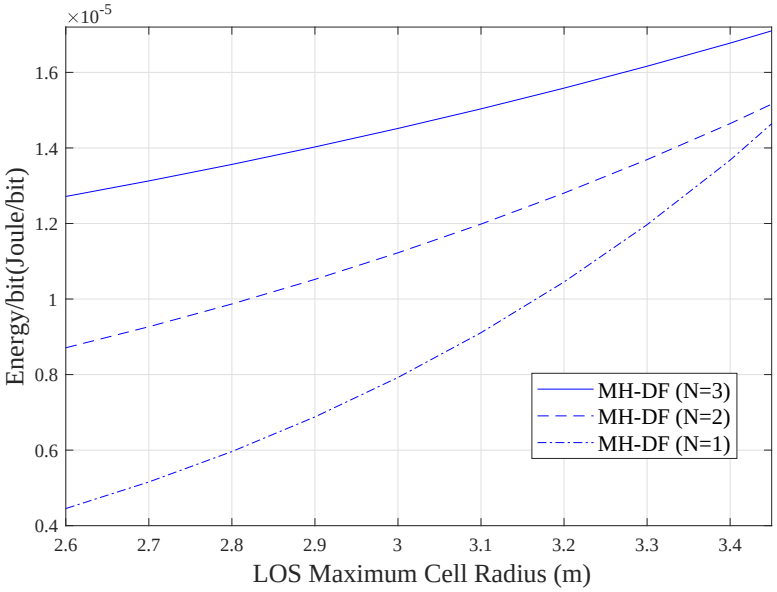

Figure 5.9 Energy-per-bit performance of multi-hop systems.

Figure 5.9 illustrates the effect of increasing the number of relays on the energy performance of the VLC system. The results show that as the number of relays increases, the system becomes less energy efficient because adding relays to the network consumes more energy, increasing the total energy consumption of the system. Obviously, the system with 3 DF relays is, all other things being equal, less energy-efficient compared to a system with 2 or 1 DF relays. For example, when the maximum cell radius is 3 m, the 3 relay system consumes almost 20% and 45% more energy than the system with 2 and 1 DF relays, respectively. It also can be seen that the systems consume more energy when the maximum cell radius of the LoS increases.

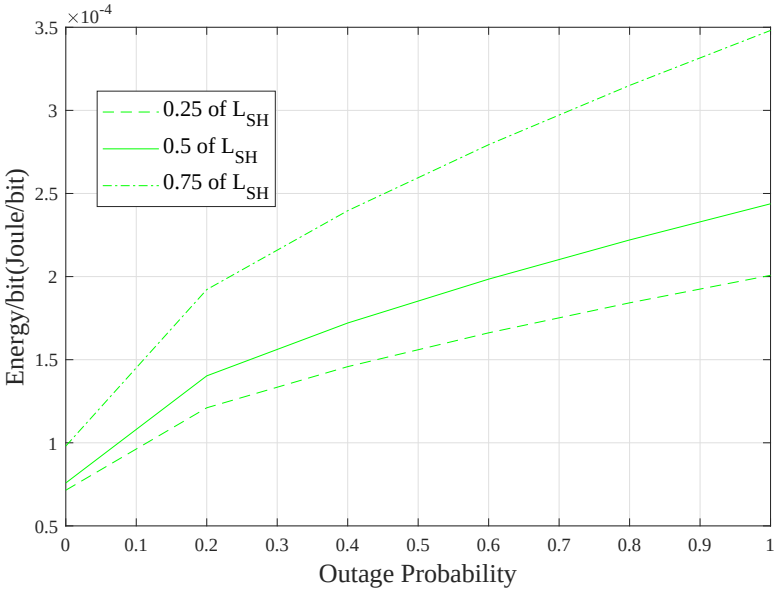

Figure 5.10 Energy consumption of the SDF system with respect to outage probability.

The last set of results presented in this chapter is Figure 5.10.The energy-per-bit consumption is plotted with respect to the outage probability of the SDF system for different source-to-relay distances. Although the SDF system with the relay placed at mid-point between the source and the destination modems (i.e, $L_{SR} = L_{RD} = 2$ m) provides better performance in terms of outage probability, the system with the relay placed closest to the source (i.e, $L_{SR} = 1$ m) consumes less energy. Indeed, the energy consumed by the latter configuration is almost 30% less compared to the mid-point modem when the outage probability is 0.5. On the other hand, the system with $L_{SR} = 2$ m outperforms the system with $L_{SR} = 3$ m in terms of energy consumption.

5.5 Summary

Relays provide reliability, throughput enhancement, and coverage improvement for communication systems particularly when the end-to-end distance between the source and destination nodes is relatively high. In this chapter, the relay-based VLC system is also considered to tackle the low data rate due to the NLoS transmission and to overcome the large shadowing and transmission-blocking caused by moving objects such as passengers. This chapter analyzed the performance of in-train relay-based VLC systems in terms of outage probability and system energy consumption. Different relay protocols were considered, namely: single-hop, multi-hop DF, SDF and IDF. Accurate and closed-form expressions for assessing outage probability and energy consumption of the different system setups were formulated, and subsequently verified by Monte Carlo simulations. The derived expressions will allow designers and engineers to optimize VLC network parameters, including number of relays in the network, distances between relays, as well as the optimum relay protocol for specific systems.

This chapter showed that SDF and IDF protocols are superior to single hop and multi-hop DF approaches in terms of outage probability and energy efficiency. However, the IDF configuration has the best energy consumption performance compared to the other VLC system configurations considered in this work. This is due to the fact that the IDF relay only takes part in the communication between the source and the destination nodes if the direct-link does not meet the required link quality. The results of this chapter also showed that increasing relay number on the network can dramatically improve the outage probability of the system but consumes more energy making the system less energy efficient.

Chapter 6

Conclusions and Suggested Future Work

This chapter presents the major conclusions of the thesis, highlights its contributions to knowledge, and suggests potential topics for future research.

6.1 Conclusions

In this thesis, the OLE system was presented as a means of communication for data delivery to trains. Deploying cooperative PLC/VLC as a reliable communication system that can provide enhanced performance and mobility to the end users inside trains was also considered in the thesis. This thesis began with the question of how an OFDM-based OLE system can deliver data to trains and can the transfer function of the OLE system be represented by the two-port network model. It then investigated which configuration of the proposed indoor communication systems can provide the best performance and is most energy efficient. The major conclusions of this thesis are summarised as:

- It was proved from the results and the pattern of the attenuation curves, which were plotted using the developed two-port network model, that this model can represent the CTF of the OLE channel. The development of this model can be achieved by simplifying the electrification system of the railway and deriving its equivalent circuit. Simple dynamic equations were used update the position and speed of the train. The developed model was used to investigate the effect of the OLE system parameters on the transmission. For example, it was found that the strength of the signal sent over the OLE system is negatively affected by the speed of the train and length of the transmission path. It was also revealed that as the attenuation increases towards high frequencies.

  To answer the question of what is the channel capacity of the OFDM-based OLE system for the given bandwidths and the given ranges of the SNR, a simulation of an OFDM based OLE system was presented in this thesis. It was confirmed that the performance of the OFDM-based OLE system improves when the SNR value increases. Furthermore, the achieved data rates from the simulated OFDM-based OLE system is promising for the given bandwidths and the given ranges of the SNR. Finally, it was concluded that the OFDM based OLE system can be used as reliable communication system for trains as the results of its performance were promising results in terms of capacity and bit-error-rate.

- The research provided knowledge of the overall capacity and outage probability of the relay-based PLC/VLC system needed to understand the performance of such an integrated system. This was achieved by exploiting the statistical properties of the PLC and VLC channels to determine the average capacity and outage probability of the proposed system. Formulating the overall capacity and outage probability of the proposed systems offers the opportunity to study the performance of in-train cascade systems and to examine the effect of the different system parameters such as relay location and relay-to-destination distance on

the performance of the proposed systems. The accuracy of these mathematical models was verified by Monte Carlo simulations.

The results of the thesis proved the accuracy of the derived expression as there agreements between the analytical results and the simulated ones. It was also confirmed that the performance of the relay-based PLC/VLC system is affected by the change of the parameters of the system. For example, it was found that location of the relay on the network can affect the total performance of the system. It was also revealed that increasing transmit power and relay gain can enhance the performance of the system. A performance comparison between the DF-based and AF-based PLC/VLC were carried out. The results of the comparison showed that the DF-based PLC/VLC system outperformed the AF-based system. However, the results revealed that the performance of both configurations is affected by system parameters such as location of relays on the network, transmit power, and relay gain.

- In order to answer the question of how can the relay-based VLC system be made more energy-efficient and provide sufficient performance, the thesis analyzed the performance of in-train relay-based VLC systems in terms of outage probability and system energy consumption. Different relaying system and configurations were considered. Accurate and closed-form expressions for the considered system configurations were derived to assessing the performance of these setups. The thesis also measured and studied the effect of number of relays on the network, source power, and vertical distance of the VLC environment, on the performance of the system. Monte Carlo simulations were used to validate the theoretical results of the derived expressions.

  It was shown that the numerical results of the derived expressions match nearly perfectly with the simulation results, which confirms the accuracy of the formulated models. It was found that using relays with the last-mile VLC system, particularly when the end-to-end distance is relatively high, can result in better performance and reliability. It was also revealed that increasing relay numbers on the network contributes to the total energy consumption of the VLC system. The outcomes of the analyses also showed that better energy efficiency of the system can be achieved by choosing an optimal system configuration. For example, it was shown that the IDF configuration is more energy efficient than the other VLC system configurations which were considered. This is due to the fact that the IDF relay only cooperates if the direct-link does not meet the required link quality.

6.2 Possible Future Research

There were limitations on the work carried out and reported in this thesis which can be improved. Following are some possible topic for future work that could improve and extend these research findings:

- This study developed the two-port network model to represent the transfer function of the OLE channel which was evaluated using computer simulations. Future work should include field measurements by which to compare the model to the reality of using the OLE as a channel for data delivery. Further, the current model could be developed to include more than one train moving on a single section of track.

- Although the MV-PLC presents an interesting solution for higher bit rates, there are technical limitations and constraints that should be considered. Signal reflection, which is a non-negligible factor in communication systems due to impedance mismatching needs to be addressed for MV-PLC system development. Noise contamination of data transmitted over MV-PLC systems is strongly weather dependent and is another technical issue that can affect data transmission over the OLE. Future work could include studying different techniques of impedance matching and noise mitigation.

- Future work could consider a cooperative PLC/VLC system for data distribution within the train coaches, investigating different integrated systems such as PLC/RF and VLC/RF. Any future study could also focus on train-to-train communication using free-space optic communication. The analysis will take into consideration the effect of outdoor environmental factors such as sunlight, rain, fog, and atmospheric disturbances.

References

[1] R. He, B. Ai, G. Wang, K. Guan, Z. Zhong, A. F. Molisch, C. Briso-Rodriguez, and C. P. Oestges. High-speed railway communications: From gsm-r to lte-r. *IEEE Vehicular Technology Magazine*, 11(3):49–58, Sept 2016.

[2] N. Lofmark D. Taylor and M. McKavanagh. Survey on operational communications-study for the evolution of the railway communications system. In *final report for the European Railway Agency, 2014*, March 2014.

[3] K. D. Masur and D. Mandoc. Lte/sae—the future railway mobile radio system: Long-term vision on railway mobile radio technologies. In *UIC Technology Report, 2009*, 2009.

[4] A. Baxter. Network rail a guide to overhead electrification. Feb. 2015.

[5] Jae-Jo Lee, Young-Jin Park, Soon-Won Kwon, Hui-Myong Oh, Hae-soo Park, Kwan-Ho Kim, Dae-Young Lee, and Young-Hwa Jeong. High data rate internet service over medium voltage power lines. In *Int. Symp. Power Line Commun. and Its Appl.(ISPLC), 2005.*, pages 405–408, Apr. 2005.

[6] L. R. M. Castor, J. A. da Silva, and M. E. V. Segatto. Medium voltage overhead power-line as a smart distribution grid for onshore oil gas industries automation and broadband data transport. In *2015 IEEE PES Innovative Smart Grid Technologies Latin America (ISGT LATAM)*, pages 641–645, Oct 2015.

[7] D. Lee, D. In, J. Lee, Y. Park, K. Kim, J. Kim, and S. Shon. A field trial of medium voltage power line communication system for AMR and DAS. In *2009 Transmission Distrib. Conf. Exposition: Asia and Pacific*, pages 1–4, Oct 2009.

[8] A. Cataliotti, D. Di Cara, and G. Tinè. Model of line to shield power line communication system on a medium voltage network. In *2010 IEEE Instrum. Meas. Technol. Conf. Proceedings*, pages 1459–1462, May 2010.

[9] K. Kastell. Communication to and in trains. In *2015 17th International Conference on Transparent Optical Networks (ICTON)*, pages 1–4, July 2015.

[10] M. Uhlirz. Adapting gsm for use in high-speed railway networks. *Dissertation, Technische Universität Wien, 1995.*, 1995.

[11] S. Barmada, A. Gaggelli, A. Musolino, R. Rizzo, M. Raugi, and M. Tucci. Design of a plc system onboard trains: Selection and analysis of the plc channel. In *2008 IEEE International Symposium on Power Line Communications and Its Applications*, pages 13–17, April 2008.

[12] S. Ahamed. Visible light communication in railways. In *The International Conference on Railway Engineering (ICRE) 2016*, pages 1–5, May 2016.

[13] A. M. Cailean, B. Cagneau, L. Chassagne, V. Popa, and M. Dimian. A survey on the usage of dsrc and vlc in communication-based vehicle safety applications. In *2014 IEEE 21st Symposium on Communications and Vehicular Technology in the Benelux (SCVT)*, pages 69–74, Nov 2014.

[14] De-Dong Sun, Tao-Rong Gong, Rui Liu, Jian Song, and Guan-Hong Wang. The design of VLC-PLC system for substation inspection. *Energy and Power Engineering*, 09:581–588, Jan. 2017.

[15] Waled Gheth, Khaled M. Rabie, Bamidele Adebisi, Muhammad Ijaz, and Georgina Harris. Channel modeling for overhead line equipment for train communication. In *Proc. Int. Symp. Power line Commun (ISPLC)*, 2020.

[16] Waled Gheth, Khaled M. Rabie, Bamidele Adebisi, Muhammad Ijaz, and Georgina Harris. Performance analysis of integrated power-line/visible-light communication systems with af relaying. In *2018 IEEE Global Communications Conference (GLOBECOM)*, 2018.

[17] W. Gheth, K. M. Rabie, B. Adebisi, M. Ijaz, and G. Harris. On the performance of df-based power-line/visible-light communication systems. In *2018 International Conference on Signal Processing and Information Security (ICSPIS)*, pages 1–4, Nov 2018.

[18] Waled Gheth, Khaled Rabie, Bamidele Adebisi, Muhammad Ijaz, and Georgina Harris. Performance analysis of cooperative and non-cooperative relaying over vlc channels. *Sensors*, 20, 06 2020.

[19] Shengfeng Xu, Gang Zhu, bo ai, and Zhangdui Zhong. A survey on high-speed railway communications: A radio resource management perspective. *Computer Communications*, 86, 04 2016.

[20] Krzysztof Bernacki, Dominik Wybrańczyk, Marcin Zygmanowski, Andrzej Latko, Jarosław Michalak, and Zbigniew Rymarski. Disturbance and signal filter for power line communication. *Electronics (Switzerland)*, 8:1–17, 03 2019.

[21] Alain Richard Ndjiongue and Hendrik Ferreira. Power line communications (plc) technology: More than 20 years of intense research. *Transactions on Emerging Telecommunications Technologies*, pages 1–20, 01 2019.

[22] Davide Russo, Antonio Gatti, A. Ghelardini, Giorgio Mancini, A. Verduci, Daniel W Amato, and Roberto Battani. Power line communication : a new approach for train passenger information systems. 2008.

[23] Tamas Becsi, Szilard Aradi, and P. Gaspar. Using train interconnection for intra-train communication via can. *Acta Polytechnica Hungarica*, 12(4):27–38, 7 2015.

[24] Muhammad Saadi, Touqeer Ahmad, Muhammad Kamran Saleem, and L. Wuttisittikulkij. Visible light communication - an architectural perspective on the applications and data rate improvement strategies. *Transactions on Emerging Telecommunications Technologies*, 06 2018.

[25] Ameur Chaabna, Abdesselam Babouri, Xun Zhang, Chuanxi Huang, and Chouabia Halim. New indoor positioning technique using spectral data compression based on vlc for performance improvement. *Optical and Quantum Electronics*, 52, 07 2020.

[26] R. K. Ahiadormey, P. Anokye, H. Jo, and K. Lee. Performance analysis of two-way relaying in cooperative power line communications. *IEEE Access*, 7:97264–97280, 2019.

[27] S. Clark. A history of railway signalling: From the bobby to the balise. In *IET Professional Development Course on Railway Signalling and Control Systems (RSCS 2010)*, pages 7–20, June 2010.

[28] M. Renner and G. Gardner. Global competitiveness in the rail and transit industry. *Worldwatch Inst., Washington, DC, USA, 2010.*, 2010.

[29] Sector overview and competitiveness survey of the railway supply industry. *European Comm., Rotterdam, The Netherlands,2012.*

[30] The unife world rail market study 'forecast 2014 to 2019. *UNIFE,Brussels, Belgium, Tech. Rep., 2014.*, 2014.

[31] Frost & Sullivan. Strategic analysis of communication based train control systems in the western european urban rail market. *Online*, July 2013.

[32] J. Farooq and J. Soler. Radio communication for communications-based train control (cbtc): A tutorial and survey. *IEEE Communications Surveys Tutorials*, 19(3):1377–1402, thirdquarter 2017.

[33] R. Alvarez and J. Roman. Etcs l2 and cbtc over lte-convergence of the radio layer in advanced train control systems. *Proc. IRSE Inst. Railway Signal Eng. Tech. Meeting, 2013*, pages 1–12, 2013.

[34] B. M. Martínez. Ertms cbtc technology convergence. *presented at MetroRail, Madrid, Spain, 2013*, April 2013.

[35] Benefits and barriers to cbtc and etcs convergence. *Proc. MetroRail Conf., London, U.K.,2012.*, March 2012.

[36] J. Farooq, L. Bro, R. T. Karstensen, and J. Soler. Performance evaluation of a multi-radio, multi-hop ad-hoc radio communication network for communications-based train control (cbtc). *IEEE Transactions on Vehicular Technology*, 67(1):56–71, Jan 2018.

[37] G. Theeg and S. Vlasenko. Railway signalling and interlocking. *Hamburg, Germany: Eurailpress, 2009.*, 2009.

[38] Q. Shan and Y. Wen. Research on the ber of the gsm-r communications provided by the em transient interferences in high-powered catenary system environment. In *2010 International Conference on Electromagnetics in Advanced Applications*, pages 757–760, Sept 2010.

[39] Y. Cao, B. Cai, T. Tang, and J. Mu. Reliability analysis of ctcs based on two gsm-r double layers networks structures. In *2009 WRI International Conference on Communications and Mobile Computing*, volume 3, pages 242–246, Jan 2009.

[40] Z.D. Zhong. Dedicated mobile communications for high-speed railway, advances in high-speed rail technology. In *Beijing Jiaotong University Press and Springer-Verlag GmbH Germany 2018*, 2018.

[41] S. Jie, Z. Xiaojin, and G. Tingting. Performance analysis of gsm-r network structure in china train control system. In *2010 International Conference on Electronics and Information Engineering*, volume 2, pages V2–214–V2–218, Aug 2010.

[42] M. Cheng, X. Fang, and W. Luo. Beamforming and positioning-assisted handover scheme for long-term evolution system in high-speed railway. *IET Communications*, 6(15):2335–2340, October 2012.

[43] H. Du, C. Wen, and W. Li. A new method for detecting and early-warning in-band interference of the gsm-r network. In *2017 IEEE 17th International Conference on Communication Technology (ICCT)*, pages 800–804, Oct 2017.

[44] A. Diaz Zayas, C. A. Garcia Perez, and P. M. Gomez. Third-generation partnership project standards: For delivery of critical communications for railways. *IEEE Vehicular Technology Magazine*, 9(2):58–68, June 2014.

[45] S. F. Ruesche, J. Steuer, and K. Jobmann. The european switch. *IEEE Vehicular Technology Magazine*, 3(3):37–46, Sept 2008.

[46] A. Sniady and J. Soler. Capacity gain with an alternative lte railway communication network. In *2014 7th International Workshop on Communication Technologies for Vehicles (Nets4Cars-Fall)*, pages 54–58, Oct 2014.

[47] J. Choi, H. Cho, H. Oh, K. Kim, M. Bhang, I. Yu, and H. Ryu. Challenges of lte high-speed railway network to coexist with lte public safety network. In *2015 17th International Conference on Advanced Communication Technology (ICACT)*, pages 543–547, July 2015.

[48] S. A. A. Shah, E. Ahmed, M. Imran, and S. Zeadally. 5g for vehicular communications. *IEEE Communications Magazine*, 56(1):111–117, Jan 2018.

[49] S. Hong, J. Brand, J. I. Choi, M. Jain, J. Mehlman, S. Katti, and P. Levis. Applications of self-interference cancellation in 5g and beyond. *IEEE Communications Magazine*, 52(2):114–121, February 2014.

[50] I. A. Hemadeh, K. Satyanarayana, M. El-Hajjar, and L. Hanzo. Millimeter-wave communications: Physical channel models, design considerations, antenna constructions, and link-budget. *IEEE Communications Surveys Tutorials*, 20(2):870–913, Secondquarter 2018.

[51] M. M. Ahamed and S. Faruque. Propagation factors affecting the performance of 5g millimeter wave radio channel. In *2016 IEEE International Conference on Electro Information Technology (EIT)*, pages 0728–0733, May 2016.

[52] Waled Gheth, Matjaz Rozman, Khaled M. Rabie, and Bamidele Adebisi. Emc measurements in indoor power line communication environments. In Ali Boyaci, Ali Riza Ekti, Muhammed Ali Aydin, and Serhan Yarkan, editors, *Int. Telecommun. Conf.*, pages 189–200, Singapore, 2018. Springer Singapore.

[53] C. J. Kikkert. Power transformer modelling and mv plc coupling networks. In *2011 IEEE PES Innovative Smart Grid Technologies*, pages 1–6, Nov 2011.

[54] W. C. Black. Power line s-parameter characterization using open-source tools. In *ISPLC2010*, pages 62–66, March 2010.

[55] C. J. Kikkert and G. Reid. Radiation and attenuation of communication signals on power lines. In *2009 7th International Conference on Information, Communications and Signal Processing (ICICS)*, pages 1–5, 2009.

[56] M. Zimmermann and K. Dostert. A multipath model for the powerline channel. *IEEE Trans. Commun.*, 50(4):553–559, Apr. 2002.

[57] Tooraj Esmailian, Frank R. Kschischang, and P. Glenn Gulak. In-building power lines as high-speed communication channels: channel characterization and a test channel ensemble. *Int. J. Commun. Syst.*, 16:381–400, 2003.

[58] Bamidele Adebisi, Abbas Khalid, Yakubu Tsado, and B. Honary. Narrowband plc channel modelling for smart grid applications. 07 2014.

[59] O. G. Hooijen. A channel model for the residential power circuit used as a digital communications medium. *IEEE Trans. Electromagn. Compat.*, 40(4):331–336, Nov. 1998.

[60] M. Zimmermann and K. Dostert. A multipath model for the powerline channel. *IEEE Trans. Commun.*, 50(4):553–559, Apr. 2002.

[61] T.Esmailian, F.R.Kschischang, and P.G.Gulak. Anin-buildingpower line channel simulatorn grid. In *In Proc. 4th Int. Symp. Power-Line Commun and it Applications (ISPLC 2000)*, Apr. 2000.

[62] Masashi Kitayama, Junichi Abe, and Shinji Tanabe. Transmission characteristics simulation on power line communications. *Electronics and Communications in Japan*, 92(3):46–55, 2009.

[63] Petr Mlynek, Jiri Misurec, Martin Koutny, and Pavel Silhavy. Two-port network transfer function for power line topology modeling. *Radioengineering*, 21, 04 2012.

[64] M. Zajc, N. Suljanovic, A. Mujcic, and J. Tasic. High voltage power line constraints for high speed communications. In *Proceedings of the 12th IEEE Mediterranean Electrotechnical Conference (IEEE Cat. No.04CH37521)*, volume 1, pages 285–288 Vol.1, May 2004.

[65] Bamidele Adebisi, Kelvin Anoh, Khaled Rabie, Augustine Ikpehai, Michael Fernando, and Andrew Wells. A new approach to peak threshold estimation for impulsive noise reduction over power line fading channels. *IEEE Systems Journal*, PP, 02 2018.

[66] M. Zimmermann and K. Dostert. Analysis and modeling of impulsive noise in broad-band powerline communications. *IEEE Transactions on Electromagnetic Compatibility*, 44(1):249–258, Feb. 2002.

[67] M. Zajc, N. Suljanovic, A. Mujcic, and J. F. Tasic. Frequency characteristics measurement of overhead high-voltage power-line in low radio-frequency range. *IEEE Transactions on Power Delivery*, 22(4):2142–2149, Oct 2007.

[68] H. A. Doost, M. H. Ghamat, and A. Rafiei. Robustness evaluation of ofdm and mc-ds-cdma systems in digital high voltage power line communication systems by using ls channel estimation technique. In *2008 3rd International Conference on Information and Communication Technologies: From Theory to Applications*, pages 1–6, April 2008.

[69] Waled Gheth, Khaled M. Rabie, and Bamidele Adebisi. Impulsive noise modeling and cancellation strategies over power line channels. In Ali Boyaci, Ali Riza Ekti, Muhammed Ali Aydin, and Serhan Yarkan, editors, *Int. Telecommun. Conf.*, pages 163–175, Singapore, 2018. Springer Singapore.

[70] A. M. Tonello, S. D'Alessandro, and L. Lampe. Cyclic prefix design and allocation in bit-loaded ofdm over power line communication channels. *IEEE Trans. Commun.*, 58(11):3265–3276, Nov. 2010.

[71] S. Liu, F. Yang, W. Ding, J. Song, and Z. Han. Impulsive noise cancellation for mimo-ofdm plc systems: A structured compressed sensing perspective. In *IEEE Glob Commun. Conf.(GLOBECOM)*, pages 1–6, Dec 2016.

[72] Qing Zhu, Zhimin Chen, and Xinyi He. Resource allocation for relay-based ofdma power line communication system. *Electronics*, 8:125, 01 2019.

[73] Bamidele Adebisi, Kelvin Anoh, and Khaled Rabie. An enhanced nonlinear companding scheme for reducing papr of ofdm systems. *IEEE Systems Journal*, 13, 06 2018.

[74] M. Ghosh. Analysis of the effect of impulse noise on multicarrier and single carrier qam systems. *IEEE Trans. Commun.*, 44(2):145–147, Feb. 1996.

[75] K. Kuri, Y. Hase, S. Ohmori, F. Takahashi, and R. Kohno. Powerline channel coding and modulation considering frequency domain error characteristics. *Proc. Int. Sympos. Power Line Commun. (ISPLC)*, pages 221 – 225, Oct. 2003.

[76] Y. H. Ma, P. L. So, and E. Gunawan. Performance analysis of OFDM systems for broadband power line communications under impulsive noise and multipath effects. *IEEE Trans. Power Del.*, 20(2):674–682, Apr. (2005). dio:10.1109/tpwrd.2005.844320.

[77] B. Adebisi, K. M. Rabie, A. Ikpehai, C. Soltanpur, and A. Wells. Vector ofdm transmission over non-gaussian power line communication channels. *IEEE Systems Journal*, 12(3):2344–2352, 2018.

[78] K. Kastell. Communication to and in trains. In *2015 17th International Conference on Transparent Optical Networks (ICTON)*, pages 1–4, July 2015.

[79] M. Taneja. A resource management framework for lte-wlan networks in high-speed trains. In *2016 2nd International Conference on Contemporary Computing and Informatics (IC3I)*, pages 155–160, Dec 2016.

[80] X. Liang, F. L. C. Ong, P. M. L. Chan, R. E. Sheriff, and P. Conforto. Mobile internet access for high-speed trains via heterogeneous networks. In *14th IEEE Proceedings on Personal, Indoor and Mobile Radio Communications, 2003. PIMRC 2003.*, volume 1, pages 177–181 Vol.1, Sept 2003.

[81] César. Briso-Rodríguez, Ke. Guan, Yin. Xuefeng, and Thomas. Kürner. Wireless communications in smart rail transportation systems. *J. Wireless Communications and Mobile Computing.*, (10), October 2017.

[82] G. Goth. New wi-fi technology racing past standards process. *IEEE Distributed Systems Online*, 9(10):1–1, Oct 2008.

[83] Émilie Masson and Marion Berbineau. *Railway Applications Requiring Broadband Wireless Communications*, chapter 2, pages 35–79. Springer International Publishing, Cham, 2017.

[84] T. Urushihara, H. Takahashi, M. Kobayashi, H. Motozuka, M. Irie, N. Shirakata, and K. Takinami. 60ghz wireless technologies for wigig/ieee 802.11ad multi-gigabit systems. In *2014 Asia-Pacific Microwave Conference*, pages 628–630, Nov 2014.

[85] G. Kalfas, N. Pleros, L. Alonso, and C. Verikoukis. Network planning for 802.11ad and mt-mac 60 ghz fiber-wireless gigabit wireless local area networks over passive optical networks. *IEEE/OSA Journal of Optical Communications and Networking*, 8(4):206–220, April 2016.

[86] M. Z. Chowdhury, M. K. Hasan, M. Shahjalal, M. T. Hossan, and Y. M. Jang. Optical wireless hybrid networks: Trends, opportunities, challenges, and research directions. *IEEE Communications Surveys Tutorials*, 22(2):930–966, Secondquarter 2020.

[87] Z. Che, J. Fang, Z. L. Jiang, X. Yu, G. Xi, and Z. Chen. A physical-layer secure coding schcme for visible light communication based on polar codes. In *2017 Conference on Lasers and Electro-Optics Pacific Rim (CLEO-PR)*, pages 1–2, July 2017.

[88] S. M. Khan, N. Saha, M. R. Rahman, M. Hasan, and M. S. Rahman. Performance improvement of mimo vlc using v-blast technique. In *2016 5th International Conference on Informatics, Electronics and Vision (ICIEV)*, pages 45–49, May 2016.

[89] L. Fan, Q. Liu, C. Jiang, H. Xu, J. Hu, D. Luo, Z. He, and Q. Huang. Visible light communication using the flash light led of the smart phone as a light source and its application in the access control system. In *2016 IEEE MTT-S International Wireless Symposium (IWS)*, pages 1–4, March 2016.

[90] L. Wei-Keng, S. Chen, C. Chen-I, and Y. Tsai. The analysis of the thermal resistance structure of leds by measuring its transient temperature variation. In *2013 8th International Microsystems, Packaging, Assembly and Circuits Technology Conference (IMPACT)*, pages 214–217, Oct 2013.

[91] S. Das, A. Chakraborty, D. Chakraborty, and S. Moshat. Pc to pc data transmission using visible light communication. In *2017 International Conference on Computer Communication and Informatics (ICCCI)*, pages 1–5, Jan 2017.

[92] K. Siddiqi, A. D. Raza, and S. S. Muhammad. Visible light communication for v2v intelligent transport system. In *2016 International Conference on Broadband Communications for Next Generation Networks and Multimedia Applications (CoBCom)*, pages 1–4, Sept 2016.

[93] Y. Wang and H. Haas. Dynamic load balancing with handover in hybrid li-fi and wi-fi networks. *Journal of Lightwave Technology*, 33(22):4671–4682, Nov. 2015.

[94] Pablo Palacios, Milton Roman Cañizares, Cesar Azurdia-Meza, David Zabala-Blanco, Ali Dehghan Firoozabadi, Fabian Seguel, Samuel Montejo Sánchez, and Ismael Soto. Interference mitigation for visible light communications in underground mines using angle diversity receivers. *Sensors*, 20:367, 01 2020.

[95] Muhammad Tabish Niaz, Fatima Imdad, Kashif Mehmood, and Hyung Seok Kim. A study of indoor vlc system based on tls receiver. *Transactions on Emerging Telecommunications Technologies*, 07 2018.

[96] Sourish Chatterjee and Deblina Sabui. Daylight integrated indoor vlc architecture: An energy-efficient solution. *Transactions on Emerging Telecommunications Technologies*, 11 2019.

[97] Shashikant Sheoran, Parul Garg, and Prabhat Sharma. Interference mitigation technique with coverage improvement in indoor vlc system. *Transactions on Emerging Telecommunications Technologies*, 30, 08 2018.

[98] D. C. O'Brien, L. Zeng, H. Le-Minh, G. Faulkner, J. W. Walewski, and S. Randel. Visible light communications: Challenges and possibilities. In *2008 IEEE 19th International Symposium on Personal, Indoor and Mobile Radio Communications*, pages 1–5, Sept 2008.

[99] A. Gupta, N. Sharma, P. Garg, and M. S. Alouini. Cascaded FSO-VLC communication system. *IEEE Wireless Communications Letters*, 6(6):810–813, Dec. 2017.

[100] W. Gheth, K. M. Rabie, B. Adebisi, M. Ijaz, G. Harris, and A. Alfitouri. Hybrid power-line/wireless communication systems for indoor applications. In *2018 11th IEEE Int. Symp. Commun. Syst., Netw. and Digit. Signal Process.(CSNDSP)*, pages 1–6, Jul 2018.

[101] W. Gheth, B. Adebisi, M. Ijaz, L. Farhan, and G. Harris. Hybrid visible-light/rf communication system for mission-critical iot applications. In *2019 IEEE 2nd British and Irish Conference on Optics and Photonics (BICOP)*, pages 1–4, 2019.

[102] Bamidele Adebisi, Albert Treytl, Abdelfatteh Haidine, Alexander Portnoy, Rafi Shan, David Lund, Hans Pille, and B. Honary. Ip-centric high rate narrowband plc for smart grid applications. *IEEE Communications Magazine*, 49:46–54, 12 2011.

[103] S. Galli, A. Scaglione, and Z. Wang. For the grid and through the grid: The role of power line communications in the smart grid. *Proc. IEEE*, 99(6):998–1027, Jun. 2011.

[104] N. Ginot, M. A. Mannah, C. Batard, and M. Machmoum. Application of power line communication for data transmission over pwm network. *IEEE Transactions on Smart Grid*, 1(2):178–185, Sept 2010.

[105] A. u. Rehman, N. Bashir, N. U. Hassan, and C. Yuen. Impact of home appliances on the performance of narrow-band power line communications for smart grid applications. In *2016 IEEE Region 10 Conference (TENCON)*, pages 3511–3514, Nov. 2016.

[106] N. Graf, I. Tsokalo, and R. Lehnert. Validating broadband plc for smart grid applications with field trials. In *2017 IEEE International Conference on Smart Grid Communications (SmartGridComm)*, pages 497–502, Oct 2017.

[107] M. O. Carrion, M. Lienard, and P. Degauque. Communication over vehicular dc lines: Propagation channel characteristics. In *2006 IEEE International Symposium on Power Line Communications and Its Applications*, pages 2–5, March 2006.

[108] A. D. Familua, K. Ogunyanda, T. G. Swart, H. C. Ferreira, R. Van Olst, and L. Cheng. Narrowband plc channel modeling using usrp and psk modulations. In *18th IEEE International Symposium on Power Line Communications and Its Applications*, pages 156–161, Mar. 2014.

[109] P. Peres, C. R. de Souza, and I. S. Bonatti. ABCD matrix: A unique tool for linear two-wire transmission line modelling. *Int. J. Elect. Eng. Educ*, 40(3):220–229, Jul. 2003.

[110] Igor Fernández, David Vega, Dominique Roggo, Robert Stiegler, Lino Capponi, Itziar Angulo, Jan Meyer, and Amaia Arrinda. Comparison of measurement methods of lv grid access impedance in the frequency range assigned to nb-plc technologies. *Electronics*, 8:1155, 10 2019.

[111] Igor Fernández, David Vega, Amaia Arrinda, Itziar Angulo, Noelia Uribe-Pérez, and Asier Llano. Field trials for the characterization of non-intentional emissions at low-voltage grid in the frequency range assigned to nb-plc technologies. *Electronics*, 8:1044, 09 2019.

[112] Bamidele Adebisi, Jonathan Stott, and Bahram Honary. Experimental study of the interference of plc transmission power levels on hf bands. In *The 10th Institution of Engineering and Technology International Conference on Ionospheric Radio Systems & Techniques (IRST 2006)*, pages 326–330. IEEE, 7 2006.

[113] Igboamalu Frank Nonso, Alain Richard Ndjiongue, and Hendrik Ferreira. Plc-rf diversity: channel outage analysis. *Telecommunication Systems*, 04 2020.

[114] K. Bhavya, N. Gangrade, and N. Kumar. Simplified integration of power line and visible light communication. In *2018 3rd International Conference on Communication and Electronics Systems (ICCES)*, pages 129–132, Oct 2018.

[115] R. K. Ahiadormey, P. Anokye, H. Jo, and K. Lee. Performance analysis of two-way relaying in cooperative power line communications. *IEEE Access*, 7:97264–97280, 2019.

[116] Mateus Filomeno, Marcello Campos, H. Vincent Poor, and Moises Ribeiro. Hybrid power line/wireless systems: An optimal power allocation perspective. *IEEE Transactions on Wireless Communications*, PP:1–1, 06 2020.

[117] M. Shimaponda-Nawa, S. Achari, D. N. K. Jayakody, and L. Cheng. Visible light communication system employing space time coded relay nodes and imaging receivers. *SAIEE Africa Research Journal*, 111(2):56–64, June 2020.

[118] X. Li, R. Zhang, and L. Hanzo. Cooperative load balancing in hybrid visible light communications and wifi. *IEEE Transactions on Communications*, 63(4):1319–1329, April 2015.

[119] S. Shao, A. Khreishah, M. Ayyash, M. B. Rahaim, H. Elgala, V. Jungnickel, D. Schulz, T. D. C. Little, J. Hilt, and R. Freund. Design and analysis of a visible-light-communication enhanced wifi system. *IEEE/OSA Journal of Optical Communications and Networking*, 7(10):960–973, October 2015.

[120] T. Holden and J. Yazdani. Hybrid security for hybrid vehicles exploring smart grid technology, powerline and wireless communication. In *2011 2nd IEEE PES International Conference and Exhibition on Innovative Smart Grid Technologies*, pages 1–5, Dec 2011.

[121] A. Cataliotti, V. Cosentino, D. Di Cara, S. Guaiana, N. Panzavecchia, G. Tinè, D. Gallo, C. Landi, M. Landi, and M. Luiso. Experimental evaluation of an hybrid communication system architecture for smart grid applications. In *2015 IEEE International Workshop on Applied Measurements for Power Systems (AMPS)*, pages 96–101, Sept 2015.

[122] L. de M. B. A. Dib, V. Fernandes, M. de L. Filomeno, and M. V. Ribeiro. Hybrid PLC/wireless communication for smart grids and internet of things applications. *IEEE Internet of Things Journal*, PP(99):1–1, 2017.

[123] J. Mafra, M. Hosami, L. Freitas, M. Martinelli, and A. Almeida. Hybrid communication module - motivations, requirements, challenges and implementations. In *2015 IEEE PES Innovative Smart Grid Technologies Latin America (ISGT LATAM)*, pages 25–29, Oct 2015.

[124] S. W. Lai and G. G. Messier. Using the wireless and plc channels for diversity. *IEEE Transactions on Communications*, 60(12):3865–3875, December 2012.

[125] M. Sayed, T. A. Tsiftsis, and N. Al-Dhahir. On the diversity of hybrid narrowband-plc/wireless communications for smart grids. *IEEE Transactions on Wireless Communications*, 16(7):4344–4360, July 2017.

[126] S. W. Lai and G. G. Messier. The wireless/power-line diversity channel. In *2010 IEEE International Conference on Communications*, pages 1–5, May 2010.

[127] A. Mathur, M. R. Bhatnagar, and B. K. Panigrahi. Performance of a dual-hop wireless-powerline mixed cooperative system. In *2016 International Conference on Advanced Technologies for Communications (ATC)*, pages 401–406, Oct 2016.

[128] K. M. Rabie, B. Adebisi, H. Gacanin, G. Nauryzbayev, and A. Ikpehai. Performance evaluation of multi-hop relaying over non-Gaussian PLC channels. *Journal of Communications and Networks*, 19(5):531–538, Oct. 2017.

[129] A. M. Tonello, F. Versolatto, and S. D'Alessandro. Opportunistic relaying in in-home PLC networks. In *2010 IEEE Global Commun. conf. GLOBECOM 2010*, pages 1–5, Dec. 2010.

[130] A. Alfitouri and K. A. Hamdi. Multiple-access capabilities of a common gateway. *IEEE Transactions on Vehicular Technology*, 66(6):5148–5159, June 2017.

[131] Min-Jae Paek, Yu-Jin Na, Wonseok Lee, Jae-Hyun Ro, and Hyoung-Kyu Song. A novel relay selection scheme based on q-learning in multi-hop wireless networks. *Applied Sciences*, 10:5252, 2020.

[132] W. Liu, J. Ding, J. Zheng, X. Chen, and C. L. I. Relay-assisted technology in optical wireless communications: A survey. *IEEE Access*, 8:194384–194409, 2020.

[133] Salvatore D'Alessandro and Andrea M. Tonello. On rate improvements and power saving with opportunistic relaying in home power line networks. *EURASIP Journal on Advances in Signal Processing, September 2012*, 2012(1):194, Sept. 2012.

[134] H. Zou, A. Chowdhery, S. Jagannathan, J. M. Cioffi, and J. Le Masson. Multi-user joint subchannel and power resource-allocation for powerline relay networks. In *2009 IEEE International Conference on Communications(ICC)*, pages 1–5, Jun. 2009.

[135] S. M. Nlom, A. R. Ndjiongue, and K. Ouahada. Cascaded plc-vlc channel: An indoor measurements campaign. *IEEE Access*, 6:25230–25239, 2018.

[136] T. Komine and M. Nakagawa. Integrated system of white LED visible-light communication and power-line communication. *IEEE Transactions on Consumer Electronics*, 49(1):71–79, Feb. 2003.

[137] H. Ma, L. Lampe, and S. Hranilovic. Integration of indoor visible light and power line communication systems. In *2013 IEEE 17th International Symposium on Power Line Communications and Its Applications*, pages 291–296, March 2013.

[138] J. Song, W. Ding, F. Yang, H. Yang, B. Yu, and H. Zhang. An indoor broadband broadcasting system based on plc and vlc. *IEEE Transactions on Broadcasting*, 61(2):299–308, June 2015.

[139] X. Ma, W. Ding, F. Yang, H. Yang, and J. Song. A positioning compatible multi-service transmission system based on the integration of vlc and plc. In *2015 International Wireless Communications and Mobile Computing Conference (IWCMC)*, pages 480–484, Aug 2015.

[140] K. M. Rabie, B. Adebisi, H. Gacanin, and S. Yarkan. Energy-per-bit performance analysis of relay-assisted power line communication systems. *IEEE Transactions on Green Communications and Networking*, 2(2):360–368, Jun. 2018.

[141] W. Bakkali, P. Pagani, and T. Chonavel. Energy efficiency performance of relay-assisted power-line communication networks. In *2015 12th Annual IEEE Consumer Communications and Networking Conference (CCNC)*, pages 525–530, Jan 2015.

[142] V. Fernandes, H. V. Poor, and M. V. Ribeiro. Dedicated energy harvesting in concatenated hybrid plc-wireless systems. *IEEE Transactions on Wireless Communications*, 19(6):3839–3853, June 2020.

[143] T. Rakia, H. Yang, F. Gebali, and M. Alouini. Optimal design of dual-hop VLC/RF communication system with energy harvesting. *IEEE Communications Letters*, 20(10):1979–1982, Oct 2016.

[144] M. R. Zenaidi, Z. Rezki, M. Abdallah, K. A. Qaraqe, and M. Alouini. Achievable rate-region of VLC/RF communications with an energy harvesting relay. In *GLOBECOM 2017 - 2017 IEEE Global Communications Conference*, pages 1–7, Dec 2017.

[145] Victor Fernandes, Thiago Oliveira, and Moises Ribeiro. The usefulness of the energy harvested from additive noises in power line and wireless media. 35:61–65, 03 2020.

[146] K. M. Rabie, B. Adebisi, and A. Salem. Improving energy efficiency in dual-hop cooperative PLC relaying systems. In *2016 International Symposium on Power Line Communications and its Applications (ISPLC)*, pages 196–200, March 2016.

[147] T. Rakia, H. Yang, F. Gebali, and M. Alouini. Dual-hop VLC/RF transmission system with energy harvesting relay under delay constraint. In *2016 IEEE Globecom Workshops (GC Wkshps)*, pages 1–6, Dec 2016.

[148] M. Kashef, M. Ismail, M. Abdallah, K. A. Qaraqe, and E. Serpedin. Energy efficient resource allocation for mixed RF/VLC heterogeneous wireless networks. *IEEE Journal on Selected Areas in Communications*, 34(4):883–893, Apr. 2016.

[149] Y. Gu and S. Aïssa. RF-based energy harvesting in decode-and-forward relaying systems: Ergodic and outage capacities. *IEEE Transactions on Wireless Communications*, 14(11):6425–6434, Nov 2015.

[150] S. S. Kalamkar and A. Banerjee. Interference-assisted wireless energy harvesting in cognitive relay network with multiple primary transceivers. In *2015 IEEE Global Communications Conference (GLOBECOM)*, pages 1–6, Dec 2015.

[151] Mariia Plakhova, Bassam Mohamed, and Pablo Arboleya. Static model of a 2x25kv AC traction system. 12 2015.

[152] A. Zupan, A. T. Teklic, and B. Filipovic-Grcic. Modeling of 25 kv electric railway system for power quality studies. In *Eurocon 2013*, pages 844–849, Jul. 2013.

[153] B. Mellitt, C. J. Goodman, and R. I. M. Arthurton. Simulator for studying operational and power-supply conditions in rapid-transit railways. *Proceedings of the Institution of Electrical Engineers*, 125(4):298–303, April 1978.

[154] C. J. Goodman, L. K. Siu, and T. K. Ho. A review of simulation models for railway systems. In *1998 International Conference on Developments in Mass Transit Systems Conf. Publ. No. 453)*, pages 80–85, April 1998.

[155] W. Mingli, C. Roberts, and S. Hillmansen. Modelling of ac feeding systems of electric railways based on a uniform multi-conductor chain circuit topology. In *IET Conf. Railway Traction Syst. (RTS 2010)*, pages 1–5, April 2010.

[156] V. o. Havryliuk. Modelling of the return traction current harmonics distribution in rails for ac electric railway system. In *2018 Int. Symp. Electromag. Compat. (EMC EUROPE)*, pages 251–254, Aug 2018.

[157] Mariia Plakhova. Implementation of the derivative-based technique for solving a 2*25kv AC bivoltage traction system. pages 1–7, 12 2015.

[158] Y. Tanaka, M. Ishikawa, and K. Kurogi. Study for electromagnetic inference under construction in boosting transformer feeding system. In *2016 19th Int. Conf. Electr. Machines and Syst. (ICEMS)*, pages 1–4, Nov 2016.

[159] J. R. Tierney and R. J. Turner. Improvement to the booster transformer/return conductor method of suppressing 50 Hz interference from a.c.-electrified railway systems. *IEE Proceedings B - Electr. Power Appl.*, 128(1):61–66, Jan. 1981.

[160] Eduardo Pilo, Luis Rouco, and Antonio Fernandez. Catenary and autotransformer coupled optimization for 2x25kv systems planning. volume 88, pages 747–756, 06 2006.

[161] E. Pilo, L. Rouco, A. Fernandez, and L. Abrahamsson. A monovoltage equivalent model of bi-voltage autotransformer-based electrical systems in railways. *IEEE Trans. Power Del.*, 27(2):699–708, Apr. 2012.

[162] Alberto Dolara and S. Leva. Calculation of rail internal impedance by using finite elements methods and complex magnetic permeability. *Int. J. Veh. Technol.*, 2009, Jan. 2009.

[163] Segun Olatinwo, Oluwagbemiga Shoewu, and N. Makanjuola. Radio wave signal attenuation in a gsm network (epe as a case study). 05 2014.

[164] Changyoung An and Heung-Gyoon Ryu. Design and performance evaluation of multidimensional ofdm system. *Wireless Personal Communications*, 113, 08 2020.

[165] C. Li, K. H. Park, and M. S. Alouini. On the use of a direct radiative transfer equation solver for path loss calculation in underwater optical wireless channels. *IEEE Wireless Communications Letters*, 4(5):561–564, Oct. 2015.

[166] K. Xu, H. Y. Yu, Y. J. Zhu, and Y. Sun. On the ergodic channel capacity for indoor visible light communication systems. *IEEE Access*, 5:833–841, 2017.

[167] K. M. Rabie and B. Adebisi. Enhanced amplify-and-forward relaying in non-gaussian plc networks. *IEEE Access*, 5:4087–4094, 2017.

[168] A. M. Tonello, S. D'Alessandro, and L. Lampe. Cyclic prefix design and allocation in bit-loaded ofdm over power line communication channels. *IEEE Trans. Commun.*, 58(11):3265–3276, Nov. 2010.

[169] A. M. Tonello, F. Versolatto, B. Bejar, and S. Zazo. A fitting algorithm for random modeling the PLC channel. *IEEE Transactions on Power Delivery*, 27(3):1477–1484, Jul. 2012.

[170] L. Zeng, D. C. O'Brien, H. L. Minh, G. E. Faulkner, K. Lee, D. Jung, Y. Oh, and E. T. Won. High data rate multiple input multiple output MIMO optical wireless communications using white led lighting. *IEEE Journal on Selected Areas in Communications*, 27(9):1654–1662, Dec. 2009.

[171] K. A. Hamdi. A useful lemma for capacity analysis of fading interference channels. *IEEE Transactions on Communications*, 58(2):411–416, Feb. 2010.

[172] M. K. Simon and M.-S. Alouini. *Digital Communication Over Fading Channels*. 2nd ed. New York: Wiley, 2005.

[173] O. Narmanlioglu, R. C. Kizilirmak, F. Miramirkhani, and M. Uysal. Cooperative visible light communications with full-duplex relaying. *IEEE Photonics Journal*, 9(3):1–11, Jun 2017.

[174] W. Yuanquan and C. Nan. A high-speed bi-directional visible light communication system based on RGB-LED. *China Communications*, 11(3):40–44, Mar 2014.

[175] M. Uysal, F. Miramirkhani, O. Narmanlioglu, T. Baykas, and E. Panayirci. IEEE 802.15.7r1 reference channel models for visible light communications. *IEEE Communications Magazine*, 55(1):212–217, Jan 2017.

[176] G. S. Spagnolo, L. Cozzella, F. Leccese, S. Sangiovanni, L. Podestà, and E. Piuzzi. Optical wireless communication and li-fi: a new infrastructure for wireless communication in saving energy era. In *2020 IEEE International Workshop on Metrology for Industry 4.0 IoT*, pages 674–678, June 2020.

[177] Pablo Palacios, Cesar Azurdia-Meza, Milton Roman Cañizares, Iván Sánchez, and Daniel Iturralde. On the performance of visible light communications in underground mines. 10 2020.

[178] Arsyad Ramadhan Darlis, Lucia Jambola, Lita Lidyawati, and Adisty Asri. Optical repeater for indoor visible light communication using amplify-forward method. *Indonesian Journal of Electrical Engineering and Computer Science*, 20:1351, 12 2020.

[179] Petr Pesek, Stanislav Zvanovec, Petr Chvojka, Norhanis Mohd, and Pooria Tabesh Mehr. Experimental validation of indoor relay-assisted visible light communications for a last-meter access network. *Optics Communications*, 451:319–322, 07 2019.

[180] Akash Gupta, Parul Garg, and Nikhil Sharma. Hard switching-based hybrid RF/VLC system and its performance evaluation. *Transactions on Emerging Telecommunications Technologies*, 30, 07 2018.

[181] L. Yin, W. O. Popoola, X. Wu, and H. Haas. Performance evaluation of non-orthogonal multiple access in visible light communication. *IEEE Transactions on Communications*, 64(12):5162–5175, Dec 2016.

[182] H. U. Sokun, A. B. Sediq, S. Ikki, and H. Yanikomeroglu. Selective DF relaying in multi-relay networks with different modulation levels. In *2014 IEEE International Conference on Communications (ICC)*, pages 5035–5041, Jun. 2014.

[183] A. Dubey, C. Kundu, T. M. N. Ngatched, O. A. Dobre, and R. K. Mallik. Incremental selective decode-and-forward relaying for power line communication. In *2017 IEEE 86th Vehicular Technology Conference (VTC-Fall)*, pages 1–6, Sep 2017.

[184] B. Rankov and A. Wittneben. Spectral efficient protocols for half-duplex fading relay channels. *IEEE Journal on Selected Areas in Communications*, 25(2):379–389, Feb. 2007.

[185] J. N. Laneman, D. N. C. Tse, and G. W. Wornell. Cooperative diversity in wireless networks: Efficient protocols and outage behavior. *IEEE Transactions on Information Theory*, 50(12):3062–3080, Dec 2004.

Appendix A

Matlab Codes

```
%--------------plc--------------------
%--calculation of transfer function-----
clc;
clear all;
close all;
%-----------------------------------
th=1.53e-3;  %-thickness of the insulation
vo=1.2566650e-6;  %-vacuum permeability
eo=8.85e-12;  %-permittivity
mc=1.256629e-6;  %-permeability of conductor
sc=5.69e7;  %conductivity of the conductor
a=1.25e-3;  %conductor radius
AA=5.26e-3;
%-----------------------------------
ZL=50;
Zs=50;
%-----------------------------------
lbr=2.5;

%-----------------------------------
fi=2e6;
ff=30e6;
fs=5e5;
fe=fi:fs:ff;
%-----------------------------------
k=1;
j=1;
l5=1:1.75438596:100;
% l2=100-l5;

    for l3=1:1.75438596:100
        l2=100-l3;
    for f=fi:fs:ff
    D=(2*a)+(2*th)+1.5e-3;  %separation of thecable
    tandc=((-5.725e-10)*f)+0.06;  %dielectric loss
    er=(-3.3333e-9*f)+3.1167;  %relative permittivity

    d=sqrt(1/(pi*f*mc*sc));    %delta factor
    R=1/(pi*a*d*sc);  %resistanec
    C=2*er*eo*(a/D);  %capacitance
    L=((vo*D)/(2*a));  %inductance
    G=(2*pi*f*C*tandc);  %conductance

    pc=sqrt((R+(1j*2*pi*f*L))*(G+(1i*2*pi*f*C))); %propagation const
    Zdc=sqrt((R+(1j*2*pi*f*L))/(G+(1i*2*pi*f*C))); %char impedance

    %-----ABCD Matrix for l1--------------
    ABCD1=[cosh(pc*l3) Zdc*sinh(pc*l3); (1/Zdc)*sinh(pc*l3) cosh(pc*l3)];

    %-----ABCD Matrix for l2--------------
    ABCD2=[cosh(pc*l2) Zdc*sinh(pc*l2); (1/Zdc)*sinh(pc*l2) cosh(pc*l2)];
%
    %-----ABCD Matrix for BRANCH-----------------
   Zdeq=50;
%     Zdeq=Zdc*coth(pc*lbr);
    ABCDbr=[1 0; 1/Zdeq 1];

    %------Source Matrix----------------------
    T0=[1 Zs; 0 1];

    %-----T matrix-------------------------
    T=T0*ABCD1*ABCDbr*ABCD2;

    %---TRANSFER FUNCTION----------------------------

    H(k,j)=10*log(abs(ZL/((T(1,1)*ZL)+(T(1,2))+(T(2,1)*ZL*Zs)+(T(2,2)*Zs))));

    k=k+1;
    end
%   T=T0*[cosh(pc*l3) Zdc*sinh(pc*l3); (1/Zdc)*sinh(pc*l3) cosh(pc*l3)];
%
% H(k,j)=10*log(abs(ZL/((T(1,1)*ZL)+(T(1,2))+(T(2,1)*ZL*Zs)+(T(2,2)*Zs))));
 k=1;
 j=j+1;

    end
figure

[X,Y]=meshgrid(fe,l5);
  mesh(X,Y,H);

% plot(fe,H);
%
% grid on
% legend('measured','calculated','Location','southwest')
```

Figure A.1 Channel response of the OLE channel.

```
clear all;
%close all;
clc;

N=64;  % number of OFDM carrier

% BER = [];
% SNR =[];
M = 1;
Bits = N*M;     %number of symbol
%OFDM_s = 31250;
OFDM_s = 10000;

%HDM = hadamard(N);
for SNR =1:2:37

for j = 1:OFDM_s
x = floor(rand(1, Bits)+0.5)';
xx = reshape(x,M,[]);

%p = qpsk(x);  % QPSK Modulation
p = bpsk(x);  % BPSK Modulation

%p = HDM.*p';

%p = Qam16(x);  % Qam 16 Modulation
s1=p;     % first symbol

%H = rayl_chan(length(p));
%H =ones(1,length(p));%
% H = plchan(length(p));
%F=4M
H1=[0.0350198942485688 - 0.116680607979154i,0.00238281911700087 - 0.0821707583038842i,-0.0176470904901776 - 0.0886679717720498i,-0.111220809
%
%F=6M
H2=[0.0128724689576761 - 0.0922005822391851i,-0.0176470904901776 - 0.0886679717720498i,-0.233552092497369 - 0.0117606224926813i,-0.017612657
%
%F=8M
H3=[0.00238281911700087 - 0.0821707583038842i,-0.111220809253268 - 0.1250888745469171,-0.0176126571881017 + 0.0884880061775780i,0.045028472
%
% Noise
 %NN = fft(CompNoise(SNR,N))/sqrt(N);  % AWGN
NN = (fft(imp_noise(SNR,N)))/sqrt(N);  % AWCN
%receiver
Y1 = H1.*s1 + NN;
Y2 = H2.*s1 + NN;
Y3 = H3.*s1 + NN;

%S = ML(Y, H)'; %  QPSK Maximum Likelihood
S1 = ML2(Y1, H1)'; %  BPSK Maximum Likelihood
S2 = ML2(Y2, H2)'; %  BPSK Maximum Likelihood
S3 = ML2(Y3, H3)'; %  BPSK Maximum Likelihood

Eror1(j)  = length(find(x~=S1));
Eror2(j)  = length(find(x~=S2));
Eror3(j)  = length(find(x~=S3));
end
%terror = sum(Eror)
BER1((SNR + 1)/2) = (sum(Eror1))/(Bits*OFDM_s);
BER2((SNR + 1)/2) = (sum(Eror2))/(Bits*OFDM_s);
BER3((SNR + 1)/2) = (sum(Eror3))/(Bits*OFDM_s);
end
SNRx =1:2:37
berx1 = BER1'
berx2 = BER2'
berx3 = BER3'
semilogy(SNRx,berx1,'b-','LineWidth',1.5);
hold on
semilogy(SNRx,berx2,'y-','LineWidth',1.5);
hold on
semilogy(SNRx,berx3,'r-','LineWidth',1.5);
axis([1 37 10^-2 1])
grid on
 legend('Frequency=5MHz', 'Frequency=10MHz','Frequency=15MHz' );
xlabel('SNR [dB]')
ylabel('BER')
```

Figure A.2 BER and average capacity of the OFDM-based OLE system.

```
close all
clear all
clc
nn=50000;
gama=1.5;
snrdB=5;
sg=1/10^(snrdB/10);
sigmard=sg;
sigmarh=sg;
sigmad=sg;

ps=1:1:10;
d1=15;
zeta=log (10)/10;
sigma1= 5*zeta;
sigma2= 5*zeta;
mu1   = 2*zeta;
mu2   = 2*zeta;
a0=9.4*10^(-3);
a1=4.2*10^(-7);
kk=0.7;
f=500;
alpha=(a0+a1*f^kk);
G=1;
L=2.15;
re=3.6;
FOV = 60;
Rp = 0.4;
n = 1.5;
A = 0.1;
G1 = 5;
T = 5;
m = -1/(log2(cos(pi/3)));
Q = (T* G1 *  A *Rp )/(2*pi);
Cc=Q;
Cmin=(Q*(m+1)*L^(m+1))^2/(re^2+L^2)^(m+3);
Cmax=(Q*(m+1)*L^(m+1))^2/(L^2)^(m+3);

c=sigmard;
b=sigmad;
for ii=1:length(ps)
    ii
    w1=0;
    Ctsr=0;
    Ctsr1=0;
    a=ps(ii);
    while w1<nn
%         h1=lognrnd(mu1,sigma1);
%         h2=lognrnd(mu1,sigma1);
               rk1=(Cc*L^(1+m) + Cc*L^(1 + m)*m)^(2/(3 + m))*(Cc^2*L^(2 + 2*m)*(1 + 2*m + m^2)*(L^2 + re^2)^(-3 - m))^(1/(3 + m));
               rk2=-(Cc*L^(1 + m) + Cc*L^(1 + m)*m)^(2/(3 + m)) + re^2 *(Cc^2* L^(2 + 2*m)*(1 + 2*m + m^2)*(L^2 + re^2)^(-3 - m))^(1/(3+ m)) *rand(1);
               h1=(-rk1./rk2).^(m+3);
               h2=(-rk1./rk2).^(m+3);
        %         DF
        snr1=(ps(ii)/sigmad)*abs(h1);
        snr2=(ps(ii)/sigmad)*abs(h2);
        snr=min(snr1,snr2);
         Ctsr=Ctsr+1/2*log2(1+snr);
%         C1=log2(1+snr1);
%         C2=log2(1+snr2);
%         Ctsr=Ctsr+1/2*min(C1,C2);
        snr11=ps(ii)*(h1);
        snr22=sigmad+(sigmad/(ps(ii)*abs(h2)));
        snrb=snr11/snr22;
        Ctsr1=(Ctsr1+1/2*log2(1+snrb));
        w1=w1+1;
    end
    Cstsr1(ii)=(Ctsr1)/nn;
    Cstsr(ii)=Ctsr/nn;
end
ps2=1:2:10;
figure(1)
plot(ps ,Cstsr,'r-');  hold on; grid on;
% plot(ps,anacsTSR1,'*');  hold on; grid on;
plot(ps ,Cstsr1,'b-');  hold on; grid on;
% plot(ps,anacsTSR2,'b*');  hold on; grid on;
legend('DF','AF');
xlabel('Input Power (Ps)');
ylabel('Average Capacity (Bits/s/Hz)');
```

Figure A.3 Average capacity for AF and DF based systems.

```
 close all
clear all
 clc
nn=5000;
gama=1.5;
snrdB=10;
sg=1/10^(snrdB/10);
sigmard=sg;
sigmarh=sg;
sigmad=sg;

d1=20;
zeta=log (10)/10;
sigma1= 5*zeta;
sigma2= 5*zeta;
mu1   = 2*zeta;
mu2   = 2*zeta;

a0=9.4*10^(-3);
a1=4.2*10^(-7);
kk=0.7;
f=500;
alpha=(a0+a1*f^kk);

ps=0.1;
c=sigmard;
b=sigmad;

L=2.15;
re=3.6;
Q1 = 60;
FOV = 60;
Rp = 0.4;
n = 1.5;
A = 0.1;
G1 = 5;
T = 5;
m = -1/(log2(cos(60)));
Q = (T* G1 *  A *Rp )/(2*pi);
Cmin=(Q*(m+1)*L^(m+1))^2/(re^2+L^2)^(m+3);
Cmax=(Q*(m+1)*L^(m+1))^2/(L^2)^(m+3);
v=Cmin:0.0001:Cmax;
for ii=1:length(v)
    ii
    w1=0;
    Ctsr1=0;
    Ctsr2=0;
    a=ps*exp(-2*alpha*d1);
 out=0;

    while w1<nn
        % plc channel
        h1=lognrnd(mu1,sigma1);

        % vlc channel
        rk1=(Q*L^(1+m) + Q*L^(1 + m)*m)^(2/(3 + m))*(Q^2*L^(2 + 2*m)*(1 + 2*m + m^2)*(L^2 + re^2)^(-3 - m))^(1/(3 + m));
        rk2=-(Q*L^(1 + m) + Q*L^(1 + m)*m)^(2/(3 + m)) + re^2 *(Q^2* L^(2 + 2*m)*(1 + 2*m + m^2)*(L^2 + re^2)^(-3 - m))^(1/(3+ m)) *rand(1);
        h2=(-rk1./rk2).^(m+3);

        snr1=(a/b)*abs (h1)^2;
        snr2=(0.1/c)*abs(h2);
        snr= min(snr1,snr2);

        if snr<v(ii)
            out=out+1;
        end
        w1=w1+1;
    end
   outAg(ii)=out/nn;
    end
vv=Cmin:0.0001:Cmax;
anacsTSR1=[-0.00746935, 0.58107, 0.721083, 0.795154, 0.84359, 0.878746, 0.905917, 0.927818, 0.946012, 0.961473, 0.974849, 0.986586];

figure
plot(v ,outAg,'b-');  hold on; grid on;
plot(vv,anacsTSR1,'*');  hold on; grid on;

legend('Simulation','Analytical');
xlabel('Source Transmit power (W)');
ylabel('Average Capacity (Bits/s/Hz)');
```

Figure A.4 Outage probability for AF based system.

```
close all
clear all
clc

nn=10000;
gama=1.5;
snrdB=10;
sg=1/10^(snrdB/10);
sigmard=sg;
sigmarh=sg;
sigmad=sg;
l=5;
d1=10;
d2=10;

zeta=log (10)/10;
sigma1= 5*zeta;
sigma2= 5*zeta;
mu1   = 2*zeta;
mu2   = 2*zeta;
a0=9.4*10^(-3);
a1=4.2*10^(-7);
kk=0.7;
f=500;
alpha=(a0+a1*f^kk);
ps=1;
c=0.1;
c=sigmard;
b=sigmad;
L=2.15;
m=1;
C=3;
re=3.6;
Cc=1;
Cmin=(Cc*(m+1)*L^(m+1))^2/(re^2+L^2)^(m+3);
Cmax=(Cc*(m+1)*L^(m+1))^2/(L^2)^(m+3);
sg=1/10^(25/10);
v=Cmin:0.01:Cmax;
for ii=1:length(v)
    ii
    w1=0;
    Ctsr=0;
    a=ps*exp(-2*alpha*d1);
    out=0;
     outAf1=0;
    outAf2=0;
    while w1<nn
        % plc channel
        h1=lognrnd(mu1,sigma1);
        % vlc channel
        rk1=(Cc*L^(1+m) + Cc*L^(1 + m)*m)^(2/(3 + m))*(Cc^2*L^(2 + 2*m)*(1 + 2*m + m^2)*(L^2 + re^2)^(-3 - m))^(1/(3 + m));
        rk2=-(Cc*L^(1 + m) + Cc*L^(1 + m)*m)^(2/(3 + m)) + re^2 *(Cc^2* L^(2 + 2*m)*(1 + 2*m + m^2)*(L^2 + re^2)^(-3 - m))^(1/(3+ m)) *rand(1);
        h2=(-rk1./rk2).^(m+3);
        snr1= a*abs(h2);
        snr2=b+c/h2;
        snr=snr1/snr2;
        Ctsr=1/2*log2(1+snr1);
         if snr1<v(ii)
            outAf1=outAf1+1;
        end
        if snr2<v(ii)
            outAf2=outDf2+1;
        end

        if snr<v(ii)
            out=out+1;
        else
            out=out+0;
        end
        w1=w1+1;
    end
    outAg(ii)=out/nn;
    outAgAf1(ii)=outAf1/nn;
    outAgAf2(ii)=outAf2/nn;
end
outageSim_AF =outAgAf1+(1-outAgAf1).*outAgAf2;
figure
plot(v ,outAg,'b-');  hold on; grid on;
plot(v,outageSim_AF,'*');  hold on; grid on;
legend('Simulation','Analytical');
xlabel('Source Transmit power (W)');
ylabel('Average Capacity (Bits/s/Hz)');
```

Figure A.5 Outage probability for DF based system.

```
close all
clear all
clc
nn=10000;
snrdB=10;
sg=1/10^(snrdB/10);sigmard=sg; c=sigmard;
L=2.85; L1=1.75; L2=1.75;L3=3.5;rs=3.6;
Q1 = 60; FOV = 60;Rp = 0.4;n = 1.5;A = 0.1;G1 = 5;
T = 5;Psh=0.33;m = -1/(log2(cos(60)));Q = (T* G1 *  A *Rp )/(2*pi);
Cmin=(Q*(m+1)*L^(m+1))^2/(rs^2+L^2)^(m+3);
Cmax=(Q*(m+1)*L^(m+1))^2/(L^2)^(m+3);v=Cmin:0.00004:Cmax;
L4=0.5:0.5:4.5;
for re=2.6:0.1:3.4
    for ii=1:length(v)
    ii
    w1=0;outDf1=0;outDf2=0; out2=0;out1=0;out3=0;
    while w1<nn
        % vlc3 channel (DIRECT LINK)
        rk3=(Q*L3^(1+m) + Q*L3^(1 + m)*m)^(2/(3 + m))*(Q^2*L3^(2 + 2*m)*(1 + 2*m + m^2)*(L3^2 + re^2)^(-3 - m))^(1/(3 + m));
        rk4=-(Q*L3^(1 + m) + Q*L3^(1 + m)*m)^(2/(3 + m)) + re^2 *(Q^2* L3^(2 + 2*m)*(1 + 2*m + m^2)*(L3^2 + re^2)^(-3 - m))^(1/(3+ m)) *rand(1);
        h3=(-rk3./rk4).^(m+3);
        snrd=(Psh/c)*abs(h3);
        %      DIRECT
        if snrd<v(ii)
            out1=out1+1;
        end
        % vlc1 channel1(SOURCE TO RELAY LINK)
        rk11=(Q*L1^(1+m) + Q*L1^(1 + m)*m)^(2/(3 + m))*(Q^2*L1^(2 + 2*m)*(1 + 2*m + m^2)*(L1^2 + re^2)^(-3 - m))^(1/(3 + m));
        rk12=-(Q*L1^(1 + m) + Q*L1^(1 + m)*m)^(2/(3 + m)) + re^2 *(Q^2* L1^(2 + 2*m)*(1 + 2*m + m^2)*(L1^2 + re^2)^(-3 - m))^(1/(3+ m)) *rand(1);
        h1=(-rk11./rk12).^(m+3);
        % vlc2 channel1 ((RELAY TO DESTINATION LINK)
        rk21=(Q*L2^(1+m) + Q*L2^(1 + m)*m)^(2/(3 + m))*(Q^2*L2^(2 + 2*m)*(1 + 2*m + m^2)*(L2^2 + re^2)^(-3 - m))^(1/(3 + m));
        rk22=-(Q*L2^(1 + m) + Q*L2^(1 + m)*m)^(2/(3 + m)) + re^2 *(Q^2* L2^(2 + 2*m)*(1 + 2*m + m^2)*(L2^2 + re^2)^(-3 - m))^(1/(3+ m)) *rand(1);
        h2=(-rk21./rk22).^(m+3);
        snr1=(Psh/c)*abs(h1);
        snr2=(Psh/c)*abs(h2);
        snr3=snr2^2;
        snr= min(snr2,snr1);
        if snr1<v(ii) || snr2<v(ii)
            out2=out2+1;
        end
        if snr1<v(ii)
            outDf1=outDf1+1;
        end
        if snr2<v(ii)
            outDf2=outDf2+1;
        end
        %         SDF
        if snrd<v(ii) && (snr1<v(ii) || snr2<v(ii))
            out3=out3+1;
        end
        w1=w1+1;
    end
    outAg1(ii)=out1/nn;
    outAg2(ii)=out2/nn;
    outAg3(ii)=out3/nn;
    outAgDf1(ii)=outDf1/nn;
    outAgDf2(ii)=outDf2/nn;
    outAg1(ii)=out1/nn;
    outAg2(ii)=out2/nn;
    outAg3(ii)=out3/nn;
    outAgDf1(ii)=outDf1/nn;
    outAgDf2(ii)=outDf2/nn;
    end
    end
    % % % SH
outageAny_SH =(-1/ (re^2)* (Q *L3^(1 + m) *(1 + m))^(2/(3 + m))*(((c *(v/Psh))).^(-(1/(3 + m))))) + (1 + L3^2/ (re^2));
% % % % DF
outageSim_DF =outAgDf1+(1-outAgDf1).*outAgDf2;
% % % % SDF
outageSim_SDF = outageAny_SH .* outageSim_DF ;
vv=Cmin:0.00004:Cmax;
figure
 plot(L4 ,outAg1,'r-.'); hold on
plot(L4 ,outAg2,'b'); hold on; grid on;
plot(L4 ,outAg3,'g-.'); hold on; grid on;
 plot(L4,outageAny_SH,'rs'); hold on; grid on;
plot(L4,outageSim_DF,'rs'); hold on; grid on;
plot(L4,outageSim_SDF,'rs')
legend('Single-hop','Non-coop. DF','Coop. SDF & ISDF','Simulation');
xlabel('Maximum Cell Radius of the  LED');
ylabel('Outage Probability');
```

Figure A.6 Outage probability of single-hop, non-cooperative DF and cooperative DF relay configurations.

```
close all
clear all
clc
eff=3;

f_MHz=30;
B=f_MHz*10^6;

Psh=[ 375.51, 784.519, 1489.49, 2613.21, 4300.9, 6720.1, 10060.7, 14535.1, 20377.7];
Pdf= [ 1100.11, 1072.66, 1311.29, 1771.71, 2487.83, 3522.79, 4957.79, 6888.73, 9424.94];
Psdf=[180.061 ,305.69 ,512.45 ,833.178, 1309.3 ,1992.65 ,2948.58 ,4260.25 ,6031.47 ];



 L=1:0.5:5;
 out=0:0.1:0.8
for ii=1:length(Psh)


     Esh(ii)=Psh(ii)/(eff*B);


end
for ii=1:length(Pdf)


    Edf(ii)=(Pdf(ii)/(eff*B))*(out(ii)+(2*(1-out(ii))));


end
for ii=1:length(Psdf)


     Esdf(ii)=(out(ii)*Psdf(ii)/(eff*B))+((1-out(ii))*2*Psdf(ii)/(eff*B));


end
for ii=1:length(Psdf)


     Eisdf(ii)= ((1-out(ii))*Psdf(ii)/(eff*B))+((out(ii)^2)*(Psdf(ii)/(eff*B)))+(out(ii)*(1-out(ii))*2*Psdf(ii)/(eff*B));



end


figure
plot(L,Esh,'r'); grid on; hold on
plot(L,Edf,'b--'); grid on; hold on
plot(L,Esdf,'g-.');grid on; hold on
plot(L,Eisdf,'k--.');grid on; hold on
legend('Single-hop','Non-coop. DF','COO. SDF','COO. ISDF');
xlabel(' Vertical Distance (m)');
ylabel('Energy/bit(Joule/bit)');
```

Figure A.7 Energy performances of the different VLC system setups (Single-hop, Noncooperative, Cooperative SDF, and Cooperative IDF).